Time crystallinity in open quantum systems

Auteur : Lacaille, Tara
Promoteur(s) : Martin, John
Faculté : Faculté des Sciences
Diplôme : Master en sciences physiques, à finalité approfondie
Année académique : 2025-2026
URI/URL : http://hdl.handle.net/2268.2/25620

University of Liège

Faculty of Sciences • Department of Physics

Time crystallinity in open quantum systems

Master thesis presented in the partial fulfillment of the requirements for the Master degree of Science in Physics

Author

Lacaille Tara

Promoter Martin John

Reading committee Schlagheck Peter
Vandewalle Nicolas
Nguyen Ngoc Duy

Academic year 2025–2026

Acknowledgements

First of all, I would like to express my gratitude to my supervisor, John Martin. I am deeply grateful for his invaluable help, his insightful advice during our weekly meetings, and his continuous availability throughout this work.

I would also like to extend my sincere thanks to Prof. P. Schlagheck, Prof. N. Vandewalle, and Prof. D. Nguyen, the members of my reading committee, for graciously accepting to read my master's thesis.

A special shout-out goes to Lucas Warland for being such an attentive listener and for his support.

Finally, I am deeply grateful to my parents and my brother. Thank you for your unconditional support throughout this entire journey.

Contents

Introduction

Symmetry is one of the organizing principles of modern physics. A symmetry is a transformation that leaves the equations governing a system invariant, and the consequences of such invariance are far-reaching: they constrain the form of interactions, fix conservation laws, and dictate which collective behaviors a system may or may not display. In the physics of many-body systems and condensed matter, symmetry plays a particularly powerful role: it provides a language to classify the distinct phases that matter can adopt. Two phases that share the same symmetries are, in a deep sense, the same kind of state whereas two phases that differ in which symmetries they realize are generally distinct. Passing from one to the other requires a phase transition. However, this picture has its limits: some phases share all the same symmetries and yet remain genuinely different, as topological phases illustrate [1]. The central and most pervasive mechanism behind this classification is spontaneous symmetry breaking.

A symmetry is said to be spontaneously broken when the Hamiltonian (or, more generally, the equations of motion) is invariant under a transformation, yet the physical state the system actually settles into is not. The microscopic laws retain the full symmetry whereas the realized state selects one option among many equivalent ones. Three ingredients make this notion precise [2].

- First, the thermodynamic limit: in a finite isolated quantum system, the exact eigenstates typically respect the symmetry, because tunneling or finite-size mixing connects the symmetry-related configurations. Genuine spontaneous symmetry breaking, with a stable broken state, is strictly a property of the limit of infinitely many degrees of freedom, $N \to \infty$, where the barrier between the equivalent states becomes insurmountable.

- Second, the order parameter: an observable whose expectation value vanishes in the symmetric phase and becomes nonzero in the broken phase, thereby labeling which of the equivalent states has been selected. Its onset is the operational signature of the broken symmetry.

- Third, the stability of the broken state. The symmetry-broken state must be robust: small perturbations that respect the symmetry should not destroy the ordering, and the symmetry-related broken states should become distinct, stable sectors in the thermodynamic limit, separated by a macroscopic rigidity. A convenient diagnostic is provided by the long-distance behavior of correlation functions of the order parameter, which remain finite across the system in the ordered phase, the hallmark of long-range order.

The spontaneous breaking of an internal symmetry is for example illustrated by the Heisenberg ferromagnet: the Hamiltonian is invariant under global spin rotations, yet below the Curie temperature the spins align along a spontaneously chosen direction, and the magnetization serves as the order parameter [3]. The breaking of a spatial symmetry is illustrated by an ordinary crystal: the microscopic Hamiltonian of particles in free space is invariant under continuous translations, yet the crystalline ground state preserves only a discrete subgroup, leaving invariance only under the discrete translations of that lattice [4]. The continuous translational symmetry of space has been spontaneously broken down to a discrete subgroup.

The example of the crystal raises a striking question. Special relativity, through Lorentz transformations, places space and time on an equal footing: spatial and temporal coordinates are intimately linked and transform into one another. If continuous spatial translation symmetry can be spontaneously broken to give rise to a discrete lattice in a crystal, could continuous temporal translation symmetry be broken in the same way, producing a state in which the observables oscillate periodically over time? Such a state, a periodic arrangement in time rather than in space, was named a time crystal by Wilczek in 2012 [5, 6].

Wilczek first asked whether this could occur classically. The obstruction is intuitive: in an ordinary classical Hamiltonian system the lowest-energy configuration is static, since kinetic energy is minimized at rest, so spontaneous motion cannot appear in the equilibrium state without contrived, singular constructions [5]. He therefore turned to the quantum case. His model consisted of particles confined to a ring threaded by an Aharonov–Bohm flux, with attractive interactions. The flux induces a persistent current, while the interactions tend to bunch the particles into a localized soliton; Wilczek argued that the combination would produce a soliton rotating steadily around the ring in the quantum ground state. A ground-state observable that varies periodically in time would constitute a spontaneous breaking of continuous time-translation symmetry, a time crystal.

This proposal was quickly challenged. Bruno first pointed out that Wilczek's rotating soliton is not the true ground state of the model: a static configuration of lower energy exists [7]. He then established a no-go theorem ruling out spontaneous ground-state (or thermal-equilibrium) rotation for a broad class of systems [8]. The intuition is that a true equilibrium ground state should not exhibit persistent time dependence in observable quantities. Since an energy eigenstate evolves only by an overall phase, expectation values of time-independent observables remain stationary; a genuinely periodic order parameter would therefore be incompatible with equilibrium ground-state order. Shortly afterwards, Watanabe and Oshikawa proved a far more general statement [9]. Adopting a precise definition of a time crystal, nontrivial time dependence of the order-parameter correlation function in the thermodynamic limit, they showed that no such time dependence can survive in the ground state or in the canonical (thermal) ensemble of any Hamiltonian with not-too-long-range interactions.

Crucially, these theorems forbid time-crystalline order only in equilibrium. They thereby pointed the way to the right setting: time crystals, if they exist at all, must be sought out of equilibrium. The natural out-of-equilibrium platform is a periodically driven (Floquet) system, governed by a time-periodic Hamiltonian $H(t) = H(t + T)$. Such a system no longer possesses continuous time-translation symmetry; it retains only the discrete symmetry $t \to t + T$. A discrete time crystal (DTC) is a phase that spontaneously breaks the discrete time-translation symmetry generated by T down to the subgroup generated by nT, with $n \geq 2$: an observable responds with a period that is an integer multiple of the drive period, i.e. at a subharmonic of the driving frequency.

A toy model illustrated in Figure 1 makes this definition tangible. Consider a chain of interacting spins randomly oriented characterized by a periodic T equation of motion. Within each period, two things happen in turn: the spins first evolve under their mutual interactions, and then, an external driving induce a global flip rotation of every spin at once (for simplicity, we take this rotation to be instantaneous). After one full period, each spin of the chain has been turned over. It is only after a second period, and therefore a second flip, that the spins return to their starting configuration. The magnetization consequently oscillates with period $2T$, twice the period of the drive: this is precisely the subharmonic response that defines the phase.

What turns this from a trivial back-and-forth into a genuine phase of matter is its robustness. Indeed, thanks to the interactions between the spins, the response stays locked to exactly $2T$ even when the rotation is imperfect: the spins still return to their initial state after two periods. More generally, we expect this rigidity for not fine-tuned parameters of the system. This

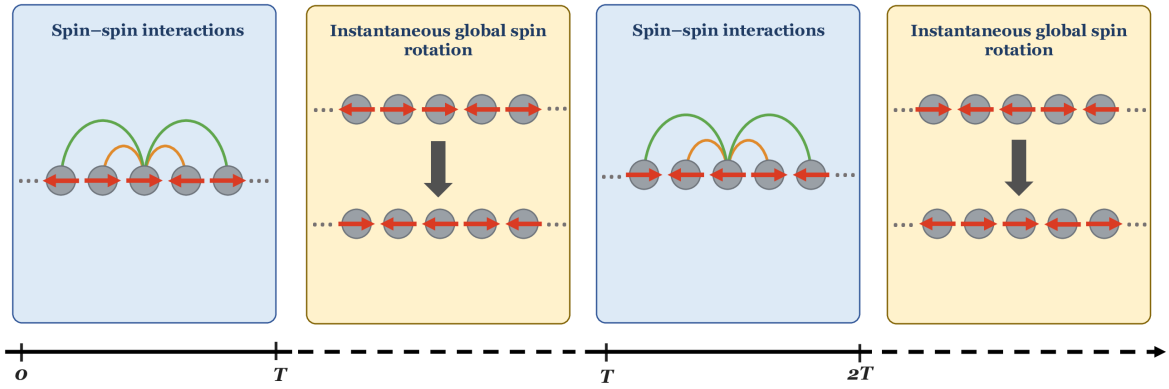

Figure 1: Paradigmatic example of a DTC. A chain of interacting spins randomly oriented is instantaneously flipped at each period T. The pattern thus repeats with period $2T$, twice the driving period, which is the subharmonic response that defines the phase.

rigidity, together with the fact that the oscillation persists indefinitely in the thermodynamic limit, is what makes the discrete time crystal a true collective phase rather than a fine-tuned coincidence.

The idea was first realized at the mean-field level by Sacha, who studied a Bose–Einstein condensate bouncing resonantly on an oscillating mirror [10]. In a mean-field description, in which each particle effectively feels the average influence of all the others, the condensate self-organizes into a motion whose period is a multiple of the drive period, spontaneously breaking the discrete time-translation symmetry.

What makes this remarkable is that periodically driven interacting systems generically heat up: under repeated driving they tend to absorb energy without bound and relax to a featureless infinite-temperature state in which no order can survive. In strongly disordered spin chains, however, this heating can be halted, and a discrete time crystal, the so-called π-spin glass, emerges [11–15]. This first route relied on disorder [11], but DTC order was subsequently shown to arise in clean systems as well [16–18], so disorder is not an essential ingredient. Experimental signatures have since been observed on several platforms, including trapped ions and nitrogen-vacancy centres in diamond [19], and later superconducting-qubit processors [20], establishing the discrete time crystal as a robust non-equilibrium many-body phase of matter.

Discrete time crystals are appealing well beyond their conceptual novelty: their rigid, robust subharmonic response makes them natural candidates for applications such as quantum metrology and sensing [21] and as robust quantum memories [22, 23]. Yet the closed-system setting in which DTCs were first defined is an idealization. Any real platform is coupled, however weakly, to an environment, and this raises a fundamental question that is the starting point of this thesis: does this phase of matter survive the introduction of a coupling to an environment? For the original π-spin-glass DTC the answer is negative. A generic local coupling to a thermal bath destroys it at long times, even when the bath itself prevents the system from heating [24].

This motivates the study of time crystals as genuinely open-system phenomena. Most work to date treats the Markovian regime, in which the dynamics is generated by a Gorini–Kossakowski–Sudarshan–Lindblad (GKSL) master equation, although a smaller body of work addresses non-Markovian settings [25]. The defining properties carried over from the closed case, subharmonic oscillation, rigidity, and persistence in the thermodynamic limit, must still hold. Strikingly, dissipation need not be an enemy of the order: suitably engineered, it can even stabilize a DTC [26]. As in the closed case, the phase leaves a characteristic fingerprint in the spectrum of the evolution, which provides a clean way to identify it. Such dissipative DTCs have been studied for example in cavity-QED models [27].

In parallel, dissipation also rehabilitated, in part, Wilczek's original continuous idea. In an

open system governed by time-independent dynamics, continuous time-translation symmetry can itself be spontaneously broken, producing persistent periodic oscillations in the thermodynamic limit, again with the requirement of rigidity. This led to the notion of a continuous (dissipative) time crystal (CTC) and, more specifically [28]. Continuous dissipative time crystals have by now been observed experimentally [29], for instance with atomic ensembles in optical cavities [30].

Both discrete and continuous time crystals are most easily approached at the mean-field level, a particularly convenient framework: the collective observables that play the role of order parameters close into a set of nonlinear differential equations, so the problem reduces to the theory of nonlinear dynamical systems, in which a CTC appears as a stable limit cycle. For a finite system the oscillation is not truly everlasting: the system eventually relaxes towards a time-independent steady state. Even then, the time-crystalline behavior shows up clearly in the spectrum of the dynamics. We note in passing that dissipative continuous time crystals have also been constructed for purely classical systems [31]. These lie outside the scope of this work, since we restrict our attention to the quantum, many-body setting in which the oscillation qualifies as a genuine collective phase of matter.

Dissipative many-body systems can support not only periodic but also chaotic collective dynamics, which gives rise to time-crystal-like phases whose temporal order is irregular. In a continuous quasi time crystal (CQTC), continuous time-translation symmetry is broken into sustained aperiodic, chaotic oscillations of the order parameter that do not decay in the thermodynamic limit [32, 33]. Such a phase was identified in a system of two coupled, driven–dissipative collective spins, each of which alone would form a CTC [32]. Unlike ordinary chaotic behavior in open systems, the oscillations do not die out in the thermodynamic limit.

The time glass, introduced very recently, is the periodically driven counterpart of this chaotic order: a non-periodic analogue of the DTC in which the order parameter oscillates aperiodically and chaotically, yet persistently in the thermodynamic limit [34]. Together, CQTCs and time glasses extend the time-crystal paradigm to genuinely chaotic quantum dynamics in open systems.

Finally, a more modest case, found in both closed and open quantum systems, deserves a separate mention: the discrete quasi time crystal. Although the term carries several definitions [35, 36] and is often regarded simply as a variant of the DTC, the distinction matters. Here the discrete time-translation symmetry is broken not into a clean subharmonic period multiplication, but into aperiodic oscillations that are nonetheless regular (quasiperiodic) rather than chaotic. It must therefore not be confused with the time-glass phase, whose temporal irregularity is genuinely chaotic.

The closed-system theory of discrete time crystals is by now mature and extensively reviewed [35, 37–40]. The picture in open quantum systems is comparatively scattered, despite a rapidly growing and increasingly varied family of phases. The objective of this thesis is to provide a unified, pedagogical overview of the different kinds of time crystals that arise in open quantum systems, classified according to the symmetry that is broken and the nature of the resulting temporal order: periodic, quasi-periodic, or chaotic.

The manuscript is structured to build this picture from the ground up. Chapter 1 lays the conceptual foundation, reviewing symmetry in quantum physics and the framework of spontaneous symmetry breaking, with the introduction of the thermodynamic limit, the order parameter and the stability of broken states, and with the harmonic crystal as the canonical example of broken spatial translational symmetry. Chapter 2 treats time crystals in closed quantum systems: the origin of the idea in Wilczek's model and its refutation by the no-go theorems, the Floquet framework for periodically driven systems, the definition of discrete time crystals, and their realization as a π-spin-glass phase in many-body-localized spin systems. Chapter 3 develops the theoretical toolbox for open quantum systems that the rest of the thesis requires: the GKSL

master equation, the Liouville-space formulation, the spectral properties of the Liouvillian, Floquet theory for open systems, and the role of symmetries in open dynamics. Chapter 4 then surveys the open-system time-crystal zoo: discrete time crystals in open systems (including the instructive case of a single dephasing spin-s); continuous time crystals and continuous quasi time crystals (including the driven–dissipative collective spin and two coupled driven–dissipative collective spins); and time glasses (including discrete quasi time crystals and the kicked–dissipative collective-spin model).

Chapter 1

Spontaneous symmetry breaking in quantum physics

This first chapter sets the conceptual stage for the whole thesis. We begin by reviewing the notion of symmetry in quantum physics, from the basic group-theoretic language to the distinction between continuous and discrete symmetries and their realization in quantum mechanics. We then turn to spontaneous symmetry breaking, introducing its essential ingredients: the thermodynamic limit, the order parameter, and the stability of symmetry-broken states. The harmonic crystal serves as the guiding example of a broken spatial translational symmetry. The objective is to build the framework that will later allow us to interpret a time crystal as the spontaneous breaking of time translation symmetry.

1.1 Symmetry in quantum physics

Time crystals are remarkable quantum many-body systems that spontaneously break time-translation symmetry. To fully comprehend this intriguing phenomenon, one must first develop a rigorous understanding of symmetry within the framework of quantum physics. In particular, the focus will be placed on the role of symmetry in many-body quantum systems, introducing the essential concepts required to define and characterize time crystals hereafter. Consequently, this discussion will not delve into the broader aspects of symmetry encountered in particle physics, but rather remain centered on the principles most relevant to condensed matter and quantum many-body theory.
The notion of symmetry applies to two distinct but related aspects of a quantum system. First, symmetry can be defined by how the Hamiltonian of the system remains invariant under certain transformations. Second, symmetry also governs the behavior of the system's states. This is typically described by how the Hamiltonian and the states transform under the action of a symmetry operation. A crucial point of discussion involves the mathematical structure underlying these symmetry transformations, which are formally described using groups.

1.1.1 Basic notion of group theory

Group A group $\mathbb{G}$ is a set of elements equipped with an internal binary operation defined everywhere

$$\times : \mathbb{G} \times \mathbb{G} \to \mathbb{G},$$

fulfilling the following properties:

1. The operation $\times$ is associative

$$\forall a, b, c \in \mathbb{G} : a \times (b \times c) = (a \times b) \times c.$$

2. The existence of a (unique) neutral element denoted by e

$$\forall a \in \mathbb{G} : a \times e = e \times a.$$

3. $\mathbb{G} \neq \{0\}$ and every non-zero element have an inverse

$$\forall a \in \mathbb{G}/\{0\}, \exists b \in \mathbb{G} : a \times b = e = b \times a.$$

Moreover, a group $\mathbb{G}$ is said to be abelian (or commutative) if

$$\forall a, b \in \mathbb{G} : a \times b = b \times a.$$

If not, the group is non-abelian (or non-commutative) [41].

Groups are abstract mathematical concepts that consist of elements defined only by the way they can be multiplied together under a very general operation. Thus, it is relevant to introduce the concept of representation.
A representation of a group $\mathbb{G}$ is a homomorphism that maps a group element $g \in \mathbb{G}$ into a linear operator G acting on a vector space V such that $\forall g, g' \in \mathbb{G}$, one has [42]

$$G(g \times g') = G(g)G(g').$$

It is straightforward to notice that the set of operators homomorph to the group is also a group equipped with the operation of linear operator multiplication. Moreover, if the dimension n of the vector space V is finite, given a basis of V, the elements of the group can be represented by a matrix $n \times n$. One will see in the following section that, in quantum physics, symmetry transformations are represented by unitary or anti-unitary operators acting on the Hilbert space of the system under study, and they will have the mathematical structure of a group. Consequently, one will henceforth consider that a group element is a linear operator.

A group is either continuous or discrete. Continuous group can be parametrized by one or more real continuous parameter whereas it is not the case for a discrete group. The number of elements in a group is called the order of the group. The order of a group may be finite, infinite but enumerable or infinite non-enumerable. A discrete group is finite or infinite enumerable whereas a continuous group is infinite non-enumerable. Moreover, the vast majority, at least those of interest in this work, of continuous groups that occur in quantum physics are called Lie groups.

Lie group A Lie group is a continuous group with the structure of a differentiable manifold [43]. The elements of the group vary smoothly when the continuous parameters are varied.g Intuitively, it represents a set of elements that can be connected continuously to one another. The number of parameters that describe a Lie group is called the dimension of the group. Thus, if an operator $G(\alpha_1, .., \alpha_N)$ represents an element of a n dimensional Lie group, it can be expanded such that

$$G(\alpha_1, .., \alpha_N) = I + i\alpha_1 G_1 + i\alpha_2 G_2 + ... + i\alpha_N G_N + \mathcal{O}(\alpha_1^2, ..., \alpha_N^2),$$

where $G_1, ..., G_N$ are the generators of the Lie algebra. The dimension of a group is therefore the number of generators that constitute it. Moreover, when the parameters $\alpha_1, ..., \alpha_N$ are infinitesimal, it is sufficient to retain only the first-order terms in the expansion above. Thus, any Lie group element $G(\alpha_1, .., \alpha_N)$ characterized by finite (non-infinitesimal) parameters $\alpha_1, ..., \alpha_N$ can be seen as the limit of an infinite composition of infinitesimal elements of the group such that

$$G(\alpha_1, .., \alpha_N) = \lim_{k \to \infty} \left(I + \sum_{i=1}^{N} \frac{\alpha_i}{k} G_i \right)^k = e^{i(\alpha_1 G_1 + ... + \alpha_N G_N)}. \tag{1.1}$$

Thus, every element of a Lie group can be represented as an exponential with the continuous parameters and the generators as arguments. The commutator between two generators, characterizing a Lie group, is a linear combination of other generators

$$[G_a, G_b] = i \sum_c f_{abc} G_c,$$

where f_{abc} are real structure constants. Of course, if a Lie group is abelian, its structure constants are zero. The set of generators associated with a Lie group forms a vector space. Thus, the vector space spanned by the generators with the extra operation of commutation is called the Lie algebra[1]. The Lie algebra is completely described by its structure constants, as the commutators of all generators are linear combinations of the generators, with coefficients given by these constants, which entirely determine the algebraic relations.

Discrete group In contrast to Lie groups, a discrete group $\mathbb{G}$ is a group where the underlying set is equipped with the discrete topology. This implies that every element is isolated from each other. Intuitively, it means that there exists a neighborhood around each elements that contains no other element of the group. Consequently, elements of a discrete group cannot be reached from the identity via a continuous variation of parameters, and the concept of a generator in the infinitesimal sense does not exist. Instead, a discrete group $\mathbb{G}$ of order n is characterized by a set of discrete generators

$$\mathbb{G} = \{G_1, G_2, \ldots, G_n\},$$

which are themselves linear operators within the group. Every element of $\mathbb{G}$ can be expressed as a finite product of these generating operators and their inverses. While the structure of a Lie group is determined by the commutators of its Lie algebra, a discrete group is defined by its presentation: a set of algebraic relations R of the form [45]

$$R(G_1, \ldots, G_n) = I.$$

These relations dictate how the generating operators commute or combine. For instance, the relation $G_1 G_2 G_1^{-1} G_2^{-1} = I$ is the discrete equivalent of a vanishing commutator, indicating that the operators G_1 and G_2 commute. Similarly, a relation such as $G_1^2 = I$ indicates that the operator G_1 is its own inverse, a common feature of parity or reflection operators in quantum mechanics.

Groups appear naturally in quantum physics. Here are a few examples that can be found:

- The unitary group $U(n)$ is a Lie group of dimension n^2. It is the set of matrices in $\mathbb{C}_n^n$ satisfying the following relation:

  $$MM^\dagger = I = M^\dagger M \quad \Leftrightarrow \quad M \in U(n).$$

  For $n = 1$, the elements of $U(1)$ are $e^{i\phi}$ with ϕ a real continuous parameter. It is an abelian group. For instance, all physical states are invariant under the action of an element of $U(1)$. For $n > 1$, $U(n)$ is no longer abelian.

[1] An algebra is simply a vector space V over a field $\mathbb{K}$, with an extra operation $\times$ called algebra multiplication which is bilinear, satisfying the following properties $\forall a, b \in \mathbb{K}$ and $\forall \mathbf{x}, \mathbf{y}, \mathbf{z} \in V$ [44]:

$$(\mathbf{x} + \mathbf{y}) \times \mathbf{z} = \mathbf{x} \times \mathbf{z} + \mathbf{y} \times \mathbf{z} \qquad \mathbf{x} \times (\mathbf{y} + \mathbf{z}) = \mathbf{x} \times \mathbf{y} + \mathbf{x} \times \mathbf{z}$$

$$(a\mathbf{x}) \times \mathbf{y} = a(\mathbf{x} \times \mathbf{y}) \qquad \mathbf{x} \times (b\mathbf{y}) = b(\mathbf{x} \times \mathbf{y})$$

.

- The special unitary group $SU(2)$ is a subgroup of the unitary group $U(2)$. It is the set of complex 2×2 unitary matrices with determinant equal to one. The three generators T_i of this group are

$$T_1 = \frac{i}{2}\sigma_x \qquad T_2 = \frac{i}{2}\sigma_y \qquad T_3 = \frac{i}{2}\sigma_z,$$

  where σ_x, σ_y and σ_z are the Pauli matrices. Thus, the dimension of the group is three and it is clearly a non-abelian group. $SU(2)$ describes spin rotation.

- The continuous translation group $(\mathbb{R}^n, +)$ equipped with the vector addition is a Lie group that is abelian. Its dimension is n. It acts on a point $x \in \mathbb{R}^n$ as

$$T_n(a) : x \mapsto x + a,$$

  where $a \in \mathbb{R}^n$ consists of continuous parameter of same values.
  For instance, time translation transformation has the mathematical structure of the group $(\mathbb{R}, +)$ whereas space translation transformation has the mathematical structure of the group $(\mathbb{R}^3, +)$.
  The discrete translation group $(\mathbb{Z}_l^n, +)$, where l is the number of elements in the group, is obtained by restricting the continuous translation group to a discrete subset. It is abelian and has no longer the structure of a Lie group. An element of this group has the same action of an element of the continuous translation group except that it is described by discrete parameters. A fundamental discrete group is the parity group $Z_2 = \{I, S\}$, defined by the single relation $S^2 = I$. This group characterizes symmetries where an operator S is its own inverse, such as the Ising symmetry or spatial parity. While translation groups $(\mathbb{R}^n, +)$ and $(\mathbb{Z}^n, +)$ usually describe shifts in space or time, the Z_2 group represents the simplest discrete reflection, acting as a "flip" on the state space. For instance, in an Ising system, it maps a spin state $|\uparrow\rangle$ to $|\downarrow\rangle$ and conversely.

1.1.2 Definition of symmetry

In a closed non-relativistic quantum system, the time evolution of a vector $|\psi(t)\rangle$, which describes the state of the system at time t, can be determined by solving the Schrödinger equation:

$$i\hbar \frac{d\,|\psi(t)\rangle}{dt} = H\,|\psi(t)\rangle\,, \tag{1.2}$$

where H is the Hamiltonian operator characterizing the dynamical behavior of the system under study. The latter is therefore the key element in the equation of motion (1.2), and can be used to define what constitutes a symmetry of the system. Moreover, since a main purpose when studying a particular system is to know the time evolution of its state, one can also define the notion of symmetry of a state in quantum physics. Unless otherwise stated, the content of this section is based entirely on Ref. [2].

Firstly, it is relevant to define what is called a symmetry in quantum theory: a symmetry is a transformation that preserves transition probabilities $|\langle\psi|\phi\rangle|^2$ between physical states $|\psi\rangle$ and $|\phi\rangle$. Additionally, Wigner's theorem informs us that any symmetry in a quantum system must be represented either by a unitary or an anti-unitary operator [46]. An operator U is said to be unitary if it satisfies $U^\dagger U = UU^\dagger = \mathbb{I}$. Thus, it is straightforward to derive the relation $\langle U\psi|U\phi\rangle = \langle\psi|\phi\rangle$, and the transition probability between two physical states $|\psi\rangle$ and $|\phi\rangle$ is therefore conserved when they are transformed by U. On the other hand, A is anti-unitary if it satisfies the relation $\langle A\psi|A\phi\rangle = \langle\psi|\phi\rangle^*$. As for a unitary operator, the transition probability between two physical states is preserved by the action of A thanks to this definition. Moreover, every anti-unitary operator can be decomposed as a product of a complex conjugation operator K, satisfying $K^2 = I$, and a unitary operator U.

One can therefore examine what makes a state symmetric and the resulting consequences. The symmetry of states can be defined as follows:

Definition. A state $|\psi\rangle$ is said to be symmetric under a unitary or an anti-unitary operator transformation U if it only acquires a relative phase factor, i.e., $U|\psi\rangle = e^{i\varphi}|\psi\rangle$.

In other words, if $|\psi\rangle$ is symmetric under U, then it is an eigenvector of U. The appearance of a phase factor has no effect as long as we remember that two state vectors differing by a phase factor describe the same physical state. To go a bit further into the previous definition, one might notice that if every physical state of a system is symmetric under an operator U, the operator is none other than an element of the group $U(1)$. This result is trivial, and one will therefore not consider this kind of symmetry transformation. Thus, the fact that a state $|\psi\rangle$ is symmetric under U is relevant when there exist other states that do not satisfy the definition above. Furthermore, the definition may be generalized for system states characterized by a density operator ρ. In this case, ρ is said to be symmetric under a unitary or anti-unitary operator U if their commutator vanishes.

One may now define what a symmetry of a system is by looking at its Hamiltonian. It is well known that an operator A acting on the Hamiltonian H of a system such that $A^\dagger HA = H$ is said to leave H invariant. We can rewrite the latter relation as $[A, H] = 0$, which means that A commutes with H. Thus, we define the symmetry of Hamiltonians as follows:

Definition. A unitary or anti-unitary operator U is a symmetry of the Hamiltoninan H if their commutator vanishes, i.e, $[U, H] = 0$.

Following the definition above, the operators U and H commute if and only if it is possible to find a complete basis of eigenvectors common to these two operators. Similarly, if $|\psi\rangle$ is an eigenstate of H associated with the eigenvalue E_ψ, then $U|\psi\rangle$ is also an eigenstate of H:

$$H(U|\psi\rangle) = U(H|\psi\rangle) = U(E_\psi|\psi\rangle) = E_\psi(U|\psi\rangle). \tag{1.3}$$

Based on this relation, we can notice an interesting property. If $|\psi\rangle$ is symmetric under U, then $U|\psi\rangle$ is the same physical state as $|\psi\rangle$, following the definition of a symmetric state. If $|\psi\rangle$ is not symmetric under U, $U|\psi\rangle$ must be a different eigenstate of H associated with the same eigenvalue E_ψ. Thus, applying U successively on $|\psi\rangle$ gives all the degenerate eigenstates of H associated with a certain eigenvalue[2]. A superposition of these degenerate eigenstates generated by U can be constructed to form a symmetric state invariant under U.

The set of all unitary operators acting on a Hilbert space $\mathcal{H}$ forms the unitary group, denoted as $U(\mathcal{H})$[3]. This group represents the most general class of transformations that preserve transition probabilities of the quantum system. For a finite-dimensional Hilbert space of dimension n, $U(\mathcal{H})$ is equivalent to the Lie group $U(n)$. In practice, the symmetry group $\mathbb{G}$ specific to a given physical system is usually a subgroup of $U(\mathcal{H})$. While $U(\mathcal{H})$ contains every possible symmetry transformation, the symmetry group $\mathbb{G}$ consists only of those operators that commute with the Hamiltonian H. If $\mathbb{G}$ is a continuous subgroup, its elements can be expressed via the exponential relation (1.1) using the generators of its associated Lie algebra. Conversely, if $\mathbb{G}$ is a

[2]This is the case only if H possesses no other symmetries.

[3]We focus here on the characterization of unitary operators only, since no anti-unitary operators appear in this master's thesis.

discrete subgroup, its elements are defined by discrete generators and algebraic relations. In the case where $\mathcal{H}$ is infinite-dimensional, $U(\mathcal{H})$ loses its structure as a finite-dimensional Lie group. However, for any continuous one-parameter symmetry, an element can still be represented in the exponential form according to Stone's theorem [47].

1.1.3 Continuous and discrete symmetry

In classical physics, when a system possesses a continuous symmetry, Noether's theorem asserts the existence of a conserved quantity. For instance, invariance under continuous time translation corresponds to the conservation of the system's energy. Noether's theorem also applies in quantum physics. However, one must distinguish between continuous and discrete symmetries, as they are physically distinct, and the theorem cannot be applied directly to the latter.

If an observable represented by a hermitian operator Q commutes with the Hamiltonian H of a system, its expectation value $\langle Q\rangle = \langle\psi(t)|\, Q\, |\psi(t)\rangle$ remains constant in time. This is evidenced by the time evolution equation of $\langle Q\rangle$:

$$\frac{d}{dt}\langle Q\rangle = \frac{1}{i\hbar}\langle[Q,H]\rangle + \left\langle\frac{\partial Q}{\partial t}\right\rangle, \tag{1.4}$$

which shows that $\langle Q\rangle$ is a constant of motion when Q has no explicit time dependence and commutes with H. In this framework, Q is referred to as the generator of the continuous symmetry transformation. The corresponding unitary transformation is expressed as:

$$U(\varepsilon) = e^{i\varepsilon Q}, \tag{1.5}$$

where ε is a real continuous parameter. While such operators are always well-defined in finite dimensions, Stone's theorem ensures that even in infinite-dimensional Hilbert spaces, any strongly continuous one-parameter unitary group is uniquely generated by a self-adjoint operator Q [47]. For example, a time-independent Hamiltonian H is a conserved quantity that generates continuous time translation symmetries via the time evolution propagator $U(t) = e^{-iHt/\hbar}$.

In contrast to the continuous case, a discrete symmetry cannot be parametrized by a real continuous parameter. Consequently, Noether's theorem, which establishes a conserved quantity for every continuous symmetry, does not directly apply. In such cases, the symmetry is represented by a specific unitary operator rather than an infinitesimal generator.
A primary example is found in Floquet systems, where the Hamiltonian possesses a discrete time-translation symmetry, $H(t+nT) = H(t)$ for $n \in \mathbb{Z}$, with T being the driving period. Here, the instantaneous Hamiltonian $H(t)$ is not a conserved quantity and does not generate the symmetry. Instead, the symmetry transformation is described by the Floquet operator U_F, which evolves the system over one full period. While U_F is a discrete symmetry operator, it can be mathematically associated with an effective Hamiltonian H_F (called the Floquet Hamiltonian) via the relation [48]

$$U_F = e^{-iH_F T/\hbar}. \tag{1.6}$$

In this context, H_F serves as the stroboscopic version of a Hamiltonian. It describes the evolution from one period of the driving to the next, even though it does not capture the continuous dynamics within the period itself. While energy is not conserved in such a driven system, a related quantity emerges. The quasi-energies are the eigenvalues of H_F, and they are conserved modulo $\hbar\omega$ with $\omega = 2\pi/T$ is the driving frequency. This periodicity in the quasi-energy spectrum is the discrete analogue of energy conservation.

1.1.4 Symmetry in quantum systems

The concept of symmetry in quantum physics being introduced, several many-body quantum systems exhibiting noteworthy properties. These include the harmonic crystal, as well as the Ising model and the Heisenberg model. These systems possess special symmetries, categorized as spatial symmetries (which involve transformations of physical coordinates like rotations or translations) or internal symmetries (which involve transformations of intrinsic properties like spin or charge in an abstract state space). These symmetries will play an important role in later discussions on spontaneous symmetry breaking and time crystals.

The harmonic crystal

A crystalline solid is described by a Hamiltonian that is homogeneous in space, reflecting a continuous translational space symmetry, since the Hamiltonian remains unchanged under arbitrary spatial shifts. For simplicity, we will consider a one-dimensional crystal, which allows us to capture the essential physics while keeping the mathematics straightforward. The latter can be viewed as an harmonic crystal characterized by the following Hamiltonian:

$$H = \sum_{j=1}^{N} \frac{p_j^2}{2m} + \frac{\kappa}{2} \sum_{j=1}^{N-1} (x_j - x_{j+1})^2, \tag{1.7}$$

where N is the number of atoms in the crystal [49]. The atom j of the crystal has a mass m, a momentum p_j and a position x_j. The harmonic potential between neighboring atoms is parametrized by κ. The crucial point to notice about this Hamiltonian is that it commutes with the total momentum operator $p_{\text{tot}} = \sum_j p_j$. Indeed, one has

$$[H, p_{\text{tot}}] = \sum_j \sum_{j'} \frac{[p_j^2, p_{j'}]}{2m} + \frac{\kappa}{2} \sum_j \sum_{j'} [(x_j - x_{j+1})^2, p_{j'}] = 0.$$

The first term on the right-hand side clearly vanishes. The second term also vanishes when expanding the quadratic term and using the canonical commutation relation $[x_j, p_{j'}] = i\hbar\delta_{j,j'}$ and the product rule for commutators[4], each contribution cancels out. The total momentum operator p_{tot} is a conserved quantity in the system and it is the generator of spatial translation symmetry. Thus, the Hamiltonian commutes with the unitary operator $U(x) = e^{-ip_{\text{tot}}x/\hbar}$ which is the space propagator over a distance x, i.e. the one-dimensional harmonic crystal thus possesses a continuous translational symmetry described by the group $(\mathbb{R}, +)$. Physically, it means that the crystal has the same properties everywhere in space.

Furthermore, the crystal is in its ground state when it is at rest (without considering the quantum vibrations of its atoms), i.e. when $p_{\text{tot}} = 0$. According to Heisenberg's uncertainty principle, a state with a well-known total momentum must have a completely uncertain center-of-mass position. In other words, the lowest energy state of the crystal is a wave function that extends over all of space. Clearly, such a delocalized state does not correspond to the kind of ground state we would expect for a piece of matter in the macroscopic world. One will see why crystals in our everyday world are perfectly localized thanks to spontaneous symmetry breaking in section 1.2.4.

Heisenberg and Ising models

The Heisenberg model is a fundamental quantum mechanical model in statistical physics that describes magnetic materials by treating the spin magnetic moment at each lattice site as a

[4] The product rule for commutators is

$$[AB, C] = A[B, C] + [A, C]B,$$

with A, B and C being linear operators.

vector that can point in any direction in three-dimensional space [50]. The Hamiltonian of this model is

$$H_H = -J \sum_{\langle i,j \rangle} \mathbf{S}_i \cdot \mathbf{S}_j, \tag{1.8}$$

where the constant J is the exchange interaction between two spins i and j and the symbol $\langle i,j \rangle$ denotes a sum over nearest neighbors. The sum can be taken over a lattice of one, two or three dimensions. For spin-1/2's, the spin operators $\mathbf{S}_i$ are given by the Pauli matrices as $\mathbf{S}_i = \hbar/2(\sigma_i^x, \sigma_i^y, \sigma_i^z)$. The Hamiltonian (1.8) has SU(2) rotational symmetry, or equivalently, is invariant under global spin rotation. Thus, one has

$$[S^x_{\text{tot}}, H_H] = 0, \qquad [S^y_{\text{tot}}, H_H] = 0, \qquad [S^z_{\text{tot}}, H_H] = 0,$$

where $S^\alpha_{\text{tot}} = \sum_i S^\alpha_i$ with $\alpha = \{x, y, z\}$. It is straightforward to show that the commutators vanish given the commutation relation $[S^\alpha_i, S^\beta_j] = i\hbar\varepsilon_{\alpha\beta\gamma} S^\gamma_i \delta_{i,j}$ and the product rule for commutators. Therefore, S^x_{tot}, S^y_{tot} and S^z_{tot} are conserved quantities of the system and are the generators of spin rotation symmetries of this system. It follows that the Heisenberg Hamiltonian also commutes with the operator $\mathbf{S}^2 = \sum_i \mathbf{S}_i \cdot \mathbf{S}_i$:

$$[H, \mathbf{S}^2] = 0.$$

It should be noted that this system could be affected by an external magnetic field, which would modify its dynamics. It is therefore necessary to add the effect of this external influence to Heisenberg's previous model by

$$H = -J \sum_{\langle i,j \rangle} \mathbf{S}_i \cdot \mathbf{S}_j - \mathbf{h} \cdot \sum_i \mathbf{S}_i, \tag{1.9}$$

where $\mathbf{h} = (h_x, h_y, h_z)$ represents the strength of the external magnetic field in each spatial direction. In this situation, the SU(2) symmetry of the Heisenberg model is explicitly broken, so that the system is no longer invariant under a global spin rotation.

A related model is the Ising model, in which the spin-1/2 can only point in two opposite directions [50]. Thus, we only consider one component of the spin, conventionally the z component. The Hamiltonian of this model is

$$H_I = -J \sum_{\langle i,j \rangle} \sigma_i^z \sigma_j^z, \tag{1.10}$$

where the constants $\hbar/2$ have been absorbed into the exchange interaction J. The Hamiltonian of the Ising model is invariant under global spin inversion:

$$\sigma_i^z \to -\sigma_i^z,$$

for all spins of the lattice. This symmetry transformation is described by the unitary operator:

$$X = e^{-i\frac{\pi}{2}\sigma^z_{\text{tot}}} = \prod_i \sigma_i^x,$$

where $\sigma^z_{\text{tot}} = \prod_i \sigma_i^z$ is the global spin operator of the system, constructed from the local spin operators. Since $X^2 = \mathbb{I}$, this system has therefore a $\mathbb{Z}_2$-symmetry (also called Ising symmetry) represented by the symmetry transformations $\{\mathbb{I}, X\}$. Similarly to the Heisenberg model, this kind of system may be submitted to an external magnetic field. The Hamiltonian then reads

$$H = -J \sum_{\langle i,j \rangle} \sigma_i^z \sigma_j^z - h \sum_i \sigma_i^\alpha. \tag{1.11}$$

If $\alpha = z$, the external field is longitudinal and the Ising symmetry is explicitly broken whereas if $\alpha = \{x, y\}$ the external field is transverse and the Ising symmetry is preserved. Furthermore, in the latter case, if the spins in the lattice interact through an infinite-range coupling, the equation (1.11) represents the Hamiltonian of the Lipkin-Meshkov-Glick (LMG) model [51].

The systems introduced previously are ordered, meaning that all parameters characterizing them are well defined. However, one may render these systems disordered by allowing their parameters to be random. For instance, the Hamiltonian (1.11) with randomly distributed spin exchange interactions and local magnetic fields,

$$H = -\sum_{\langle i,j \rangle} J_{ij}\, \sigma_i^z \sigma_j^z + \sum_i h_i\, \sigma_i^\alpha, \tag{1.12}$$

describes a disordered quantum spin system [52]. The interaction strength J_{ij} between neighboring spins now depends on the specific pair of spins (i, j), and each spin is subject to a local magnetic field h_i whose intensity and direction vary randomly from one site to another. Such disordered spin systems will prove extremely useful in the study of the emergence of time crystallinity in closed quantum systems.

1.2 Spontaneous symmetry breaking

This section introduces the concept of spontaneous symmetry breaking (SSB), which plays a central role in understanding time crystals, as these systems spontaneously break time-translation symmetry. SSB explains why certain systems can exist in a non-symmetric state at equilibrium. We will focus on the most relevant aspects of SSB regarding spatial and internal symmetries in quantum many-body systems, outlining foundational concepts such as the thermodynamic limit, the order parameter, and the mathematical tools used to detect its occurrence. Throughout this section, one-dimensional many-body systems, such as one-dimensional crystals, will serve as concrete examples. While one-dimensional systems with short-range interactions cannot exhibit SSB at any finite temperature[5] ($T > 0$ K), and therefore do not display it in practice, they provide a mathematically accessible framework and an intuitive interpretation of the phenomenon. Consequently, we will operate within the traditional framework of closed quantum systems at absolute zero temperature, where SSB in one-dimensional systems remains theoretically possible. Unless otherwise stated, the content of this section is based entirely on Ref. [2].

A system described by a Hamiltonian that is invariant under a unitary transformation typically admits a symmetric equilibrium state. Indeed, in quantum mechanics, such a symmetric system either possesses a unique symmetric groundstate or a degenerate manifold of groundstates. In this section, we focus on systems with a unique symmetric ground state and do not address the case of a degenerate ground-state manifold, as its analysis requires a deeper treatment of SSB and is not relevant to our discussion. Nevertheless, in everyday experience, one rarely encounters perfectly symmetric objects. The question of how systems settle into stable states that appear to violate the underlying symmetries is explained by the phenomenon of spontaneous symmetry breaking.

Definition. Spontaneous symmetry breaking (SSB) is the phenomenon in which a stable state of a system is not symmetric under a symmetry of its Hamiltonian.

[5] In 1D and 2D systems with continuous symmetry and short-range interactions, the Mermin-Wagner theorem dictates that thermal fluctuations prevent the establishment of long-range order at any finite temperature [53–55]. For 1D systems with discrete symmetries and short-range interactions, spontaneous symmetry breaking is forbidden because of the dominant entropic effect at finite temperature, whereas in 2D systems, SSB can occur. [55, 56]

More broadly, when the stable state of a system $|\psi\rangle$ is not left invariant under a symmetry transformation U that commutes with the Hamiltonian, the system is said to have spontaneously broken the symmetry. A complete set of distinct symmetry-broken states with the same energy can be defined by successively applying U to $|\psi\rangle$, since each application generates a different state according to the definition of a symmetric state given in section 1.1.2. For instance, a solid is invariant under spatial translations, while being truly localized in space. Translating the solid to another localized position yields a distinct state of the solid, yet with the same energy. The set of all these inequivalent but degenerate states corresponds to the solid being localized at all possible positions. Moreover, the collection of degenerate stable broken-symmetry state must be invariant under symmetry transformations that form a subgroup of the symmetry group of the system. Returning to the example of the solid, whereas the states above concern the solid as a whole, its internal periodic structure is left invariant by the discrete subgroup of lattice translations of the continuous translation group. The continuous symmetry is thus not destroyed but reduced to a discrete one, which is precisely the mechanism behind discrete time crystals.

The goal now is to explain how the stable state of a system may spontaneously break the symmetry of the system. The general idea behind SSB is easily formulated: as a collection of quantum mechanical particles grows larger, the object as a whole becomes ever more unstable against small perturbations. In the end, for infinite large system, even an infinitesimal perturbation is enough to cause the collective system to break the underlying symmetry of the Hamiltonian. In fact, SSB arises from the emergence of a singularity in the thermodynamic limit.

1.2.1 The thermodynamic limit

The thermodynamic limit is a mathematical tool used to describe macroscopic systems by considering them as infinitely large while keeping their average density constant. Formally, it corresponds to taking the number of particles N and the volume V of the system to infinity while maintaining a fixed particle density ρ:

$$N \to \infty, \qquad V \to \infty, \qquad \rho = \frac{N}{V} = \text{constant}. \tag{1.13}$$

In this limit, intensive quantities such as density or temperature remain constant, whereas extensive quantities like entropy or particle number grow without bound.

The singular nature of the thermodynamic limit is the reason why SSB can occur. Indeed, the physics of an infinitely large system is qualitatively distinct from that of any finite system, no matter how large. In the thermodynamic limit, symmetry-broken states become orthogonal to one another and degenerate eigenstates with the symmetric ground state of the Hamiltonian. This singular behavior can be expressed through the non-commutativity of limits involving a physical quantity O, called the order parameter, that measures the degree of symmetry breaking of a state. Consider a many-body system that possesses a certain symmetry and add to its Hamiltonian an external perturbation, controlled by a parameter h, which explicitly breaks this symmetry. Let $O(|\psi\rangle, N, h)$ be the observable chosen to characterize the symmetry properties of the system. It depends on the system size N, the control parameter h, and the ground state $|\psi\rangle$ of the perturbed system. If spontaneous symmetry breaking occurs, the limits $\lim_{N\to\infty}$ and

$\lim_{h\to 0}$ do not commute:

$$\lim_{N\to\infty}\lim_{h\to 0} O(|\psi\rangle, N, h) = 0, \tag{1.14}$$

$$\lim_{h\to 0}\lim_{N\to\infty} O(|\psi\rangle, N, h) \neq 0. \tag{1.15}$$

The first expression shows that for any finite system, the ground state remains symmetric when the perturbation is exactly zero. The second shows that if the system is made macroscopic before removing the perturbation, the system remains trapped in a symmetry-broken state, revealing the singular character of the thermodynamic limit. Thus, these non-commuting limits imply that considering larger and larger many-body systems, a weaker and weaker perturbation must provoke the spontaneous broken symmetry. Moreover, the singular nature of the thermodynamic limit merely requires that the two limits do not commute, that is, that they yield different values depending on the order in which they are taken. The specific results obtained in Eqs. 1.15, namely zero versus a nonzero value, are only one particular instance of this.

SSB is a phenomenon that can be rigorously defined only in the thermodynamic limit. Only in this limit do the symmetric ground state and the symmetry-breaking states become exactly degenerate, allowing the system to occupy one of the symmetry-breaking states. Consequently, it is only in the thermodynamic limit that a symmetry-breaking state becomes an eigenstate of the Hamiltonian and can be regarded as the true ground state of the system. In finite systems, the ground state is unique and symmetric, as required by the symmetry of the Hamiltonian. If the system is found in a non-symmetric state, there always exists a finite tunneling probability between the different configurations, preventing any of them from being truly stable. For sufficiently large systems, however, the situation changes qualitatively. The overlap between a symmetry-broken state and the exact symmetric ground state becomes exponentially small as the number of particles increases, while the tunneling time between degenerate macroscopic configurations grows exponentially with system size (the gap Δ decreases exponentially). As a consequence, these non-symmetric states behave as effectively stable and become quasi-degenerate with the true ground state on all experimentally relevant timescales, thereby representing the physical states observed in practice and being regarded as the ground state of the system. Meanwhile, the exact symmetric ground state becomes increasingly unstable as the system size grows. This can be understood by noting that, in a finite system, the true ground state $|0\rangle$ is a superposition of a non-symmetric state $|\sigma\rangle$ and its symmetry-transformed partners $U|\sigma\rangle$. For sufficiently large systems, any arbitrarily small perturbation (for instance, due to the environment) will drive the system out of this symmetric superposition and into one of the symmetry-broken configurations that will therefore be considered stable.

Let us take the example of a one-dimensional chain of N spin-1/2 particles characterized by the Ising Hamiltonian introduced earlier:

$$H = -J\sum_{i=1}^{N-1}\sigma_i^z\sigma_{i+1}^z - h\sum_{i=1}^{N}\sigma_i^x, \tag{1.16}$$

with $0 < h \ll J$. This system possesses a global $\mathbb{Z}_2$-symmetry, represented by the operator X introduced in section 1.1.4. Hence, the eigenstates of the system must also be eigenstates of X with eigenvalues ± 1. The eigenstates consequently come in pairs of cat states $|+\rangle$ and $|-\rangle$. For example, it can be the states $|+\rangle \approx \frac{1}{\sqrt{2}}(|\uparrow\uparrow\ldots\rangle + |\downarrow\downarrow\ldots\rangle)$ and $|-\rangle \approx \frac{1}{\sqrt{2}}(|\uparrow\uparrow\ldots\rangle - |\downarrow\downarrow\ldots\rangle)$[6]. The energy splitting between this pair is given by $\Delta = E_+ - E_-$ and scales as $\Delta \sim e^{-N/\xi}$, with ξ a characteristic length. As we move toward the thermodynamic limit, the energy splitting Δ

[6]These approximations are very accurate as soon as one considers $0 < h \ll J$.

vanishes exponentially. In this limit, the states $|+\rangle$ and $|-\rangle$ become perfectly degenerate. It allows for the existence of a non-symmetric ground state, as any linear combination of the degenerate pair is now a valid stationary state of the system in the thermodynamic limit. Indeed, the tunneling time τ between symmetry-broken states diverges as $\tau \sim \Delta^{-1}$. This transition marks the point where SSB becomes physically possible, as the system can remain trapped in a state that no longer reflects the full symmetry of the Hamiltonian.

In conclusion, SSB occurs strictly only in the thermodynamic limit, since finite systems require a small external perturbation to select a symmetry-broken state. This limit captures the emergent macroscopic behavior of large but finite systems with remarkable accuracy. It thus provides the appropriate framework for a rigorous description of SSB. For this reason, in what follows we shall adopt the thermodynamic limit as our working setting. Furthermore, the method presented above based on non-commuting limits is a very effective way to reveal the occurrence of SSB in many-body systems. However, simpler tools can also be employed to highlight SSB of global symmetries, such as the two-point correlation function or the cluster decomposition property.

1.2.2 The order parameter

In statistical mechanics, an order parameter acts as a diagnostic tool to distinguish two different phases of matter. In the context of SSB, the two different phases to distinguish are the phase when the stable state of the system is symmetric and the phase when the stable state of the system is non-symmetric. In quantum mechanics, one may define a local observable $\mathcal{O}(x)$ called the order parameter operator, whose expectation value gives the local order parameter $O(x)$:

$$O(x) = \langle\psi|\mathcal{O}(x)|\psi\rangle\,, \tag{1.17}$$

This quantity must have different values depending on whether the state $|\psi\rangle$ is symmetric or not. Indeed, a definition of the order parameter can be

$$O(x) = 0 \text{ if } |\psi\rangle \text{ is symmetric,}$$
$$O(x) \neq 0 \text{ if } |\psi\rangle \text{ is non-symmetric.}$$

The central idea behind the order parameter is that it must take different values depending on whether the state in question is symmetric or not, in order to distinguish between them. While the local order parameter $O(x)$ gives information about the symmetry breaking at a certain position, the global order parameter O can be defined to exhibit the broken symmetry of the whole system:

$$O = \langle\psi|\mathcal{O}|\psi\rangle\,,$$

where $\mathcal{O}$ is defined as

$$\mathcal{O} = \int_V \mathcal{O}(x)d^3x.$$

Thus, computing the order parameter in the ground state of the system must indicate the emergence of SSB. Another effective way to detect SSB is through the analysis of the two-point correlation function, which captures how local observables are correlated across the system:

$$C(x,x') = \langle\psi|\mathcal{O}^\dagger(x')\mathcal{O}(x)|\psi\rangle\,, \tag{1.18}$$

or equivalently, the correlation function can be defined in terms of the global order parameter operator $\mathcal{O}$:

$$C = \frac{\langle\psi|\mathcal{O}^\dagger\mathcal{O}|\psi\rangle}{V^2} \tag{1.19}$$

The behavior of the two-point correlation function can be classified into two distinct categories[7]:

$$\lim_{|x-x'|\to\infty}\lim_{V\to\infty} C(x,x') \propto \begin{cases} f(x-x') & \text{long-range ordered/crystalline ordered} \\ e^{-|x-x'|/l} & \text{disordered} \end{cases} \tag{1.20}$$

where $f(x-x')$ is a non-zero constant if the system exhibits long-range order, or a periodic function if it exhibits crystalline order. The length scale l is called the correlation length and for long-range ordered or crystalline ordered system, it must diverge. If a state $|\psi\rangle$ is long-range ordered or crystalline ordered, it breaks the symmetry of the system. In fact, the two-point correlation function can indicate a tendency toward SSB even in finite-size systems whose exact ground state remains symmetric. Although, the order parameter is strictly zero in such cases, the two-point function reveals nontrivial correlations over large distances.

1.2.3 Stability of states

In te case of SSB, the exact groundstate of a system is infinitely sensitive to perturbations, which therefore always yield a broken-symmetry state in the thermodynamic limit. However, such symmetric states are also generically unstable all by themselves. To illustrate this concept, let's take the Hamiltonian of the Ising model where one considers an external transverse field:

$$H_I = -J\sum_{<i,j>}\sigma_i^z\sigma_j^z - h\sum_i \sigma_i^x. \tag{1.21}$$

If we consider the external field to be small compare to the interaction between spins, i.e, $J \gg h > 0$, the groundstate of this Hamiltonian may be approximate by a superposition of all spins up and all spins down:

$$|\psi\rangle \approx \frac{1}{\sqrt{2}}(|\uparrow\uparrow ...\rangle - |\downarrow\downarrow ...\rangle), \tag{1.22}$$

Thus measuring S_i^z at the site i will collapse the superposed ground state onto the component corresponding to the observable value of S_i^z. For instance, if a local measurement of S_i^z reveals a up spin, the entire state after the measurement has collapsed to $|\uparrow\uparrow ...\rangle$, and subsequently measuring S_j^z at any site j will always yield up. The expectation value of the local observable S_j^z has changed due to the measurement of S_i^z, which means that the ground state (1.22) is unstable against local measurement. Conversely, the broken symmetry state $|\uparrow\uparrow ...\rangle$ is stable against local measurement since the measurement of $S^z(x)$ will not influence the local measurement at another positions. Local measurements typically and rapidly collapse an unstable symmetric state into one of its possible symmetry-broken configurations. Stability against local measurements is particularly important when considering a system's coupling to its environment. Even weak environmental interactions effectively measure local observables, such as the magnetization S_i^z, and thus make symmetric states practically unobservable. This idea can be quantified through the concept of cluster decomposition. A state $|\psi\rangle$ is said to satisfied the cluster decomposition if and only if for all local observables $a(x)$ and $b(x')$ we have

$$\lim_{|x-x'|\to\infty}\lim_{V\to\infty} \langle a(x)b(x')\rangle - \langle a(x)\rangle\langle b(x')\rangle \to 0. \tag{1.23}$$

In this case, the state $|\psi\rangle$ is short-range correlated and it is long-range correlated if the cluster decomposition is not satisfied. It means that the measurements of $a(x)$ and $b(x')$ are uncorrelated when x and x' are fart apart. In the context of SSB, $a(x)$ and $b(x')$ must be the local order parameter operator and its adjoint respectively. The exact groundstate of Hamiltonians susceptible to SSB are almost always cat states, like the ground state (1.22), and they do not

[7]Note that the division of states into long-range ordered/crystalline ordered and disordered is not exhaustive, but it is the one that is relevant to this thesis.

satisfy the cluster decomposition contrary to broken-symmetry states. The latter always do satisfy the cluster decomposition property. Hence, the study of stability of the exact symmetric groundstate state is interesting because it must be long-range correlated for all systems that exhibit SSB.

1.2.4 The harmonic crystal

One of the most prominent examples of SSB is the breaking of spatial translation symmetry that occurs in a crystalline lattice. To illustrate this, we consider a one-dimensional harmonic crystal characterized by the Hamiltonian (1.7) introduced in section 1.1.4. The discussion below can be straightforwardly generalized to a higher-dimensional harmonic crystal. In what follows, the Hamiltonian is recast in terms of bosonic creation and annihilation operators. After applying a Fourier transform, the Hamiltonian is diagonalized using a Bogoliubov transformation [57], following the derivations in Refs. [49, 58]. Although this framework is more mathematically involved than the traditional approach of introducing particle equilibrium positions [2], it offers the distinct advantage of dropping this assumption, thereby explicitly capturing the motion of the crystal's center of mass.

The momentum operator p_j and the position operator x_j can both be expressed in terms of the creation operator $b_j^\dagger$ and the annihilation operator b_j such that

$$p_j = i\sqrt{\frac{\hbar}{2}}(2m\kappa)^{\frac{1}{4}}[b_j^\dagger - b_j], \qquad x_j = \sqrt{\frac{\hbar}{2}}\left(\frac{1}{2m\kappa}\right)^{\frac{1}{4}}[b_j^\dagger + b_j], \tag{1.24}$$

and equivalently,

$$b_j = \frac{1}{\sqrt{2\hbar}}\left[(2m\kappa)^{\frac{1}{4}}x_j + i\left(\frac{1}{2m\kappa}\right)^{\frac{1}{4}}p_j\right], \quad b_j^\dagger = \frac{1}{\sqrt{2\hbar}}\left[(2m\kappa)^{\frac{1}{4}}x_j - i\left(\frac{1}{2m\kappa}\right)^{\frac{1}{4}}p_j\right]. \tag{1.25}$$

This transformation is canonical: given the canonical commutation relations $[x_i, p_j] = i\hbar\,\delta_{ij}$, the definitions (1.24) ensure that the bosonic commutation relations $[b_i, b_j^\dagger] = \delta_{ij}$ are satisfied. Inserting Eqs. (1.24) into the Hamiltonian (1.7), it becomes

$$H = \frac{\hbar}{4}\sqrt{\frac{2\kappa}{m}}\sum_{j,j'}\left[2(b_j^\dagger b_j + b_j b_j^\dagger) - (b_j^\dagger + b_j)(b_{j'}^\dagger + b_{j'})\right]. \tag{1.26}$$

Considering a harmonic crystal with periodic boundary conditions to eliminate edge effects and mimic an infinite system, we perform a Fourier transformation on the bosonic operators $b_j^\dagger$ and b_j:

$$b_j^\dagger = \frac{1}{\sqrt{N}}\sum_k e^{-ikaj}b_k^\dagger, \qquad b_j = \frac{1}{\sqrt{N}}\sum_k e^{ikaj}b_k, \tag{1.27}$$

where a is the lattice constant and k runs over the discrete wave vectors of the first Brillouin zone, $k = 2\pi n/Na$. Introducing these Fourier transformations into Eq. (1.26) leads to the following form of the Hamiltonian:

$$H = \hbar\sqrt{\frac{\kappa}{2m}}\sum_k\left[A_k b_k^\dagger b_k + \frac{B_k}{2}(b_k^\dagger b_{-k}^\dagger + b_k b_{-k}) + 1\right], \tag{1.28}$$

where $A_k = 2 - \cos(ka)$ and $B_k = -\cos(ka)$. This Hamiltonian is not diagonal yet, since the terms $b_k^\dagger b_{-k}^\dagger$ and $b_k b_{-k}$ respectively create and annihilate two bosons at the same time. To

resolve this issue, a Bogoliubov transformation must be performed on the bosonic operators $b_k^\dagger$ and b_k. We define two new bosonic operators $\beta_k^\dagger$ and β_k:

$$b_k^\dagger = \cosh(u_k)\beta_{-k}^\dagger - \sinh(u_k)\beta_k, \qquad b_{-k} = \cosh(u_k)\beta_k - \sinh(u_k)\beta_{-k}^\dagger, \tag{1.29}$$

where the new operators satisfy the bosonic commutation relations $[\beta_i, \beta_j^\dagger] = \delta_{ij}$. The parameters u_k satisfy $u_k = u_{-k}$ and are chosen such that the Hamiltonian is brought into diagonal form. This requires

$$\cosh(2u_k) = \frac{A_k}{\sqrt{A_k^2 - B_k^2}}, \qquad \sinh(2u_k) = \frac{B_k}{\sqrt{A_k^2 - B_k^2}}. \tag{1.30}$$

By substituting Eqs. (1.29) into the Hamiltonian (1.28), it takes the form

$$H = \hbar\sqrt{\frac{\kappa}{m}} \sum_k 2\sin\left|\frac{ka}{2}\right| \left(\beta_k^\dagger \beta_k + \frac{1}{2}\right) + \text{const} \tag{1.31}$$

$$= 2\hbar\sqrt{\frac{\kappa}{m}} \sum_k \sin\left|\frac{ka}{2}\right| \left(n_k + \frac{1}{2}\right), \tag{1.32}$$

where the additive constant is a zero-point contribution that we drop, energy being defined only up to an arbitrary constant. In this form, the Hamiltonian is finally diagonal. It describes a set of independent bosonic modes labeled by the wave vector k. Each mode behaves as a quantized harmonic oscillator with frequency

$$\omega_k = 2\sqrt{\frac{\kappa}{m}}\, \sin\left|\frac{ka}{2}\right|. \tag{1.33}$$

The operator n_k counts the number of bosons (phonons) occupying the mode k, and each mode contributes an energy $\hbar\omega_k \left(n_k + \frac{1}{2}\right)$. Physically, this represents the lattice vibration spectrum, characterized by phonons, where each k-mode corresponds to a collective excitation of the lattice with quantized energy levels.

However, the canonical transformation given by Eq. (1.29) is not well-defined as $k \to 0$. Indeed, Eqs. (1.30) show that the parameter u_k diverges in this limit, so that $\cosh(u_k) \to \infty$ and $\sinh(u_k) \to \infty$. The $k = 0$ mode must therefore be considered separately in the Hamiltonian (1.28). With $A_0 = 1$ and $B_0 = -1$, one has

$$H_{k=0} = \hbar\sqrt{\frac{\kappa}{2m}} \left[b_0^\dagger b_0 - \frac{1}{2}(b_0^\dagger b_0^\dagger + b_0 b_0) + 1\right] \tag{1.34}$$

$$= \hbar\sqrt{\frac{\kappa}{2m}} \left[1 - \frac{1}{2}(b_0^\dagger - b_0)^2\right], \tag{1.35}$$

where we used the commutation relation $[b_0, b_0^\dagger] = 1$. Applying the inverse Fourier transformation (1.27) together with Eqs. (1.25) to $H_{k=0}$, and using $b_0 = \frac{1}{\sqrt{N}} \sum_j b_j$, one finds

$$H_{k=0} = \hbar\sqrt{\frac{\kappa}{2m}} \left[1 - \frac{1}{2N} \sum_{j,l} (b_j^\dagger - b_j)(b_l^\dagger - b_l)\right] \tag{1.36}$$

$$= \hbar\sqrt{\frac{\kappa}{2m}} \left[1 + \frac{1}{N} \sum_{j,l} \frac{p_j p_l}{\hbar(2m\kappa)^{\frac{1}{2}}}\right] \tag{1.37}$$

$$= \frac{\sum_{j,l} p_j p_l}{2Nm} + \text{const} \tag{1.38}$$

$$= \frac{p_{tot}^2}{2Nm} + \text{const}, \tag{1.39}$$

where $p_{tot} = \sum_j p_j$ is the total momentum of the entire system, or equivalently its center-of-mass momentum. This zero-momentum part of the Hamiltonian thus describes the obvious fact that the crystal as a whole carries a kinetic energy associated with the combined mass Nm of all its constituents, up to an additive constant. The full Hamiltonian of the one-dimensional harmonic crystal is therefore

$$H = H_{k\neq 0} + H_{k=0} = 2\hbar\sqrt{\frac{\kappa}{m}}\sum_{k\neq 0}\sin\left|\frac{ka}{2}\right|\left(n_k + \frac{1}{2}\right) + \frac{p_{tot}^2}{2Nm}, \tag{1.40}$$

where the additive constant has been dropped. Since $H_{k=0}$ and $H_{k\neq 0}$ commute, each eigenstate of H has a well-defined value for both parts of the Hamiltonian. We will therefore analyze only the collective part of the Hamiltonian and completely ignore the internal part.
The eigenvalues E_p of the collective Hamiltonian (1.39) are those of a free particle of mass mN and are of the form $E_p \propto \frac{n^2}{2Nm}$, with n an integer. These energies form the thin spectrum and decrease as the number of particles in the crystal increase. Consequently, all states in the collective portion of the spectrum become degenerate with the ground state in the thermodynamic limit. Thus, it costs no energy to generate collective excitations, so a wave packet formed from total-momentum eigenstates with a well-defined center-of-mass position has the same energy expectation value as the zero-momentum state, thereby signaling SSB. However, outside this limit, the ground state of the Hamiltonian obviously has total momentum equal to zero. Hence, the total momentum being determined, the ground state must have maximum uncertainty on the center of mass of the position of the crystal which means that translation space symmetry is not broken for a finite one-dimensional harmonic crystal.

For a finite crystal, one must introduce a symmetry-breaking field, treated as a perturbation to the collective part of the Hamiltonian, and determine the strength required to make it possible to construct a superposition of crystal eigenstates with a well-defined center-of-mass position [2]. To this purpose, we must add a symmetry-breaking field of the form $Bx_{tot}^2/2$, with $x_{tot} = \frac{1}{N}\sum_j x_j$, to the Hamiltonian (1.39). It yields a harmonic oscillator equation for the collective position coordinate. Its ground state wavefunction is well known and is given by:

$$\psi_0(x_{tot}) = \left(\frac{m\omega N}{\pi\hbar}\right)^{\frac{1}{4}} e^{-\frac{m\omega N}{2\hbar}x_{tot}^2}, \tag{1.41}$$

where $\omega = \sqrt{B/mN}$ and $\sigma = \sqrt{\frac{\hbar}{m\omega N}}$ is its width in position space. The ground state of the harmonic crystal in the presence of a symmetry-breaking perturbation is a gaussian wave packet for the center of mass coordinate in real space which corresponds to an equivalent superposition of total momentum states: the symmetry breaking field B couples the different thin spectrum states of the crystal. The occurrence of SSB can again be identified through the singular nature of the thermodynamic limit, manifested by the two non-commuting limits:

$$\lim_{N\to\infty}\lim_{B\to 0}|\psi_0(x_{tot})|^2 = \text{constant},$$
$$\lim_{B\to 0}\lim_{N\to\infty}|\psi_0(x_{tot})|^2 = \delta(x_{tot}).$$

The first equation above indicates that, for a system of any finite size, the perturbation can always be chosen sufficiently weak so that the ground state wave function remains essentially delocalize over space. By contrast, the second line shows that in the thermodynamic limit, localization occurs even in the presence of an infinitesimal potential, which effectively means that the wave function localizes spontaneously. In this latter case, the continuous space translational symmetry of the crystal as a whole is spontaneously broken. Although real crystals are finite, the singular nature of the thermodynamic limit implies that, as the crystal becomes larger and larger, an increasingly weaker perturbation suffices to render its ground state a localized wave packet.

Chapter 2

Time crystals in closed quantum systems

Building on the framework of spontaneous symmetry breaking, we introduce time crystals in the setting of closed quantum systems. We first recall the origin of the idea in Wilczek's proposal and the no-go theorems that rule out time-crystalline order in equilibrium. This naturally leads to periodically driven systems: we develop Floquet theory for closed systems, define the discrete time crystal, and present its realization as a π-spin-glass phase in disordered, many-body-localized spin systems. The objective is to understand why equilibrium time crystals are forbidden and to define discrete time crystals, a genuine non-equilibrium phase of matter.

2.1 Origin of time crystals

In the framework of special relativity, our understanding of physics shifted as time ceased to be considered absolute and instead became integrated with space into a four-dimensional manifold known as spacetime. Because time behaves mathematically as a fourth "spatial" coordinate, it may be interesting to explore the spontaneous breaking of time-translation symmetry. As we know, crystals break continuous spatial translation symmetry, spontaneously organizing their atoms into a discrete structure that exhibits discrete symmetry. This may suggest that a physical system could potentially and spontaneously break continuous time-translation symmetry into a discrete one. In 2012, Frank Wilczek was the first to formally introduce the concept of a time crystal, a theoretical phase of matter that extends the conventional definition of a crystal from space into the time domain. Wilczek's foundational work encompassed both classical time crystals, developed in collaboration with A. Shapere [5], and quantum time crystals, which he explored on his own [6]. His central idea involved studying physical systems described by a time-independent Hamiltonian. In a standard crystal, the lowest-energy state is spatially periodic, and Wilczek drew the analogy that, for a time crystal, the ground state would exhibit periodic behavior in time.

A crucial finding of this initial theoretical investigation was that a time crystal, a physical system that spontaneously break time translation symmetry in an equilibrium system, cannot exist in classical systems. Indeed, in classical physics, a system with a time-independent Hamiltonian that exhibits motion in its ground state seems absurd, as this would amount to invoking the concept of a perpetual motion machine. As a matter of fact, in order to find the lowest energy state for a classical system, we must find an extremal value of its Hamiltonian H:

$$\frac{\partial H}{\partial p} = 0, \qquad \frac{\partial H}{\partial x} = 0. \tag{2.1}$$

Thus, it means that it is impossible to find a classical system in motion, since the first condition above implies that the lowest energy state cannot exhibit any, as

$$\dot{x} = \frac{dx}{dt} = \frac{\partial H}{\partial p} = 0. \tag{2.2}$$

However, if one assumes that the energy of a classical system is given by

$$E = \frac{\dot{x}^4}{4} - \frac{\dot{x}^2}{2}, \tag{2.3}$$

it appears that the lowest energy of the particle corresponds to a motion $\dot{x} = \pm 1$ [5]. The contradiction of this result with the conclusion based on Eq. (2.2) can be resolved by realizing that the energy given by Eq. (2.3) cannot be converted to an Hamiltonian smoothly since it is a multi-valued function of the momentum with cusps that correspond precisely to energies minima at $\dot{x} = \pm 1$ where the Hamilton equations are not defined.
Hence, since the analysis of the classical case shows that it fails to identify a classical time crystal in the Hamiltonian formalism, the next step is to investigate the possibility of quantum time crystals. Indeed, it is well known that quantum systems exhibit behaviors that would never be considered possible in a classical framework.

2.1.1 Frank Wilczek's model

This section presents a summary of the first theoretical proposal of a time crystal, introduced by Frank Wilczek in Ref. [6]. Let us consider a charged particle confined on a circular unit ring in a region where the magnetic field $\mathbf{B}$ is null but the vector potential $\mathbf{A}$ is different from zero. The position of the particle on this ring is depicted by the angle ϕ. The presence of a non-zero $\mathbf{A}$ requires that there must exist a region of space where $\mathbf{B}$ is non-null in the area of the ring. However, the wavefunction that characterizes the particle is forbidden to enter this region. This system is called an Aharonov-Bohm ring and the Hamiltonian characterizing the dynamics of the charged particle is given by [59]

$$H = \frac{(\pi_\phi - \alpha)^2}{2}, \tag{2.4}$$

where the mass m of the particle and $\hbar$ are taken to be equal to one. Furthermore, $\pi_\phi = i\partial/\partial\phi$ is the canonical angular momentum conjugated to ϕ and α is the magnetic flux through the ring. Thus, if one considers the many-body system of N bosons in this ring, where their interactions is described by attractive Dirac δ-interactions, the Hamiltonian of this many-body systems is

$$H = \sum_{j=1}^{N} \frac{(\pi_j - \alpha)^2}{2} + V(\phi_1, \ldots, \phi_N) = \sum_{j=1}^{N} \frac{(\pi_j - \alpha)^2}{2} - \frac{\lambda}{2} \sum_{j \neq k,1}^{N} \delta(\phi_j - \phi_k) \tag{2.5}$$

with the understanding that H acts on periodic functions, so the δ-interaction is well defined. The strength of the interaction between two bosons is characterized by λ which is positive given that an attractive interaction is considered. To solve the Schrödinger equation involving the latter Hamiltonian, we work in the mean field approximation taking the product ansatz:

$$\Psi(\phi_1, \ldots, \phi_N) = \prod_{j=1}^{N} \psi(\phi_j), \tag{2.6}$$

and we solve an approximate one-body evolution equation for ψ. To do so, we define the effective potential V_{eff}:

$$V_{\text{eff}}(\phi_1, \ldots, \phi_N) = \sum_{j=1}^{N} W(\phi_j) \quad \text{with} \quad W(\phi_j) = \int \prod_{k \neq j} d\phi_k \, \psi^*(\phi_k) \, V \, \psi(\phi_k), \tag{2.7}$$

satisfying the following relation:

$$\langle \Psi | V | \Psi \rangle = \langle \Psi | V_{\text{eff}} | \Psi \rangle \,. \tag{2.8}$$

Thus, the effective Schrodinger equation for Ψ is:

$$i\frac{\partial \Psi}{\partial t} = \left[\sum_{j=1}^{N} \frac{(\pi_j - \alpha)^2}{2} + V_{\text{eff}}(\phi_1, \ldots, \phi_N) \right] \Psi. \tag{2.9}$$

Hence, if we apply the Dirac-Frenkel variational principle to the latter equation, we can reduce it to the one-body non-linear Schrodinger equation (NLSE) adjusted to the system for ψ:

$$i\frac{\partial \psi}{\partial t} = \frac{1}{2}(\pi - \alpha)^2 \psi - \lambda(N-1)|\psi|^2 \psi. \tag{2.10}$$

This equation is obtained using a mean-field approach. Accordingly, the ground state described by Eq. (2.10) provides a good approximation to the true many-body ground state when the number of bosons N is large and the interaction strength λ is small. In the joint limit $N \to \infty$ and $\lambda \to 0$, while keeping the mean total interaction energy $\lambda(N-1)$ constant, the ground state of the NLSE coincides with the ground state of the full many-body system.

If we consider the case of vanishing magnetic flux, i.e. $\alpha = 0$, and if the total effective interaction is sufficiently strong $\big(\lambda(N-1) > \pi^2\big)$, it becomes energetically favorable for the particles to cluster together. As a result, the mean-field solution ψ breaks spatial translational symmetry and becomes inhomogeneous in space. The stationary solution of Eq. (2.10) is then given by a Jacobi elliptic function, which for $\lambda(N-1) \gg 1$, can be well approximated by

$$\psi(\phi) \approx \frac{\sqrt{\lambda(N-1)}}{2}\, e^{i\frac{[\lambda(N-1)]^2}{8}t}\, \cosh^{-1}\!\left(\frac{\lambda(N-1)}{2}(\phi + \beta) \right), \tag{2.11}$$

where the parameter β reflects the degeneracy of the non-symmetric states arising from spontaneous symmetry breaking. To obtain this solution, we impose both the periodicity condition $\psi(\phi + 2\pi) = \psi(\phi)$ and the normalization condition on ψ. This solution corresponds to the well-known bright soliton of the NLSE on the line. In our case $\big(\lambda(N-1) \gg 1\big)$, the soliton has a small width and can therefore be deformed, at negligible energy cost, to fit on a unit circle. This implies that the mean-field approach predicts that all bosons in the ground state occupy a localized wavefunction, forming a localized Bose–Einstein condensate.

In the presence of a magnetic flux, i.e. for $\alpha \neq 0$, Wilczek postulates and constructs a time-dependent ground state of the NLSE based on the following idea. According to Faraday's law, if the magnetic flux is increased adiabatically from zero until the angular velocity $\dot{\phi}$ reaches the value α, the condensate of localized bosons is set into motion. Wilczek therefore argued that the localized ground state obtained for $\alpha = 0$ evolves, during this acceleration process, into a time-dependent state, ultimately reaching a time-dependent ground state once $\dot{\phi}$ equals α. Moreover, each particle acquires an energy $\alpha^2/2$, which can be interpreted as the rotational kinetic energy gained through this process. In the end, this ground state is expected to spontaneously break both spatial and temporal translational symmetries and to remain in perpetual motion in the limits $N \to \infty$ and $\lambda \to 0$, while keeping $\lambda(N-1) = \text{const}$.
However, Wilczek postulates that the state described above is the ground state of the system based primarily on physical intuition, without further justification. This claim has therefore prompted significant debate within the physics community. Indeed, subsequent analyses have shown that his conclusion does not hold for the system he considered. Hereafter, even a no-go theorem has been established, demonstrating that an equilibrium system cannot possess a time-dependent ground state.

2.1.2 No-go theorems

Shortly after the publication of Wilczek's article postulating the existence of a time crystal in a quantum system, the first critical responses appeared [7, 60]. P. Bruno was the first to point out that the state identified by Wilczek as the ground state was, in fact, not the true ground state of the system. Indeed, the model introduced by Wilczek suffers from several fundamental issues [7]. The most significant one concerns the violation of energy conservation in the presence of an external environment (e.g., the electromagnetic field). Specifically, if one considers N charged bosons rotating on a ring, the rotating density lump would radiate energy despite being in its supposed ground state. Wilczek himself recognized this paradox and proposed to suppress the coupling to the environment by considering higher multipole moments or by placing the system inside a cavity. However, this proposal was not entirely convincing. Another paradoxical feature of Wilczek's model arises from the dependence of the ground-state energy on the magnetic flux parameter α. In particular, comparing the cases $\alpha = 0$ and $\alpha = \dot{\phi}$, the groundstate appears to gain energy. In the classical lump limit ($\lambda(N-1) \to \infty$), however, the groundstate energy is completely insensitive to the magnetic flux α, and the system exhibits a static ground state, in contradiction with Wilczek's result. Bruno therefore showed that, in the specific model proposed by Wilczek, the purported non-stationary ground state is not the true groundstate. Rather, the true groundstate is stationary. He subsequently formulated a more general no-go theorem that rigorously rules out the possibility of spontaneous rotation in the groundstate (or in thermal equilibrium) for a broad class of systems on an Aharonov–Bohm ring [8].

Bruno's no-go theorem can be summarized as follows. Consider an assembly of N particles (bosons or fermions) with masses m_i, moving on a one-dimensional Aharonov–Bohm ring of radius R, threaded by a magnetic flux and described by the Hamiltonian

$$H_\alpha^{(\Omega)}(\boldsymbol{\phi}, t) = \sum_{i=1}^{N} \left[\frac{\hbar^2 \left(\pi_i - \alpha_i\right)^2}{2 m_i R^2} + V_i(\phi_i - \Omega t) \right] + \sum_{i<j} U_{ij}(\phi_i - \phi_j), \tag{2.12}$$

where $V_i(\phi_i - \Omega t)$ is the external potential experienced by particle i, rigidly rotating with angular velocity Ω. This potential is interpreted as a symmetry-breaking perturbation responsible for the explicit breaking of time-translation symmetry. The Hamiltonian (2.12) therefore constitutes a generalization of the Hamiltonian (2.5) introduced in the previous section. It can be shown that the energy eigenvalues of the Hamiltonian above, for both $\Omega = 0$ and $\Omega \neq 0$, satisfy the relation

$$E_{\alpha,n}^{(\Omega)} - E_{\alpha,n}^{(0)} = \frac{I_{\alpha,n}\, \Omega^2}{2} + \mathcal{O}(\Omega^3), \tag{2.13}$$

where $E_{\alpha,n}^{(0)}$ denotes the energy eigenvalue associated with the nth eigenstate of the time-independent Hamiltonian $H_\alpha^{(0)}(\boldsymbol{\phi})$, and $E_{\alpha,n}^{(\Omega)}$ corresponds to the nth eigenstate of the time-dependent Hamiltonian $H_\alpha^{(\Omega)}(\boldsymbol{\phi}, t)$. The quantity $I_{\alpha,n}$ is identified as the moment of inertia associated with the nth energy level. The central result is that the moment of inertia of the ground state, $I_{\alpha,0}$, is strictly positive if rotational symmetry is broken, and vanishes otherwise. Therefore, in order to properly assess the possibility of spontaneous symmetry breaking, one must first take the thermodynamic limit $N \to \infty$, and only afterward consider the limit $V \to 0$ of the symmetry-breaking potential. This procedure must be applied to the difference between the ground-state energies per particle, $\varepsilon_{\alpha,0}^{(\Omega)}$ and $\varepsilon_{\alpha,0}^{(0)}$. If $\varepsilon_{\alpha,0}^{(\Omega)} < \varepsilon_{\alpha,0}^{(0)}$, spontaneous breaking of time-translation symmetry cannot occur, since the symmetric and non-symmetric groundstates are not degenerate, or the non-symmetric state has a lower energy. However, assuming the occurrence of spontaneous breaking of rotational symmetry, one finds

$$\varepsilon_{\alpha,0}^{(\Omega)} - \varepsilon_{\alpha,0}^{(0)} = \lim_{V \to 0} \lim_{N \to \infty} \frac{E_{\alpha,0}^{(\Omega)} - E_{\alpha,0}^{(0)}}{N} > 0, \tag{2.14}$$

for any finite value of $\Omega \neq 0$. Bruno therefore demonstrated the impossibility of Wilczek's proposed spontaneously rotating quantum time crystals in the ground state. Moreover, he showed that the same conclusion holds when the system is in thermal equilibrium at a finite temperature. A first remark concerning the discussion above is that, in Wilczek's original model, the thermodynamic limit was not explicitly invoked. This is because the analysis relied on mean-field theory, which enforces symmetry breaking at the outset. To obtain results valid beyond mean-field theory, it is necessary to employ the Bogoliubov method (or an equivalent approach) in order to rigorously establish spontaneous symmetry breaking. A second remark is that the moment of inertia $I_{\alpha,n}$ appearing in Eq. (2.13) may become negative in the thermodynamic limit for certain excited states, which allows for the possibility of time-crystal behavior in excited eigenstates.

However, since the previous no-go theorem apply only for many-body systems on an Aharonov–Bohm ring, it is therefore restricted to a special class of Hamiltonians. In 2015, a much more general no-go theorem was presented by Watanabe and Oshikawa (WO) [9]. They gave a proof that rules out the possibility of time crystals, as originally defined, in the ground state or in the thermal equilibrium of a general Hamiltonian, which consists of short-range interactions Hamiltonian. Indeed, as we have seen in section 1.2, spontaneous symmetry breaking in many-body systems does not necessarily need the introduction of a symmetry-breaking field to be exposed, but can also be defined in terms of correlation functions. As a reminder, a system has long-range order if the equal-time correlation function of the local order parameter operator $\phi(x,t)$ satisfies in the thermodynamic limit:

$$\lim_{V\to\infty} \langle \phi(\mathbf{x},t)\phi(\mathbf{x}',t)\rangle \to \text{constant} \neq 0, \tag{2.15}$$

for $|\mathbf{x}-\mathbf{x}'|$ much greater than any microscopic scales and V is the volume of the system[1]. Since systems which exhibit spontaneous crystalline order has a long-range correlation who approaches a space periodic function:

$$\lim_{V\to\infty} \langle \phi(\mathbf{x},t)\phi(\mathbf{x}',t)\rangle \to f(\mathbf{x}-\mathbf{x}'), \tag{2.16}$$

WO presented a precise spatiotemporal definition for time crystals, that is, the system is a time crystal if the correlation function defined with the global order parameter operator $\Phi(t)$ of $\phi(\mathbf{x},t)$:

$$\lim_{|\mathbf{x}-\mathbf{x}'|\to\infty} \lim_{V\to\infty} \langle \phi(\mathbf{x}',t)\phi(\mathbf{x},0)\rangle = \lim_{V\to\infty} \frac{\langle \Phi(t)\Phi(0)\rangle}{V^2} = \lim_{V\to\infty} \frac{\langle e^{iHt}\Phi(0)e^{-iHt}\Phi(0)\rangle}{V^2} \to f(t), \tag{2.17}$$

exhibits a nontrivial periodic oscillation $f(t)$ in relation to time t. This limit evaluates the long-range spatial behavior of a two-time correlation function. Equation (2.17) is therefore a generalization of the spontaneous crystalline order for time. One might think that we could define time crystals based on the time dependence of equal-position correlation functions. Should we adopt this definition, however, rather trivial systems would qualify as time crystals. "Crystal" should be reserved for systems that exhibit correlated, coherent behaviors, which are captured by long-distance correlation functions, be it an ordinary crystal or a time crystal.
Based on this definition, WO proved, at zero temperature, the following inequality

$$\frac{1}{V^2} |\, \langle 0|\Phi(0)e^{-i(H-E_0)t}\Phi(0)|0\rangle - \langle 0|\Phi^2(0)|0\rangle \,| \leq C\frac{t}{V}, \tag{2.18}$$

with a constant C that can depend on $\Phi(0)$ and H but not on t or V. This inequality holds for local Hamiltonians and non-local Hamiltonians with exponentially decaying interactions or power-law decaying interactions $r^{-\alpha}$ ($\alpha > 0$). This result implies quite generally that time

[1] Contrary to the definition of long-range order in section 1.2, the latter is defined in the Heisenberg picture.

crystals defined by Eq. (2.17) are not possible in ground states. Indeed, in the thermodynamic limit and for any fixed t, the inequality (2.18) become $|f(t) - f(0)| = 0$ so it means that the correlation function $f(t)$ remains constant and is therefore time independent. This conclusion can be extended to the case of thermal equilibrium states at finite temperature.

In conclusion, the spontaneous breaking of continuous time-translation symmetry cannot occur in the ground state of a closed quantum system with short-range interactions. However, time-translation symmetry breaking may arise when the system is prepared in an excited eigenstate, as pointed out by *Syrwid et al.* [61]. Moreover, it remains an open question whether a time-independent Hamiltonian with long-range interactions can support a time-dependent ground state, thereby potentially circumventing the constraints imposed by the WO no-go theorem [62–64]. Nevertheless, this subtle issue has attracted limited attention, as WO also proposed the existence of time crystals in non-equilibrium systems, a direction that has since proven to be highly fruitful.

2.2 Discrete time crystals

Since a time-crystal phase appears to be absent in equilibrium closed quantum systems, attention has shifted toward the possibility of realizing time-crystalline behavior in non-equilibrium settings, in particular in periodically driven systems. In such systems, continuous time-translation symmetry is explicitly broken by the presence of an external time-dependent drive, and the dynamics are therefore governed by a time-periodic Hamiltonian. This naturally leads to the concept of discrete time crystals (DTCs), also known as Floquet time crystals.
The central idea behind DTCs is to consider a many-body system subjected to a periodic drive with period T, such that its Hamiltonian satisfies $H(t) = H(t+T)$ and thus possesses a discrete time-translation symmetry. The goal is then to identify systems that spontaneously evolve into states exhibiting a subharmonic response, namely observables that oscillate with a period that is an integer multiple of the driving period. Crucially, this oscillatory behavior must persist indefinitely in the thermodynamic limit and remain robust over a finite range of system parameters. Such phenomena constitute a genuinely new class of non-equilibrium phases of matter, stabilized not by equilibrium thermodynamics, but by dynamical constraints and many-body interactions.
Thus, in this section, we first develop the theoretical framework underlying Floquet quantum systems that is relevant for defining and characterizing DTCs. We then provide a rigorous definition of DTCs, highlighting the generalization of the concept of spontaneous symmetry breaking, previously introduced for internal and spatial symmetries, to the temporal domain, together with the conditions under which this non-equilibrium phase can occur. Finally, we discuss disordered spin systems which are known to exhibit discrete time crystal behavior.
A brief summary of the phenomenological properties of a DTC is provided in Table I, which appears in the Conclusion.

2.2.1 Floquet theory in closed quantum systems

Floquet systems are systems subjected to a time-periodic driving with period T, such that the Hamiltonian exhibits temporal periodicity, $H(t) = H(t+T)$. Floquet theory provides a powerful framework to describe such configurations and has been developed for classical systems, closed quantum systems, and even open quantum systems. In this section, however, we focus on the main results of Floquet theory for closed quantum systems that are relevant to the understanding of discrete time crystals. Originally introduced by Gaston Floquet in 1883 in the context of classical differential equations [65], this theory was later used in the framework of quantum mechanics [66], and can be regarded as the temporal analogue of Bloch theory in

condensed matter physics [48]. It enables a systematic solution of the Schrödinger equation for Hamiltonians that are explicitly time-dependent and periodic. Floquet's theorem can be stated as follows [66, 67]:

Floquet's theorem:
The linearly independent solutions of the time-dependent Schrödinger equation

$$i\hbar\frac{d\,|\psi(t)\rangle}{dt} = H(t)\,|\psi(t)\rangle\,,$$

where the Hamiltonian is periodic in time, *i.e.* $H(t) = H(t+T)$ for all t, can be written in the following form:

$$|\psi_\alpha(t)\rangle = e^{-\frac{i}{\hbar}\varepsilon_\alpha t}\,|\phi_\alpha(t)\rangle\,, \quad \forall\,\alpha \in \mathbb{Z}, \tag{2.19}$$

where $|\phi_\alpha(t)\rangle$ have the same time periodicity as the Hamiltonian. The quantities ε_α are called the quasi-energies of the system, and the states $|\phi_\alpha(t)\rangle$ are referred to as Floquet states. By virtue of the linearity of the Schrödinger equation, an arbitrary state of the system can be expressed as a linear combination of Floquet states:

$$|\psi(t)\rangle = \sum_{\alpha=1}^{N} c_\alpha\, e^{-\frac{i}{\hbar}\varepsilon_\alpha t}\,|\phi_\alpha(t)\rangle\,, \tag{2.20}$$

where N is the dimension of the Hilbert space of the system and c_α are complex coefficients determined by the initial state.

Substituting the solutions (2.19) in the time-dependent Schrödinger equation leads to an eigenvalue equation for quasi-energies ε_α that can be written as

$$\left(H(t) - i\hbar\frac{d}{dt}\right)|\phi_\alpha(t)\rangle = \varepsilon_\alpha\,|\phi_\alpha(t)\rangle\,. \tag{2.21}$$

Since the Hamiltonian $H(t)$ and the Floquet states $|\phi_\alpha(t)\rangle$ are periodic, their Fourier components can be defined as follows:

$$H(t) = \sum_{m\in\mathbb{Z}} e^{-im\omega t}H_m, \qquad\qquad |\phi_\alpha(t)\rangle = \sum_{m\in\mathbb{Z}} e^{-im\omega t}\,|\phi_{\alpha,m}\rangle\,, \tag{2.22}$$

where $\omega = 2\pi/T$. Substituting these expressions into Eq. (2.21) leads to the following eigenvalue problem for quasi-energy ε_α:

$$\sum_{n\in\mathbb{Z}}(H_{m+n} - m\omega\delta_{m,n})\,|\phi_{\alpha,n}\rangle = \varepsilon_\alpha\,|\phi_{\alpha,m}\rangle\,. \tag{2.23}$$

This expression constitute an infinite system of coupled equations that can be solved to find the solutions of $|\phi_{\alpha,m}\rangle$ and ε_α. The new mapping from the time-dependent equation (2.21) didn't involve any approximation so it means that it always holds when any sort of time-periodic quantum systems is considered. Furthermore, an important consequence of Eq. (2.21) is that it has no explicit time dependence which mean that various established techniques from equilibrium statistical physics can be used to solve the non-equilibrium system [68].
Quasi-energies represent the effective, time-averaged energy levels of a system whose instantaneous energy is constantly being perturbed by a periodic drive and describe the temporal evolution of the energy of the Floquet states. Even if the Floquet spectrum is not bounded, it should be noted that the quasi-energies are only defined modulo $\hbar\omega$, i.e $\varepsilon_\alpha = \varepsilon_\alpha + k\hbar\omega$ with k an integer. Indeed, if the quasi-energy $\varepsilon_\alpha + k\hbar\omega$ is considered, Eq. (2.21) becomes

$$\left(H(t) - \frac{d}{dt}\right)e^{ik\omega t}\,|\phi_\alpha(t)\rangle = (\varepsilon_\alpha + k\hbar\omega)\,|\phi_\alpha(t)\rangle\,, \tag{2.24}$$

and from Eq. (2.22),

$$e^{ik\omega t}\left|\phi_\alpha(t)\right\rangle = \sum_{m\in\mathbb{Z}} e^{-i(m+k)\omega t}\left|\phi_{\alpha,m}\right\rangle = \sum_{j\in\mathbb{Z}} e^{-ij\omega t}\left|\phi_{\alpha,m}\right\rangle = \left|\phi_\alpha(t)\right\rangle, \tag{2.25}$$

where we defined $j = m+k$. Thus, this property allows us to consider only an interval of N values of the quasi-energies without loss of generality to study the evolution of a periodic driven system.

If we consider that the state of a system at time t_0 is $|\psi(t_0)\rangle$, the state of the system $|\psi(t)\rangle$ at time t is given by applying the time propagator $U(t,t_0)$:

$$\left|\psi(t)\right\rangle = U(t,t_0)\left|\psi(t_0)\right\rangle, \tag{2.26}$$

with

$$U(t,t_0) = \mathcal{T}\exp\left[-\frac{i}{\hbar}\int_{t_0}^{t} H(t')dt'\right], \tag{2.27}$$

where $\mathcal{T}$ is the time-ordering operator. For systems characterized by a time-independent Hamiltonian H, the time propagator is simply

$$U(t,t_0) = \exp\left[-\frac{i}{\hbar}H(t-t_0)\right]. \tag{2.28}$$

In the context of Floquet systems, the time propagator, denoted $U_F(t,t_0)$, possesses special properties [48, 66]. In particular, the time propagator over a period T can be considered to construct a discrete quantum map, propagating an initial state across many fundamental periods. To establish this, let us consider the time propagator over nT periods, with n an integer, and we take $t_0 = 0$:

$$U_F(nT,0) = \mathcal{T}\exp\left[-\frac{i}{\hbar}\int_0^{nT} H(t')dt'\right] \tag{2.29}$$

$$= \mathcal{T}\exp\left[-\frac{i}{\hbar}\sum_{k=1}^{n}\int_{(k-1)T}^{kT} H(t')dt'\right] \tag{2.30}$$

$$= \mathcal{T}\prod_{k=1}^{n}\exp\left[-\frac{i}{\hbar}\int_{(k-1)T}^{kT} H(t')dt'\right]. \tag{2.31}$$

This result is the consequence of the periodicity of the Hamiltonian. Furthermore, the terms in the result above do commute since they are equal over a full period. Thus, the time-ordering operator $\mathcal{T}$ can be moved in front of the product:

$$U_F(nT,0) = \prod_{k=1}^{n}\mathcal{T}\exp\left[-\frac{i}{\hbar}\int_{(k-1)T}^{kT} H(t')dt'\right] = \left[U_F(T,0)\right]^n. \tag{2.32}$$

Consequently, $U_F(T,0)$ is called the stroboscopic Floquet propagator and is defined as

$$U_F(T,0) = \exp\left[-\frac{i}{\hbar}H_F T\right], \tag{2.33}$$

where H_F is a time-independent hermitian operator called the Floquet Hamiltonian[2]. Knowledge of the stroboscopic Floquet propagator is sufficient to describe the stroboscopic dynamics of the system, provided one is not interested in the micromotion, i.e, the dynamics within a single period. Furthermore, Floquet systems possess the discrete time translation symmetry which is

[2]The Floquet Hamiltonian H_F depends explicitly on the choice of the initial time t_0 used to define the stroboscopic evolution.

the infinite, abelian, discrete group $\mathbb{Z}$ generated by the Floquet propagator $U_F(T,0)$. Hence, the evolution over a period T of an initial Floquet state $|\phi_\alpha(0)\rangle$ is given by

$$U_F(T,0)\,|\phi_\alpha(0)\rangle = e^{-\frac{i}{\hbar}\varepsilon_\alpha T}\,|\phi_\alpha(T)\rangle = e^{-\frac{i}{\hbar}\varepsilon_\alpha T}\,|\phi_\alpha(0)\rangle\,, \tag{2.34}$$

which means that Floquet states are also the eigenstates of the discrete time evolution operator $U_F(T,0)$. More precisely, the Floquet states $|\alpha\rangle = |\phi_\alpha(nT)\rangle$ are equivalent $\forall n \in \mathbb{Z}$ and are the eigenstates of the Floquet Hamiltonian H_F associated to the quasi-energies ε_α:

$$H_F\,|\alpha\rangle = \varepsilon_\alpha\,|\alpha\rangle\,. \tag{2.35}$$

The stroboscopic evolution of a Floquet system is equivalent to the evolution of a time-independent system characterized by the Floquet Hamiltonian H_F at discrete times nT, with $n \in \mathbb{Z}$.

2.2.2 Definition of DTCs

The initial idea behind the definition of time crystallinity was to identify a time-independent many-body system that spontaneously breaks continuous time-translation symmetry at equilibrium. However, previously established no-go theorems rule out the existence of such behavior in a broad class of time-independent systems. Following the work of WO [9], attention therefore shifted toward the possibility of time-crystalline behavior in non-equilibrium systems. In particular, studies of periodically driven systems have led to a reinterpretation of the original definition of a time crystal, giving rise to the concept of discrete time crystals [38].
A discrete time crystal is a non-equilibrium quantum phase of matter that arises in periodically driven many-body systems. More specifically, it is characterized by the spontaneous breaking of discrete time-translation symmetry in Floquet systems. A necessary condition for a Floquet system to be identified as a discrete time crystal is the existence of a physical observable exhibiting a subharmonic response to the external driving, *i.e.* an oscillation with a period that is an integer multiple of the driving period.
However, this condition alone is not sufficient to characterize a system as a discrete time crystal. Indeed, certain quantum systems may display subharmonic oscillations only as a transient dynamical effect or for particular fine-tuned initial states. In such cases, the observed behavior is merely a consequence of the system's dynamics rather than a manifestation of a new phase of matter. To qualify as a discrete time crystal, the subharmonic oscillation must be rigid. Rigidity implies that the oscillation remains stable under small perturbations or variations of the system parameters. The rigidity of the subharmonic oscillation must have a many-body origin. Furthermore, the subharmonic response must be independent of the choice of a broad class of initial states, occurring generically rather than for specially prepared states.
Finally, in the thermodynamic limit, the subharmonic oscillation must persist for infinitely long times. This requirement reflects the true spontaneous breaking of discrete time-translation symmetry and allows one to distinguish a stable discrete time crystal from prethermal discrete time crystals[3], as well as from accidental oscillations that survive only for finite durations.
Taken together, these criteria provide a rigorous phenomenological definition of discrete time crystals in closed quantum systems and delineate the conditions under which a periodically driven system hosts this novel non-equilibrium phase of matter [17, 70, 71]:

[3] A prethermal discrete time crystal is a periodically driven many-body system that exhibits a rigid but transient subharmonic response before thermalization [69]. Unlike stable discrete time crystals, this behavior persists only for a finite time in the thermodynamic limit. The lifetime of the prethermal regime does not scale exponentially with system size, but instead grows exponentially with the driving frequency and depends on the strength of the many-body interactions [35].

DTCs definition:
Considering a Floquet system subjected to a periodic driving with period T, which possesses a discrete time-translation symmetry, i.e. $H(t+T) = H(t)$, and a class of initial states $|\psi\rangle$, let $O(t) = \langle\psi|\mathcal{O}(t)|\psi\rangle$ denote the value of an order parameter operator at time t. A discrete time crystal must fulfill the three following conditions:

1. **Discrete time-translation symmetry breaking:** the order parameter satisfies $O(t+T) \neq O(t)$ even though the Hamiltonian is periodic, $H(t+T) = H(t)$. For a DTC, periodicity is recovered only after an integer number $n > 1$ of driving periods, $O(t+nT) = O(t)$.

2. **Rigidity of the oscillations:** $O(t)$ shows a fixed oscillation period nT without fine-tuned Hamiltonian parameters.

3. **Persistence to infinite time:** the non-trivial period oscillation nT must persist for infinitely long times in the thermodynamic limit.

A discrete time crystal does not constitute a trivial phase that can generically arise in a Floquet system. Indeed, periodic driving of a many-body system typically injects energy into the system on average. As a consequence, for arbitrary initial states, the system heats up and eventually reaches an ergodic regime [72, 73]. In this long-time limit, the system approaches an infinite-temperature state[4], which precludes the possibility of breaking discrete time-translation symmetry. One might ask whether exceptions to this behavior exist. In particular, some many-body systems are integrable and thus avoid uncontrolled heating. However, such systems relax to a time-periodic generalized Gibbs ensemble. Crucially, this steady state remains periodic with the same period as the external drive, and therefore does not display discrete time-translation symmetry breaking either [74–76]. Hence, it was believed that many-body systems subjected to periodic driving would exhibit either behavior.
However, Floquet many-body localization (F-MBL) provides a mechanism by which a closed quantum many-body system subjected to a periodic driving can avoid thermalizing to an infinite-temperature state and thus avoid quantum decoherence [15]. This phenomenon arises in disordered many-body systems, where the presence of disorder localizes the dynamics in state space and forbids the system from heating up under periodic driving. This mechanism enables the observation of novel out-of-equilibrium quantum phases that are induced and protected by interactions. Within the F-MBL regime, a particularly important phase is the π-spin glass (πSG), which can host a discrete time crystal phase characterized by a robust subharmonic response [77]. Furthermore, we should emphasize that since πSG is a spin glass phase, it does not exhibit any spatial order [52]. Hence, it cannot display spatio-temporal order so the definition (2.17) of a time crystal proposed by WO can not be directly adapted to discrete time crystals by considering $f(t)$ exhibiting subharmonic oscillation. Hence, in general, a system displaying discrete time crystal order without spatial order should preserve information about its initial state in addition to subharmonic dynamics. This motivates the following definition [70]:

[4] An infinite temperature state is a state of maximum entropy where every possible quantum configuration of a system is occupied with equal probability. In this regime, the state of the system is characterized by a density operator which is proportional to the identity operator, $\rho \propto \mathbb{I}$, meaning that the system has lost all specific information about its initial conditions. Mathematically, this occurs because as $T \to \infty$ in the Gibbs Ensemble state:

$$\rho = \frac{1}{Z} e^{-\frac{H}{k_b T}}, \tag{2.36}$$

the energy dependence vanishes, rendering all energy levels statistically equivalent.

Discrete time crystal order definition:
A quantum state $|\psi\rangle$ evolving under a Floquet unitary operator U_F with driving period T is said to exhibit discrete time crystal order if there exists a local observable $O(\mathbf{x}, t)$ satisfying two conditions. First, the equal-time correlation function remains finite at arbitrarily large separations in the thermodynamic limit:

$$\lim_{|\mathbf{x}-\mathbf{x}'|\to\infty} \lim_{V\to\infty} \langle\psi|O(\mathbf{x},0)O(\mathbf{x}',0)|\psi\rangle \neq 0. \tag{2.37}$$

Second, the normalized time-dependent correlation function

$$\lim_{|\mathbf{x}-\mathbf{x}'|\to\infty} \lim_{V\to\infty} \frac{\langle\psi|O(\mathbf{x},t)O(\mathbf{x}',0)|\psi\rangle}{\langle\psi|O(\mathbf{x},0)O(\mathbf{x}',0)|\psi\rangle}, \tag{2.38}$$

approaches a nonzero periodic function $f(t)$. The period of this function is nT, where $n > 1$ is an integer, indicating a subharmonic response of the system relative to the driving period.

Discrete time crystals according to the phenomenological definition, were believed to exist exclusively within the F-MBL framework. Nevertheless, experimental systems exhibiting a discrete time crystal phase, as well as subsequent theoretical studies, have demonstrated that discrete time-crystalline behavior can also emerge in clean (*i.e.* non-disordered) many-body systems. In particular, systems with long-range interactions [18], such as those described by the Lipkin-Meshkov-Glick model [16], systems operating in strongly interacting regimes [17], or even clean short-range interacting systems [78], can exhibit discrete time crystal phases even in the absence of disorder.
In fact, a discrete time crystal was first proposed in a clean system within the framework of cold-atom setups [10]. By bouncing ultracold atomic clouds on an oscillating mirror under the influence of gravity and initially preparing the system in its steady Floquet state, it was shown that the introduction of a small perturbation, such as atomic losses or a measurement of particle positions, can collapse the system into a more stable state whose periodicity is an integer multiple of the driving period. To analyze this kind of system, a mean-field approximation can be employed. From this semiclassical point of view, the many-body Hamiltonian is reduced to a nonlinear Schrödinger equation, such as the Gross–Pitaevskii equation. The resulting dynamics manifest as a stable periodic orbit in phase space, reflecting the fact that classical-like resonant particle orbits can also emerge in the quantum regime for interacting many-body systems. The nonlinear interactions provide a self-correcting mechanism that prevents the wave packet from dispersing and thereby stabilizes the subharmonic response.

In a system exhibiting spontaneous breaking of discrete time translation symmetry, the structure of the Floquet spectrum and the nature of its eigenstates are fundamentally distinct from those of a thermalizing system [77, 79]. To support a DTC phase, the Floquet eigenstates cannot be short-range correlated [11]. In the many-body regime, these eigenstates typically emerge as cat states. The latter structure is necessary for spontaneous symmetry breaking to occur in the thermodynamic limit. The spectrum itself is characterized by specific spectral pairing. For a DTC with a subharmonic response of period nT, the Floquet quasi-energies appear in nearly degenerate pairs separated by a precise phase shift. Indeed, the Floquet eigenstates come in pairs, whose quasi-energies are separated by exactly π/nT. Hence, the spontaneous breaking of discrete time-translation symmetry is intrinsically connected to the spontaneous breaking of a global internal $\mathbb{Z}_m$ symmetry, which is responsible for the emergence of a subharmonic response with period mT[5] [16].

[5]This symmetry is either explicitly present in the Hamiltonian that characterizes the system or in its Floquet propagator [70].

Let us illustrate these ideas using a toy model constructed to exhibit a discrete time-crystal phase and to provide further intuition for the concepts introduced above. We consider a kicked clock model described by the general Hamiltonian [80]:

$$H(t) = H_s + \sum_{k\in\mathbb{Z}} \delta(t - kT)K, \tag{2.39}$$

where H_s and K are time-independent operators. The stroboscopic Floquet propagator U_F can be decomposed as

$$U_F = e^{-\frac{i}{\hbar}K} e^{-\frac{i}{\hbar}H_s T} = X e^{-\frac{i}{\hbar}H_s T} \tag{2.40}$$

where we set $X = e^{-\frac{i}{\hbar}K}$. It represents a time-independent free dynamics dictated by H_s spaced out by kicks (at intervals T) controlled by the operator X. Furthermore, for simplicity, let us assume that H_s possesses an internal $\mathbb{Z}_m$ symmetry, and that the operator X represents the symmetry transformation between elements of $\mathbb{Z}_m$. Then, X must commute with H_s. We consider here the case of a system possessing an internal $\mathbb{Z}_2$ symmetry. In the thermodynamic limit, spontaneous symmetry breaking implies that the eigenstates of H_s come in degenerate pairs, $|\uparrow\rangle$ and $|\downarrow\rangle$, permuted by the symmetry transformation X:

$$X|\uparrow\rangle = |\downarrow\rangle \quad \text{and} \quad X^2 = 1 \tag{2.41}$$

However, in a many-body system of finite size L, the eigenstates of H_s must simultaneously diagonalize the symmetry transformation X. Consequently, these eigenstates are cat states:

$$|\pm\rangle = \frac{1}{\sqrt{2}}(|\uparrow\rangle \pm |\downarrow\rangle). \tag{2.42}$$

The corresponding eigenvalues of H_s are $\varepsilon_\pm = \varepsilon \pm \Delta$. If the system is likely to exhibit spontaneous symmetry breaking, the splitting must be exponentially small with the increasing of the system size L. The quasienergies ε_F of the full Floquet operator U_F are obtained by including the eigenvalues of the symmetry operator X ($+1$ for $|+\rangle$ and -1 for $|-\rangle$). Given the eigenvalue equation $U_F|\pm\rangle = e^{-i\varepsilon_F^\pm T}|\pm\rangle$:

- $U_F|+\rangle = e^{-i\varepsilon_+ T}|+\rangle$
- $U_F|-\rangle = -e^{-i\varepsilon_- T}|-\rangle = e^{i\pi}e^{-i\varepsilon_- T}|-\rangle$

Since the drive frequency is defined as $\omega = 2\pi/T$, the phase $e^{i\pi}$ corresponds to a quasienergy shift of $\pi/T = \omega/2$:

$$\varepsilon_F^+ = \varepsilon + \Delta, \qquad \varepsilon_F^- = \varepsilon - \Delta + \frac{\omega}{2}. \tag{2.43}$$

The spectrum of U_F consists of pairs of eigenvalues that differ by $\omega/2$ up to exponential accuracy in the system size. Hence, any initial state will have components on both the $|+\rangle$ and $|-\rangle$ states of each pairs such that the system will thus coherently oscillate at frequency $\omega/2$, up to a dephasing time $t \sim \Delta^{-1}$ which diverges exponentially with the system size. For example, let us consider a long range correlated initial state $|\uparrow\uparrow\ldots\rangle$ and assume $\Delta \ll 1$. This state can be written as a superposition of two cat states,

$$|\uparrow\uparrow\ldots\rangle = \frac{1}{\sqrt{2}}\left(|+\rangle + |-\rangle\right), \tag{2.44}$$

where $|\pm\rangle = \frac{1}{\sqrt{2}}\left(|\uparrow\uparrow\ldots\rangle \pm |\downarrow\downarrow\ldots\rangle\right)$. After one evolution period, the state of the system becomes $|\downarrow\downarrow\ldots\rangle$, while after another period it returns to $|\uparrow\uparrow\ldots\rangle$. This alternating dynamics must give rise to period-doubled subharmonic oscillations of a physical observable, which serves as the order parameter characterizing this behavior. More generally, a subharmonic response with an integer period $m > 2$ can arise in systems exhibiting an internal $\mathbb{Z}_m$-symmetry [80]. A rigorous study of the robustness of the system must be carried out in order to confirm the emergence of a discrete time crystal.

2.2.3 Discrete time crystallinity in disordered spins systems

Let us study the discrete time crystal introduced in Ref. [11]. It consists of a disordered spin-1/2 system with short-range interactions, which can be influenced by external magnetic field perturbations. The system is governed by the Hamiltonian

$$H_s = \sum_i J_i \sigma_i^z \sigma_{i+1}^z + \sum_i h_i^z \sigma_i^z + \sum_i h_i^x \sigma_i^x, \tag{2.45}$$

where J_i, h_i^z, and h_i^x are uniformly distributed such that

$$J_i \in [0.5, 1.5], \quad h_i^z \in [0, 1], \quad h_i^x \in [0, h]. \tag{2.46}$$

The regime of interest corresponds to the case where the local transverse field perturbations, with maximum value h, are small compared to the random interactions J_i. Moreover, after each period T, the system is subjected to a transverse magnetic field pulse which perfectly flips all the z-spin components:

$$H_F = \frac{\pi}{2} \sum_i \sigma_i^x. \tag{2.47}$$

Hence, the time-periodic Hamiltonian can be modeled as a kicked clock model, as introduced in Section 2.2.2:

$$H(t) = H_s + H_F \sum_{n \in \mathbb{Z}} \delta(t - nT). \tag{2.48}$$

The stroboscopic Floquet operator, which characterizes the evolution of the system over a single period T, is thus given by[6]

$$U_F = \exp\left(-iH_s T\right) \exp\left(-iH_F\right). \tag{2.49}$$

This system becomes analytically solvable when we consider no transverse magnetic perturbation, i.e., for $h = 0$. In this limit, the eigenstates of H_s are simply the product states of the individual Pauli matrices σ_i^z. Let us denote such a many-body eigenstate as $|\{s_i\}\rangle$, with $s_i = \pm 1$, such that $\sigma_k^z |\{s_i\}\rangle = s_k |\{s_i\}\rangle$. The action of the Hamiltonian on these states yields $H_s|\{s_i\}\rangle = \left(E_+(\{s_i\}) + E_-(\{s_i\})\right)|\{s_i\}\rangle$, where we separate the energy into an interaction term $E_+(\{s_i\}) = \sum_i J_i s_i s_{i+1}$ and a longitudinal field term $E_-(\{s_i\}) = \sum_i h_i^z s_i$.
Because the pulse H_F acts as a perfect global spin-flip operator, the true Floquet eigenstates of U_F are superpositions of states with opposite spins orientation:

$$|\Phi^{\pm}\rangle = \frac{1}{\sqrt{2}} \left(e^{iTE_-(\{s_i\})/2} |\{s_i\}\rangle \pm e^{-iTE_-(\{s_i\})/2} |\{-s_i\}\rangle \right). \tag{2.50}$$

The corresponding Floquet eigenvalues are given by $\pm \exp\left(-iTE_+(\{s_i\})\right)$. Since discrete time translation symmetry requires that the eigenstates of the Floquet operator U_F cannot be written as short-range correlated product states, this condition is perfectly satisfied here due to the macroscopic long-range correlations inherent to these Schrödinger cat states. In the thermodynamic limit, these symmetric and antisymmetric superposition states become exactly degenerate in quasi-energy. This degeneracy allows for the spontaneous breaking of the internal $\mathbb{Z}_2$ symmetry, meaning the system physically localizes into one of the definite spin configurations, such as $|\{s_i\}\rangle$. Consequently, the periodic drive forces the system to continuously switch back and forth between the two symmetry-broken states, leading to the robust subharmonic oscillations characteristic of a discrete time crystal.
In order to study what arises when we consider $h \neq 0$, numerical analyzes have been made to study the behavior of the system. Figure 2.1 shows the time evolution of the computed averaged expectation value of the Pauli spin operators averaged over 146 disorder configurations and over the spatial interval $i \in [50, 150]$ and considering the initial state of the system to be

[6] We will set $\hbar = 1$ throughout this section.

$[\cos(\pi/8)\,|\uparrow\rangle + \sin(\pi/8)\,|\downarrow\rangle]^{\otimes L}$ for system size $L = 200$, $h = 0.3$ and $T = 1$. The spin-flip part of the Floquet operator is applied instantaneously and after an initial transient, the expectation values oscillate at frequency π/T, half the drive frequency.

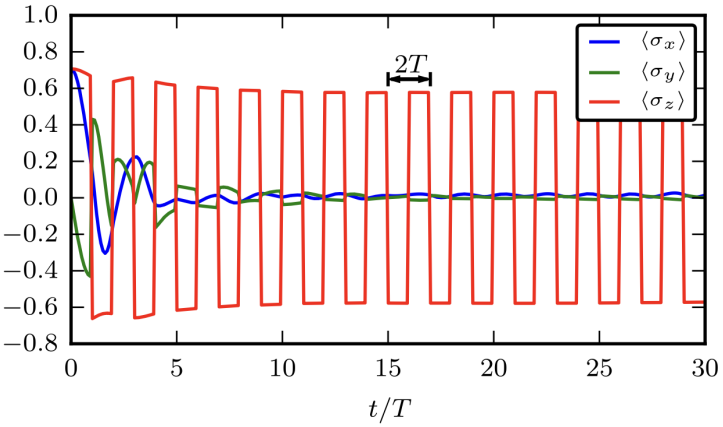

Figure 2.1: Time evolution of the average spin observables $\langle\sigma^x\rangle$, $\langle\sigma^y\rangle$ and $\langle\sigma^z\rangle$ with short range correlated initial state following the dynamics induced by the Hamiltonian 2.48 with $h = 0.3$ and $T = 1$. $\langle\sigma^x\rangle$ and $\langle\sigma^y\rangle$ decay rapidly in time, whereas $\langle\sigma^z\rangle$ exhibits subharmonic oscillations. Reprinted figure from Ref. [11].

Furthermore, we expect that the subharmonic oscillation is persistent for infinite time in the thermodynamic limit. Thus, to extract the time on which the magnetization decays, we define the quantity

$$Z(t) = (-1)^t \langle\sigma^z(t)\rangle \text{sign}(\langle\sigma^z(0)\rangle), \tag{2.51}$$

that characterizes the time evolution of the magnetization starting from random initial product states that are polarized in the z direction. In Figure 2.2, $Z(t)$ has been computed over 500 disorder realizations, for a fixed position i and for three different system size $L = 8, 10, 12$ and for $h = 0.3$ and $T = 1$. We can observe that there is an initial decay of this quantity, which for the parameters chosen here occurs around $t/T = 10$, and then a plateau that extends up to a time that diverges exponentially in the system size. This therefore indicates that the persistent magnetization and subharmonic oscillations observed in Figure 2.1 persist in the thermodynamic limit.

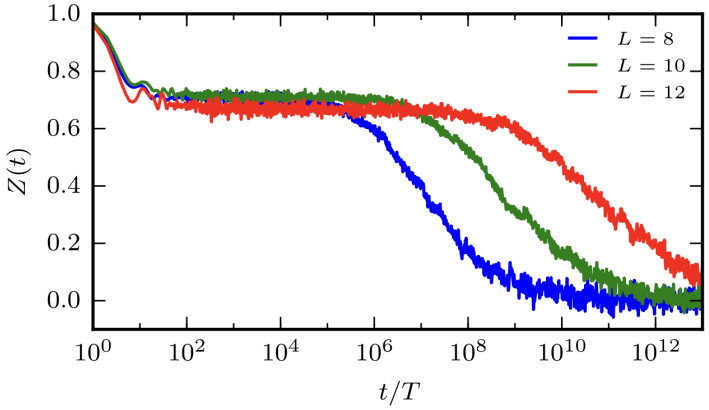

Figure 2.2: Time evolution of the magnetization $Z(t)$, defined in Eq. (2.51), averaged over 500 disorder realizations and initialized in random product states polarized along the z-direction following the dynamics induced by the Hamiltonian (2.48), for $h = 0.3$ and $T = 1$. The curves correspond to system sizes $L = 8$, 10, and 12. Reprinted figure from Ref. [11].

In Ref. [81], the authors considered quite a similar system as the one above with $h = 0$ but they considered that the random interaction are uniformly distributed such that

$$J_i \in [0.8J_z, 1.2J_z], \tag{2.52}$$

with J_z an interaction parameter. Furthermore, they considered a parameter ϵ which act as a perturbation of the phase rotation such that

$$H_F = \left(\frac{\pi}{2} - \epsilon\right) \sum_i \sigma_i^x. \tag{2.53}$$

Thus, they provided a phase diagram in Fig. 2.3 as a function of the interaction strength J_z and the rotation error ϵ with $T = 1$, a discrete time crystal phase emerge in the presence of the interactions and is robust with spin rotation perturbation ϵ. There is also a symmetry unbroken phase which correspond to many body localization but without discrete time translation symmetry breaking and a thermal phase which corresponds to the trivial paramagnet. The main claim of the paper is that there is a phase transition from a discrete time crystal phase to trivial paramagnet which is of the Ising type. They also considered long range interactions which discrete time crystal behavior seems to be even more robust with that.

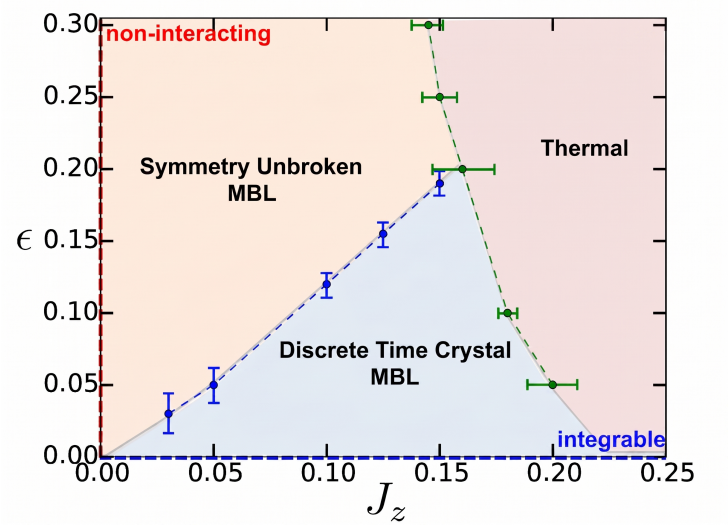

Figure 2.3: Phase diagram of the discrete time crystal, characterized by the Hamiltonian (2.48) with $h = 0$ and the kick (2.53), as a function of the interaction strength J_z and the pulse imperfections ϵ. The discrete time crystal phase appears only in the presence of interactions and is robust with respect to changes of ϵ. Reprinted figure from Ref. [81].

Chapter 3

Open quantum systems theory

In order to investigate how the concept of time crystals may be extended and enriched when the influence of an external environment is taken into account, it is essential to first establish the theoretical framework of open quantum systems. Therefore, before addressing the specific features of time crystals in such contexts, we begin by introducing the fundamental concepts and mathematical tools of open quantum systems that will be relevant for our work. The content of this chapter is based entirely on Refs. [71, 82, 83].

An open quantum system is a quantum system S which is coupled to another quantum system B, referred to as the environment[1]. The composite system $S + B$ is assumed to be closed and therefore evolves according to a unitary dynamics. In contrast, the subsystem of interest S is influenced both by its internal dynamics and by its interaction with the surroundings, which generates system-environment correlations. As a result, it does not in general conserve its energy and does not evolve under a purely unitary Hamiltonian dynamics. The Hilbert spaces associated with the system and the environment are denoted by $\mathcal{H}_S$ and $\mathcal{H}_B$, respectively. The Hilbert space of the total system is then given by the tensor product

$$\mathcal{H} = \mathcal{H}_S \otimes \mathcal{H}_B.$$

The total Hamiltonian $H(t)$ governing the dynamics of the composite system can be written as

$$H(t) = H_S \otimes I_B + I_S \otimes H_B + H_{SB}(t), \tag{3.1}$$

where H_S and H_B are the Hamiltonians of the system and the environment, respectively, and $H_{SB}(t)$ describes their interaction. The time evolution of the total density operator $\rho_{SB}(t)$ is governed by the Liouville-von Neumann equation:

$$\dot{\rho}_{SB}(t) = -\frac{i}{\hbar}\left[H(t), \rho_{SB}(t)\right]. \tag{3.2}$$

Since our primary interest lies in the dynamics of the open system S, we introduce the reduced density operator

$$\rho_S(t) = \mathrm{Tr}_B\big(\rho_{SB}(t)\big) = \sum_{k_B} \langle k_B|\rho_{SB}(t)|k_B\rangle, \tag{3.3}$$

where $\{|k_B\rangle\}$ is an orthonormal basis of $\mathcal{H}_B$, and Tr_B denotes the partial trace over the environmental degrees of freedom. Thus, the state of the system can in principle be determined at any time by solving Eq. (3.2) and then applying Eq. (3.3). However, the motivation for the study of the open system S is that, in many physically important situations, a complete mathematical

[1] When we speak of an open quantum system S, we shall use the general term environment for the system B coupled to it. The quantum system B is called a reservoir when it possesses an infinite number of degrees of freedom such that its mode frequencies form a continuum. It is further called a bath when this reservoir is in a state of thermal equilibrium.

model of the combined system's dynamics is much too complicated. The environment may represent, for example, a reservoir or a heat bath consisting of infinitely many degrees of freedom, in which case an exact treatment requires the solution of an infinite hierarchy of coupled equations of motion. Even if a solution is known, one is still confronted with the task of isolating and determining the relevant physical quantities by averaging over the remaining, irrelevant degrees of freedom. Moreover, one often encounters situations in which the modes of the environment are neither known exactly nor controllable. One therefore seeks to develop a simpler description within a reduced state space formed by a restricted set of physically relevant variables, which is achieved by employing various analytical methods and approximation techniques. Thus, in what follows, we focus exclusively on describing the evolution of the system S by introducing the concept of a dynamical map in open quantum systems. More specifically, we introduce the Gorini-Kossakowski-Sudarshan-Lindblad (GKSL) master equation, which provides a general and consistent description of the time evolution of open quantum systems undergoing Markovian processes, since we restrict our analysis in the following to this type of process.

3.1 GKSL master equation

A quantum map in quantum mechanics is a mathematical transformation, called a superoperator, that transforms a quantum state, described by a density operator, into another one in order to represent a physical process. If we want to characterize the time evolution of the state ρ of a system, we must introduce the concept of quantum dynamical map. A quantum dynamical map is a family of linear maps $\{\Phi_t\}_{t\geq 0}$ such that, for each $t \geq 0$,

$$\Phi_t : \mathcal{L}(\mathcal{H}) \to \mathcal{L}(\mathcal{H}), \tag{3.4}$$

and whose restriction to the set of density operators $\rho \in \mathcal{L}(\mathcal{H})$[2] defines the time evolution of the system:

$$\rho(t) = \Phi_t(\rho(0)). \tag{3.5}$$

For any $t \geq 0$, the map Φ_t is required to be:

- linear,
- trace-preserving: $\mathrm{Tr}[\Phi_t(\rho)] = \mathrm{Tr}[\rho]$,
- Positivity preserving
- Hermiticity-preserving,

and to satisfy the initial condition $\Phi_0 = \mathbb{I}$. A map satisfying these three conditions is said to be a positive and trace-preserving map (PTM). If we are interested in the evolution of an open quantum system S, a dynamical map Φ_t that acts only on S can be extended to the entire system, where the environment B is also taken into account, such that

$$(\Phi_t \otimes \mathbb{I}^d)\rho_{SB}(0) = \rho_{SB}(t) \geq 0, \tag{3.6}$$

and it should still preserve the positivity of the state of the system. This is valid only in the Markovian approximation, where the environment is not affected by the system. Furthermore, this result must hold for any $d \leq \dim(\mathcal{H}_B)$ if Φ_t is a dynamical map. Thus, any valid dynamical map of an open quantum system is a completely positive and trace-preserving map (CPTM). Furthermore, we generally assume that the state of the system ρ_S is initially uncorrelated with the state of the environment at $t = 0$, since we consider that the system and the environment begin to interact at this moment and that the system can usually be regarded as well controlled.

[2] $\mathcal{L}(\mathcal{H})$ is the set of linear transformations acting on a Hilbert space $\mathcal{H}$.

We also assume that the environment is large enough that its interaction with the open quantum system does not cause it to evolve. Thus, let us assume that the initial state of the entire system $S+B$ is given by $\rho_{SB}(0) = \rho_S(0) \otimes \rho_B$. We choose a basis $\{|k_B\rangle\}$ for the environment and denote by $U_{SB}(t)$ the time-evolution operator of $S+B$ over a time t. In this way, every CPTM can be decomposed as:

$$\begin{aligned}\Phi_t[\rho_S(0)] = \rho_S(t) &= \mathrm{Tr}_B[U_{SB}(t)(\rho_S(0)\otimes\rho_B)U_{SB}^\dagger(t)] \\ &= \sum_{k_B} \langle k_B|U_{SB}(t)(\rho_S(0)\otimes\rho_B)U_{SB}^\dagger(t)|k_B\rangle \\ &= \sum_{k_B}\sum_{k'_B} p_{k'_B} \langle k_B|U_{SB}(t)|k'_B\rangle \rho_S(0) \langle k'_B|U_{SB}^\dagger(t)|k_B\rangle\end{aligned}$$

where we have used $\rho_B = \sum_{k_B} p_{k_B} |k_B\rangle \langle k_B|$. We can therefore define the operator $D_{k_B,k'_B} = \sqrt{p_{k'_B}} \langle k_B|U_{SB}(t)|k'_B\rangle$ such that

$$\Phi_t[\rho_S(0)] = \sum_{k_B,k'_B} D_{k_B,k'_B}\rho_S(0)D_{k_B,k'_B}^\dagger = \sum_\alpha D_\alpha\rho_S(0)D_\alpha^\dagger, \tag{3.7}$$

where we have combined the two indices k_B and k'_B into a single index α. Here, D_α and $D_\alpha^\dagger$ are time-dependent and are called the measurement operators. They satisfy

$$\sum_\alpha D_\alpha^\dagger D_\alpha = \mathbb{I}, \tag{3.8}$$

in order to ensure the trace-preserving condition of $\rho_S(t)$. The measurement operators represent the different ways in which a quantum system can evolve as a result of its interaction with its environment, with each operator corresponding to one possible outcome of the evolution.
From this decomposition of dynamical maps, we can now derive the differential form of CPTMs. Let us consider an infinitesimal time interval dt over which the state of the system $\rho(t)$ evolves from time t. Furthermore, we assume that the interaction between the system and the environment is Markovian, i.e. the state of the system at time $t+\mathrm{dt}$ depends only on its state at time t and not on its history prior to time t. In this case, the CPTM characterizing a Markovian process must satisfy the semigroup property:

$$\Phi_{t_1+t_2} = \Phi_{t_1} \circ \Phi_{t_2}, \qquad \forall t_1, t_2 \geq 0. \tag{3.9}$$

The dynamical map can thus be written as

$$\rho(t+\mathrm{dt}) = \sum_\alpha D_\alpha\rho(t)D_\alpha^\dagger. \tag{3.10}$$

Since we consider an infinitesimal time evolution of the system, we can expand the measurement operators so that the probability of a jump occurring is of first order in time:

$$\begin{aligned}D_0 &= \mathbb{I}_S - L_0\mathrm{dt}, \\ D_\alpha &= \sqrt{\mathrm{dt}}L_\alpha, \qquad \alpha \in \mathbb{N}_0^+,\end{aligned} \tag{3.11}$$

since we must have $D_0 = \mathbb{I}_S$ and $D_{\alpha\neq 0} = 0$ at $t = 0$. The measurement operator D_0 corresponds to the evolution of the system when the environment does not affect it, while the other measurement operators D_α correspond to the different outcomes induced by the influence of the environment. Moreover, by inserting Eq. (3.11) into Eq. (3.8) and retaining terms of first order in dt, we find:

$$L_0 + L_0^\dagger = \sum_{\alpha\neq 0} L_\alpha L_\alpha^\dagger. \tag{3.12}$$

Furthermore, L_0 can be decomposed as the sum of a Hermitian term and a non-Hermitian term:

$$L_0 = \frac{L_0 + L_0^\dagger}{2} + \frac{L_0 - L_0^\dagger}{2}, \tag{3.13}$$

which is equivalent to

$$L_0 = \frac{1}{2}\sum_{\alpha\neq 0} L_\alpha L_\alpha^\dagger + iB, \tag{3.14}$$

where we have used Eq. (3.12) and B is a Hermitian operator. However, when we consider a unitary dynamics generated by a Hamiltonian H_S, it is straightforward to see that a single measurement operator, $D_0 = \exp(-iH_S t/\hbar)$, suffices to describe the dynamical map, so that in this case

$$L_0 = \frac{i}{\hbar} H_S. \tag{3.15}$$

Equations (3.14) and (3.15) give the final result

$$L_0 = \frac{1}{2}\sum_{\alpha\neq 0} L_\alpha L_\alpha^\dagger + \frac{i}{\hbar} H_S. \tag{3.16}$$

Let us expand Eq. (3.10) using relations (3.11):

$$\rho_S(t + \mathrm{d}t) = \rho_S(t) - L_0\rho(t)\mathrm{d}t - \rho_S(t)L_0^\dagger \mathrm{d}t + \sum_{\alpha\neq 0} L_\alpha \rho_S(t) L_\alpha \mathrm{d}t + \mathcal{O}(\mathrm{d}t^2). \tag{3.17}$$

Considering a differentiable family of CPTM $\{\Phi_t\}_{t\geq 0}$ between t and $t+\mathrm{d}t$, and using Eq. (3.16), equation (3.17) finally yields the following Markovian master equation:

$$\frac{d\rho}{dt} = -\frac{i}{\hbar}[H_S, \rho_S] + \sum_{\alpha\neq 0}\left(L_\alpha \rho_S L_\alpha^\dagger - \frac{1}{2}\{L_\alpha^\dagger L_\alpha, \rho_S\}\right), \tag{3.18}$$

and every CPTM semigroup can therefore be described via this differential form. Its most general form is called the Gorini-Kossakowski-Sudarshan-Lindblad (GKSL) master equation:

$$\dot{\rho} = \mathcal{L}(\rho), \tag{3.19}$$

where $\mathcal{L}(\cdot)$, called the Liouvillian, is the generator of a quantum dynamical semigroup:

$$\Phi_t = e^{i\mathcal{L}t}, \tag{3.20}$$

and takes the following general form to describe the evolution of an open quantum system:

$$\mathcal{L}(\cdot) = -\frac{i}{\hbar}[H, \cdot] + \sum_\alpha \gamma_\alpha \left(L_\alpha \cdot L_\alpha^\dagger - \frac{1}{2}\{L_\alpha^\dagger L_\alpha, \cdot\}\right), \tag{3.21}$$

where

- H is the Hamiltonian of the system, to which a Lamb-shift contribution H_{LS} can be added when the interaction with the environment modifies the energy levels of the system,
- L_α are the Lindblad operators, which describe the dissipative effect of the environment on the system at a rate γ_α,
- the first term of the Liouvillian represents the unitary evolution of the system, also called the coherent part, whereas the second term represents the irreversible evolution of the system through the effects of dissipation and decoherence caused by the environment; this second term is usually denoted by the dissipation superoperator $\mathcal{D}(\cdot)$.

While we have shown that the GKSL master equation can be viewed as the differential form of a semigroup of CPTM, it can also be derived rigorously from a microscopic model with a clear physical interpretation. This derivation starts from the von Neumann equation for the total system and, by tracing over the environment, yields the reduced dynamics of the subsystem S:

$$\dot{\rho}_S = -\frac{i}{\hbar}\,\mathrm{Tr}_B\big([H_{SB}, \rho_{SB}]\big). \tag{3.22}$$

To proceed, three key approximations are introduced. First, the system-environment coupling is assumed to be weak (Born approximation). Second, the environment is assumed to relax rapidly compared to the system's dynamics (Markov approximation). Finally, rapidly oscillating terms are neglected (secular approximation). Under these conditions, the dynamics of an open quantum system is governed by a quantum dynamical semigroup, and is therefore described by a CPTM whose generator takes the GKSL form. Hence, in what follows, we restrict our attention to Markovian open quantum systems satisfying these conditions, such that their dynamics can be described by the GKSL master equation.

3.2 Liouville space

Observables in quantum physics are described by linear operators acting on a Hilbert space $\mathcal{H}$[3] characterizing the system under study. Furthermore, the state of an open quantum system is represented by the density operator, which is also a linear operator on $\mathcal{H}$. The set of linear operators acting on a Hilbert space $\mathcal{H}$,

$$A : \mathcal{H} \to \mathcal{H}, \qquad |\psi\rangle \mapsto A\,|\psi\rangle\,, \quad \forall\,|\psi\rangle \in \mathcal{H}, \tag{3.23}$$

forms a vector space, commonly denoted by $\mathcal{B}(\mathcal{H})$. When this space is equipped with the Hilbert–Schmidt inner product,

$$\langle A, B\rangle_{HS} = \mathrm{tr}(A^\dagger B), \qquad A, B \in \mathcal{B}(\mathcal{H}), \tag{3.24}$$

it becomes a Hilbert space. This Hilbert space is often referred to as the Liouville space and is denoted by $\mathcal{L}(\mathcal{H})$.
In the theory of open quantum systems, this space provides the natural framework for describing states in terms of density operators. In this context, the Hilbert–Schmidt inner product plays a role analogous to the inner product on $\mathcal{H}$ and is directly related to physical quantities, as it allows one to express expectation values of observables through expressions of the form $\mathrm{tr}(A\rho)$, thereby encoding measurement outcomes and statistical properties of the system.
The usual representation of an operator A in Liouville space is given by a matrix of dimension $\dim(\mathcal{H}) \times \dim(\mathcal{H})$, whose elements are defined with respect to an orthonormal basis $\{|i\rangle\}$ of $\mathcal{H}$ as

$$A = \sum_{i,j} A_{ij}\,|i\rangle\langle j|\,, \qquad \text{with} \quad A_{ij} = \langle i|\,A\,|j\rangle\,. \tag{3.25}$$

However, operators in $\mathcal{L}(\mathcal{H})$ can be represented as column vectors in $\mathcal{H} \otimes \mathcal{H}$, just like elements of $\mathcal{H}$, through the isomorphic vectorization (also called the Choi-Jamiolkowski isomorphism) process

$$A = \sum_{i,j} A_{ij}\,|i\rangle\langle j| \;\longmapsto\; |A\rangle\!\rangle = \sum_{i,j} A_{ij}\,|i\rangle \otimes |j\rangle^*\,. \tag{3.26}$$

[3]Here we restrict the description of the Liouville space considering finite-dimensional Hilbert spaces $\mathcal{H}$.

so that the scalar product of two elements $A, B \in \mathcal{L}(\mathcal{H})$ under this vector mapping is equivalent to the Hilbert–Schmidt inner product:

$$\begin{aligned}\langle\langle A|B\rangle\rangle &= \sum_{m,n} A^*_{mn} B_{mn} \\ &= \sum_{m,n} (A_{nm})^\dagger B_{mn} \\ &= \sum_n (A^\dagger B)_{nn} = \mathrm{tr}(A^\dagger B),\end{aligned} \tag{3.27}$$

and we therefore have

$$|A\rangle\rangle = \sum_i \langle\langle A|C_i\rangle\rangle |C_i\rangle\rangle, \tag{3.28}$$

where $\{|C_i\rangle\rangle\}$ is an orthonormal basis of $\mathcal{H} \otimes \mathcal{H}$.
From a more pictorial point of view, the vectorization of an operator $A \in \mathcal{L}(\mathcal{H})$, with $\dim(\mathcal{H}) = N$, can be written as

$$A \equiv \begin{pmatrix} A_{11} & \cdots & A_{1n} \\ \vdots & \ddots & \vdots \\ A_{n1} & \cdots & A_{nn} \end{pmatrix} \mapsto |A\rangle\rangle \equiv \begin{pmatrix} A_{11} \\ \vdots \\ A_{1n} \\ \vdots \\ A_{nn} \end{pmatrix}. \tag{3.29}$$

Consider superoperators $\varepsilon(\cdot)$ acting on the Liouville space $\mathcal{L}(\mathcal{H})$:

$$\varepsilon(\cdot) : \mathcal{L}(\mathcal{H}) \to \mathcal{L}(\mathcal{H}), \qquad \rho \mapsto \varepsilon(\rho), \quad \rho \in \mathcal{L}(\mathcal{H}), \tag{3.30}$$

such that, by linearity, under vectorization one obtains

$$\varepsilon(\rho) \;\longmapsto\; |\varepsilon(\rho)\rangle\rangle = \boldsymbol{\varepsilon}\, |\rho\rangle\rangle, \tag{3.31}$$

where $\boldsymbol{\varepsilon}$ represents an operator in $\mathcal{L}(\mathcal{H} \otimes \mathcal{H})$[4]. Let us consider $\dim(\mathcal{H}) = N$ and let $\{|C_k\rangle\rangle\}$ be an orthonormal basis of $\mathcal{H} \otimes \mathcal{H}$; then $\boldsymbol{\varepsilon}$ can be decomposed as:

$$\boldsymbol{\varepsilon} = \sum_{i,j} \langle\langle C_i|\varepsilon(C_j)\rangle\rangle |C_i\rangle\rangle\langle\langle C_j|, \tag{3.32}$$

with

$$\langle\langle C_k|\varepsilon(C_k)\rangle\rangle = \mathrm{tr}[C_k^\dagger \varepsilon(C_k)] \tag{3.33}$$

which can be represented by the $N^2 \times N^2$ matrix

$$\begin{pmatrix} \langle\langle C_1|\varepsilon(C_1)\rangle\rangle & \cdots & \langle\langle C_1|\varepsilon(C_{N^2})\rangle\rangle \\ \vdots & \ddots & \vdots \\ \langle\langle C_{N^2}|\varepsilon(C_1)\rangle\rangle & \cdots & \langle\langle C_{N^2}|\varepsilon(C_{N^2})\rangle\rangle \end{pmatrix}. \tag{3.34}$$

The Hilbert–Schmidt inner product allows us to introduce the concept of the adjoint superoperator, which, for all $A, B \in \mathcal{L}(\mathcal{H})$, satisfies

$$\langle\langle A|\varepsilon(B)\rangle\rangle = \langle\langle \varepsilon^\ddagger(A)|B\rangle\rangle \tag{3.35}$$

It satisfies the following property: if the superoperator ε is defined as

$$\varepsilon(\cdot) = A \cdot B, \qquad A, B \in \mathcal{L}(\mathcal{H}),$$

[4]From now on, we adopt the unambiguous convention that $\mathcal{E}(\cdot)$ denotes the superoperator acting on $\mathcal{L}(\mathcal{H})$, while $\mathcal{E}$ denotes its vectorized operator acting on $\mathcal{H} \otimes \mathcal{H}$.

then

$$\varepsilon(\cdot) = A \cdot B \mapsto \varepsilon^{\ddagger} = A^{\dagger} \cdot B^{\dagger}, \tag{3.36}$$

and the vectorization of the adjoint of a superoperator is the Hermitian conjugate of the vectorized operator. For instance, the adjoint of the Liouvillian defined in the previous section is therefore

$$\mathcal{L}^{\ddagger}(\cdot) = -\frac{i}{\hbar}[H, \cdot] + \sum_{\alpha} \gamma_{\alpha} \left(L_{\alpha}^{\dagger} \cdot L_{\alpha} - \frac{1}{2}\{L_{\alpha}^{\dagger} L_{\alpha}, \cdot\} \right). \tag{3.37}$$

Furthermore, if the superoperator ε defined above acts on an operator $C \in \mathcal{L}(\mathcal{H})$, it can be vectorized as

$$\varepsilon(C) = ACB \mapsto |ACB\rangle\!\rangle = \boldsymbol{\varepsilon}|C\rangle\!\rangle = (A \otimes B^{T})|C\rangle\!\rangle. \tag{3.38}$$

Since the Liouvillian given by Eq. (3.21), introduced in the previous section, is a superoperator, it can be vectorized using the property of Eq. (3.38) as

$$\mathcal{L} = -\frac{i}{\hbar}(H \otimes \mathbb{1} - \mathbb{1} \otimes H^{T}) + \sum_{\alpha} \gamma_{\alpha} \left[L_{\alpha} \otimes L_{\alpha}^{*} - \frac{1}{2}(L_{\alpha}^{\dagger} L_{\alpha} \otimes \mathbb{1} + \mathbb{1} \otimes (L_{\alpha}^{\dagger} L_{\alpha})^{T}) \right], \tag{3.39}$$

which is therefore a linear operator acting on $\mathcal{H} \otimes \mathcal{H}$, and the vectorized form of $\mathcal{L}^{\ddagger}(\cdot)$ is simply $\mathcal{L}^{\dagger}$. The introduction of the vectorization procedure proves useful for analyzing certain features of the evolution, particularly those that can be inferred from the spectral decomposition of the Liouvillian in its operator form.
In what follows, we will employ both formalisms, switching unambiguously between them as dictated by the context and by the advantages offered by each representation.

3.3 Spectral properties of the Liouvillian

In this section, we present the main properties of the Liouvillian and its spectrum, as their structure plays a central role in the characterization of time crystals in open quantum systems described by the GKSL master equation.
The GKSL master equation, with a time-independent Liouvillian $\mathcal{L}$ as the generator of the dynamics, admits the following solution:

$$|\rho(t)\rangle\!\rangle = e^{\mathcal{L}t}|\rho(0)\rangle\!\rangle, \tag{3.40}$$

where $e^{\mathcal{L}t}$ is the propagator of the dynamics and $|\rho(0)\rangle\!\rangle$ is the initial state of the open quantum system under study. The dynamics of an open system can be understood by analyzing the spectrum of the Liouvillian matrix $\mathcal{L}$. A first important point is that $\mathcal{L}$ is not necessarily Hermitian nor normal, and therefore not always diagonalizable. We will focus here on the case of a diagonalizable Liouvillian, and simply note that a non-diagonalizable Liouvillian can nevertheless be brought into a Jordan form. We define left and right eigenvectors since, for a non-Hermitian operator, the Hermitian conjugate of a right eigenvector is not necessarily a left eigenvector:

$$\begin{aligned} \mathcal{L}|r_{\mu}\rangle\!\rangle &= \lambda_{\mu}|r_{\mu}\rangle\!\rangle, \\ \mathcal{L}^{\dagger}|l_{\mu}\rangle\!\rangle &= \lambda_{\mu}^{*}|l_{\mu}\rangle\!\rangle. \end{aligned} \tag{3.41}$$

Here are some relevant properties of the spectral decomposition of the Liouvillian:

1. The eigenvectors of $\mathcal{L}$ or $\mathcal{L}^{\dagger}$ corresponding to different eigenvalues are linearly independent. Moreover, they can be chosen to form a bi–orthonormal set, i.e. $\langle\!\langle l_{\mu}|r_{\nu}\rangle\!\rangle = \delta_{\mu\nu}$.

2. The eigenvalues of $\mathcal{L}$ are either real or come in complex-conjugate pairs. The positivity of the evolution requires the eigenvalues to have a non-positive real part, $\mathrm{Re}(\lambda_{\mu}) \leq 0$. Moreover, the Liouvillian always possesses the eigenvalue $\lambda_0 = 0$.

3. The Liouvillian $\mathcal{L}$ ($\mathcal{L}^\dagger$) shares the same right (left) eigenvectors as the propagator $e^{\mathcal{L}t}$ ($e^{\mathcal{L}^\dagger t}$), and the eigenvalues of the latter are $\mathrm{e}^{\lambda_\mu t}$ ($\mathrm{e}^{\lambda_\mu^* t}$).

From these properties, the evolution of the state of the system can be decomposed as

$$|\rho(t)\rangle\!\rangle = \sum_{n,j} c_{n,j}(0)\, \mathrm{e}^{\lambda_n t} |r_{n,j}\rangle\!\rangle, \qquad c_{n,j}(0) = \langle\!\langle l_{n,j}|\rho(0)\rangle\!\rangle, \tag{3.42}$$

where $|r_{n,j}\rangle\!\rangle$ are the right eigenvectors of $\mathcal{L}$ associated with the eigenvalues λ_n.
If the system possesses a single eigenvalue λ_0 with zero real part, then the asymptotic state is unique and corresponds to a stationary steady state:

$$|\rho(t\to\infty)\rangle\!\rangle = \sum_j c_{0,j}(0)\, |r_{0,j}\rangle\!\rangle. \tag{3.43}$$

However, the system may possess additional eigenvalues with zero real part. This motivates the introduction of the asymptotic space, defined as the subspace spanned by the eigenvectors associated with eigenvalues whose real part is zero:

$$\mathrm{As}(\mathcal{H}) = \mathrm{span}\left\{|r_{n,j}\rangle\!\rangle : \ \mathrm{Re}(\lambda_n) = 0\right\}. \tag{3.44}$$

While the asymptotic states of the system belong to $\mathrm{As}(\mathcal{H})$, not every element of this space necessarily represents a valid quantum state. Moreover, in general, the elements of $\mathrm{As}(\mathcal{H})$ are non-decaying rather than strictly stationary, since eigenvalues with non-zero imaginary parts induce time-dependent phases.
Finally, one can define the dissipative gap Δ as

$$\Delta = \min_n |\mathrm{Re}(\lambda_n)|, \quad \text{such that} \quad \mathrm{Re}(\lambda_n) \neq 0, \tag{3.45}$$

which usually sets the characteristic timescale for the convergence towards the asymptotic state of the system.

3.4 Floquet theory in open quantum systems

The study of periodically driven quantum systems naturally leads to the framework of Floquet theory, which provides a powerful way to analyze dynamics under time-periodic generators. While this theory is well established for isolated systems, its extension to open quantum systems and more precisely, in our case, to open quantum systems described by a Liouvillian dynamics, where dissipation and decoherence play a role, reveals a much richer structure.
In Markovian open quantum systems, the time evolution of the density matrix $\rho(t)$ is governed by a quantum master equation of Liouvillian form:

$$\partial_t \rho = \mathcal{L}_t \rho, \tag{3.46}$$

where $\mathcal{L}_t$ is the time-dependent Liouvillian superoperator, which has the same form as in equation (3.21), with the Hamiltonian and the jump operators now being time-dependent. When the system is subject to periodic driving with period T, the Liouvillian satisfies

$$\mathcal{L}_{t+T} = \mathcal{L}_t, \tag{3.47}$$

making the dynamics explicitly time-periodic.
For such systems, the formal solution to the evolution equation is given by the Dyson time-ordered exponential:

$$\mathcal{E}(t) = \mathcal{T} \exp\left(\int_0^t ds\, \mathcal{L}(s)\right), \tag{3.48}$$

where $\mathcal{T}$ denotes the time-ordering operator. In contrast to the time-independent case, the instantaneous spectral properties of $\mathcal{L}(t)$ do not directly determine the long-time behavior. Instead, the central object of interest is the Floquet propagator, defined as the evolution map over one full period:

$$\mathcal{E}_F = \mathcal{T} \exp\left(\int_0^T ds\, \mathcal{L}(s)\right). \tag{3.49}$$

This map fully characterizes the stroboscopic dynamics, i.e., the evolution of the system at discrete times $t_n = nT$, through repeated application:

$$\mathcal{E}(t_n) = \mathcal{E}_F^n. \tag{3.50}$$

The Floquet map $\mathcal{E}_F$ is a CPTM. As a consequence, its eigenvalues λ_α lie within or on the unit disk in the complex plane, and at least one eigenvalue is exactly equal to one. The corresponding eigenoperator defines the stroboscopic steady state ρ_{ss}, satisfying

$$\mathcal{E}_F(\rho_{\text{ss}}) = \rho_{\text{ss}}. \tag{3.51}$$

More generally, the eigenvalue equation

$$\mathcal{E}_F(\rho_\alpha) = \lambda_\alpha \rho_\alpha \tag{3.52}$$

provides a spectral decomposition of the dynamics. If the Floquet map is diagonalizable, its eigenmodes form a complete basis for operators, allowing any initial state to be expanded as

$$\rho(0) = \rho_{\text{ss}} + \sum_{\alpha \geq 1} c_\alpha \rho_\alpha. \tag{3.53}$$

Under stroboscopic evolution, each mode evolves independently:

$$\rho(nT) = \rho_{\text{ss}} + \sum_{\alpha \geq 1} c_\alpha (\lambda_\alpha)^n \rho_\alpha. \tag{3.54}$$

The long-time behavior is governed by the eigenvalues with the largest magnitudes. In particular, in the Floquet picture, the asymptotic subspace is spanned by the eigenmodes whose eigenvalues lie on the unit circle, often referred to as the peripheral spectrum. These modes give rise to nontrivial steady states and persistent oscillations, which are central to phenomena such as time crystals.

For dissipative systems, all eigenvalues satisfy $|\lambda_\alpha| \leq 1$, and eigenvalues strictly inside the unit disk correspond to decaying modes. The slowest decay rate is set by the eigenvalue λ_1 with the second-largest magnitude. This defines the dissipative Floquet gap:

$$\Delta_F = -\frac{1}{T} \ln |\lambda_1|, \quad \text{with} \quad \lambda_1 = \max_{n \neq 0}(|\lambda_n|) \quad \text{such that} \quad |\lambda_n| \leq \lambda_0, \tag{3.55}$$

which quantifies the rate at which the system approaches its steady state. It plays a crucial role in identifying dynamical phase transitions in driven open systems.

A key distinction from isolated systems is that, in the presence of dissipation, the Floquet propagator generally cannot be expressed as the exponential of a time-independent effective Liouvillian. This lack of reduction to an effective static description highlights the fundamentally richer dynamics of periodically driven open quantum systems.

In order to simplify the expression of the Floquet quantum map $\mathcal{E}_F$ and to perform an analytical study of Floquet open quantum systems, we consider periodic kicks acting on the unitary dynamics, described by the time-dependent Hamiltonian:

$$H(t) = H_0 + H_1 \sum_n \delta(t - nT), \quad n \in \mathbb{Z}, \tag{3.56}$$

where H_0 represents the static part of the Hamiltonian, H_1 corresponds to an instantaneous kick applied periodically at times nT, and the dissipative part of the Liouvillian remains time-independent. In this case, the Floquet map is given by

$$\mathcal{E}_F(\rho) = U_{\mathrm{K}} \mathrm{e}^{\mathcal{L}_0 T}(\rho) U_{\mathrm{K}}^\dagger, \tag{3.57}$$

with $\mathcal{L}_0$ the Liouvillian of the static dissipative evolution and $U_{\mathrm{K}} = \exp(-iH_1)$ the unitary kick operator. Furthermore, since the Floquet map is a superoperator, it can be vectorized into an operator using Eq. (3.38):

$$\mathcal{E}_F = U_{\mathrm{K}} \otimes U_{\mathrm{K}}^* \exp(\mathcal{L}_0 T). \tag{3.58}$$

A remark about the Floquet map characterizing kicked systems is that its spectrum is generally not the same as that of $e^{\mathcal{L}_0}$, since the unitary kick operator typically alters the spectrum of a CPTM [71].

3.5 Symmetry in open quantum systems

As a brief reminder, in closed quantum systems, a symmetry is simply a unitary operator that commutes with the Hamiltonian, inducing a conserved quantity. When the system is coupled to an environment, however, this single condition is no longer sufficient: the dissipative channels introduced by the jump operators $\{L_k\}$ can either respect or break the symmetry independently of H, giving rise to a richer classification. One must therefore distinguish between symmetries that constrain the full microscopic dynamics, both coherent and dissipative, and those that act only at the level of the density-matrix evolution as a whole. A strong symmetry yields a genuinely conserved quantity even in the presence of dissipation, whereas a weak symmetry merely constrains the structure of the steady-state manifold without protecting any local conserved quantity. Indeed, in open quantum systems whose evolution is described by the GKSL master equation, two distinct notions of symmetry can be defined:

- A unitary operator U is called a strong symmetry of the Liouvillian $\mathcal{L}$ if it commutes with both the Hamiltonian and each Lindblad operator individually:

$$[U, H] = 0 \qquad \text{and} \qquad [U, L_k] = 0 \quad \forall\, k. \tag{3.59}$$

  As a consequence, the Hilbert space $\mathcal{H}$ decomposes into invariant subspaces labeled by symmetry sectors, each evolving independently. The steady state is then generally not unique: there is one for each symmetry sector. In the closed-system limit ($L_k = 0$), condition (3.59) reduces to $[U, H] = 0$, or equivalently $UHU^\dagger = H$.

- The notion of weak symmetry is less restrictive: U is a weak symmetry if $\mathcal{L}$ commutes with the adjoint action of U,

$$\mathcal{L}\Big(U\rho U^\dagger\Big) = U\,\mathcal{L}(\rho)\,U^\dagger \qquad \Longleftrightarrow \qquad \mathcal{L}\,\mathcal{U} = \mathcal{U}\,\mathcal{L}, \tag{3.60}$$

  where $\mathcal{U}(\cdot) = U \cdot U^\dagger$. Unlike a strong symmetry, U need not commute with each L_k separately. The consequence is more moderate: it is the Liouville space that decomposes into symmetry sectors, rather than $\mathcal{H}$ itself. The Liouvillian can be block-diagonalized, but this does not necessarily imply multiple steady states. Every strong symmetry is, in particular, a weak symmetry, but the converse does not hold in general.

Both notions admit anti-unitary counterparts, which are not of concern here. Furthermore, for any steady state ρ_{ss} satisfying $\mathcal{L}(\rho_{\mathrm{ss}}) = 0$ and any symmetry U_i, the state $U_i \rho_{\mathrm{ss}} U_i^\dagger$ is also a steady state, and the expectation value of an observable A in that state reads

$$\langle A \rangle_{U_i \rho_{\mathrm{ss}} U_i^\dagger} = \mathrm{tr}\Big[U_i^\dagger A\, U_i\, \rho_{\mathrm{ss}}\Big] = \langle U_i^\dagger A\, U_i \rangle_{\rho_{\mathrm{ss}}}. \tag{3.61}$$

Chapter 4

Time crystals in open quantum systems

This chapter is the core of the thesis and surveys the landscape of time crystals that emerge in open quantum systems. We first treat discrete time crystals in the dissipative setting, including the instructive case of a single dephasing spin-s. We then turn to continuous time crystals and continuous quasi time crystals, illustrated by a driven collective spin and by two coupled driven–dissipative collective spins. Finally, we study time glasses, illustrated by a kicked collective-spin model. The objective is to reformulate, define and classify these phases under GKSL dynamics, and to present our own contribution to their analysis.
A summary of the properties of the different types of time crystals in open quantum systems presented in this chapter is provided in Table II, which appears in the Conclusion.

4.1 Discrete time crystals in open quantum systems

As seen in chapter 2, discrete time crystals are a genuine out-of-equilibrium phase of matter, characterized by the spontaneous breaking of the discrete time-translation symmetry of a periodically driven system. This discussion, however, has so far been restricted to closed quantum systems, which correspond to an idealized situation: in practice it is impossible to isolate a system completely from its environment. Realistically, one must therefore account for the effects of the environment and ask whether this phase of matter survives. In fact, the π-spin-glass DTC that arises in disordered spin systems, stabilized by many-body localization, does not survive once the system is coupled to an environment [24].

This fragility shows that the notion of a discrete time crystal cannot simply be transposed from the closed to the open setting. It must be reformulated in the language of open quantum systems (OQS). In the present work we adopt the Markovian description provided by the GKSL master equation, which governs the most widely studied class of dissipative time crystals. Within this framework our aim is twofold. First, to clarify the role played by dissipation, which is far from being purely detrimental: while it destroys the MBL-protected DTC, a suitably engineered dissipation can also stabilize time-crystalline order that would not exist in the closed system [26]. Second, to establish how the phase can be defined and identified in this open setting.

4.1.1 Definitions and properties

Now that the relevant theoretical tools have been introduced, we can present the central idea underlying the concept of a discrete time crystal. The phenomenological definition of discrete time crystals in isolated systems, provided in section 2.2.2, must be appropriately adapted to the framework of OQS, while preserving the essential defining properties [71]:

- First, for an OQS to be characterized as a discrete time crystal, the discrete time-translation symmetry of the governing equation of motion must be spontaneously broken. This symmetry breaking is manifested through a suitable order parameter exhibiting subharmonic oscillations.
- Second, these subharmonic oscillations must be robust over a wide range of system parameters; equivalently, they must be stable against perturbations.
- Third, the subharmonic response must persist indefinitely in time in the thermodynamic limit.

While the concept of time crystals relies on the spontaneous breaking of discrete time-translation symmetry, it is often naturally associated with signatures that emerge in the thermodynamic limit. In this regime, many OQS that exhibit time crystallinity can be effectively described using a mean-field approach, which reduces the dynamics to a set of nonlinear equations governing the evolution of the relevant observables. Consequently, a large fraction of studies on discrete time crystals adopt this framework, in which the spontaneously broken discrete time-translation symmetry is characterized by a limit cycle, or by subharmonic oscillations around a stable state [27, 84–86]. This classical framework facilitates the study of time crystallinity and helps to identify the phase transition and the relevant parameters describing the discrete time crystal behavior. However, such approaches typically neglect genuine quantum correlations and also fail to predict the dynamical behavior of finite-size systems: in any finite dissipative system, the system usually settles into a time-independent steady state ρ_{ss} after a sufficiently long time. Thus, a fully quantum treatment, one that can characterize the finite system and capture its convergence toward the mean-field behavior when increasing the system size, calls for a more precise definition rooted in the properties of OQS.
Since discrete time crystals must exhibit both synchronization among the microscopic degrees of freedom and subharmonic temporal dynamics of the synchronized collective motion, the correlation function given by Eq. (2.17), used to define time crystals in section 2.1.2, can be generalized to the framework of OQS and serve as a useful tool to identify this kind of behavior. The correlation function can be defined as

$$C_M(t) = \langle M(t)M(0)\rangle_{\text{ss}} = \text{Tr}[M(t)M(0)\rho_{\text{ss}}], \tag{4.1}$$

where M is the total order parameter, obtained by integrating the local order parameter $m(x)$ over all space:

$$M = \frac{1}{V^2}\int m(x)dx, \tag{4.2}$$

and ρ_{ss} is the steady state of the system and V is the volume of the system [34]. In the thermodynamic limit, the behavior of the correlation function is given by

$$C_M^{\infty}(t) = \lim_{V\to\infty} C_M(t). \tag{4.3}$$

In particular, the equal-time correlation $C_M^{\infty}(0)$ captures spatial correlations and acts as a static order parameter. Hence, using the autocorrelation function $C_M^{\infty}(t)$ in the thermodynamic limit, we can characterize discrete time crystals:

Correlation-based definition of discrete time crystals [34, 87]:
Discrete time crystals are defined by the persistence of a finite order parameter, $C_M^{\infty}(0) > 0$, together with persistent subharmonic oscillations of the correlation function, i.e. $C_M^{\infty}(t) = C_M^{\infty}(nT)$ with $n > 1$ an integer and T the period of the external driving.

This behavior exhibited by discrete time crystals can be distinguished from a disordered phase, corresponding to a phase in which no spontaneous symmetry breaking appears ($C_M^\infty(t) = 0$), and from a static, spatially long-range-ordered phase ($C_M^\infty(t) = \text{constant} \neq 0$), in which the correlation function is time-independent, as discussed in section 1.2.2. Of course, this property alone is not sufficient to define a discrete time crystal, since discrete time crystals must also be robust to perturbations.
Another way to characterize discrete time crystals, when the dissipative dynamics of the OQS can be described by the GKSL master equation, is in terms of the spectral properties of the Floquet map $\mathcal{E}_\mathrm{F}$. Within this framework, *Riera-Campeny et al.* [71] proposed a definition and an identification criterion for discrete time crystals in open quantum systems based on the Floquet propagator:

Spectral definition of DTCs:
Consider an OQS whose dynamics is governed by a GKSL master equation with a time-periodic Liouvillian, i.e. $\mathcal{L}_{t+T} = \mathcal{L}_t$. The evolution over one period defines a completely positive trace-preserving map, known as the Floquet map $\mathcal{E}_\mathrm{F}$, which captures the stroboscopic dynamics of the system.
An OQS is said to exhibit discrete time-crystalline behavior if the associated Floquet propagator satisfies the following three conditions:

1. **Discrete time-translation symmetry breaking:** There exists at least one eigenvalue $\varepsilon_* \neq 1$ of $\mathcal{E}_\mathrm{F}$ with $|\varepsilon_*| = 1$ such that $\varepsilon_*^N = 1$ for some integer N.
2. **Rigidity of the oscillations:** The eigenvalue ε_* must be linearly robust; that is, given a deformation of the evolution $\mathcal{E}_\mathrm{F} \mapsto \mathcal{E}_\mathrm{F} + \eta\mathcal{V}$, the susceptibility $\mathcal{X}^{(1)} = \left|\left(\frac{\partial \varepsilon_*}{\partial \eta}\right)_{\eta=0}\right| = 0$.
3. **Persistence at infinite time:** The decay timescale of the subharmonic oscillations is fixed by the dissipative Floquet gap $\Delta_\mathrm{F} = -\frac{1}{T}\ln|\varepsilon_*|$, which must vanish in the thermodynamic limit.

The first condition of the definition is related to the stroboscopic evolution of the OQS subjected to periodic kicks. Let us consider a Floquet propagator characterizing a kicked OQS that has the eigenvalues $\{1, e^{i\pi}\}$ in its peripheral spectrum. The state of the system after a large number of oscillations is well approximated, thanks to Eq. (3.54), by

$$\lim_{N\to\infty} \rho(NT) = \lim_{N\to\infty} \mathcal{E}_\mathrm{F}^N(\rho(0)) \approx \rho_\mathrm{ss} + c_*(e^{i\pi})^N\rho_*, \tag{4.4}$$

where c_* is a coefficient related to the initial condition and ρ_* is the eigenstate associated with the eigenvalue $e^{i\pi}$. Thus, this is the behavior of an OQS in a discrete time-crystal phase, with subharmonic oscillations of periodicity $2T$.
The second condition is necessary but not sufficient for a strong definition of a discrete time crystal in an open quantum system. Indeed, time crystallinity is regarded as a non-equilibrium phase of matter, so one would expect a discrete time crystal to be robust to perturbations at all orders, and not only at first order as in [71]. While the aim of this master's thesis is to provide a complete overview of the concept of time crystals, we will not pursue this direction. As we will see, this "weak" definition of a discrete time crystal allows time-crystalline signatures to be observed in systems without collective interactions. However, systems with collective interactions must be considered in order to obtain more robust subharmonic oscillations, since collective jump operators are crucial for producing oscillations that are more robust to rotation-error perturbations, as shown for a short-range open XY model [71].

The third condition makes it possible to link the persistence of subharmonic oscillations in the infinite-time limit with a relevant parameter characterizing the rate at which the steady state is reached. Indeed, if there exists a value other than the trivial eigenvalue 1 in the peripheral spectrum, the system reaches a non-equilibrium steady state in the infinite-time limit.

In the following section, we present the "weak" discrete time crystal through the example of a dephasing single qubit, which, as we will see, satisfies the definition based on the Floquet spectrum. We will therefore focus on this latter definition in order to become more familiar with the concept, while in section 4.3.3 we will present a system that supports discrete time crystallinity, exhibiting spontaneous symmetry breaking in the true sense of the term.

4.1.2 Dephasing of a single spin-s quantum system

In this section, we present a simple and intuitive OQS that satisfies the spectral definition of discrete time crystals introduced in the previous section, in order to illustrate the underlying mechanism. Specifically, we consider a dephasing single-qubit system exhibiting period-doubled subharmonic oscillations, as introduced in Ref. [71]. We then generalize this construction to higher-spin systems subjected to dephasing, demonstrating the emergence of higher-order subharmonic oscillations. In the following, we consider the spin operators S^α with $\alpha = x, y, z$, associated with the spin-s under study. Furthermore, we set $\hbar = 1$.

Qubit (spin-1/2)
Let us consider a single qubit subjected to pure dephasing. The dynamics is governed by the Liouvillian

$$\mathcal{L}(\rho) = \frac{1}{2}\left[S^z, \rho\right] + \kappa\left(S^z \rho S^z - \rho\right), \tag{4.5}$$

where κ denotes the dephasing rate. The eigenvalues of the Liouvillian are

$$\{\lambda_i\} = \{0, -2\kappa - i, -2\kappa + i\}, \tag{4.6}$$

and the asymptotic subspace is spanned by the eigenoperators associated with the zero eigenvalue,

$$\mathrm{As}(\mathcal{H}) = \{|0\rangle\langle 0|,\ |1\rangle\langle 1|\}. \tag{4.7}$$

Now consider applying a unitary kick of the form $U_\mathrm{K} = \exp(-i\pi S^x/2) = -iS^x$. Using Eq. (3.58), the corresponding Floquet propagator reads

$$\mathcal{E}_\mathrm{F} = S^x \otimes S^x\ \exp(\mathcal{L}T), \tag{4.8}$$

and its spectrum is given by

$$\{\varepsilon_i\} = \{1, -1, e^{-2\kappa T}, e^{-2\kappa T}\}. \tag{4.9}$$

The four eigenvalues are illustrated in Figure 4.1a for $\kappa = 0.1$ and $T = 1$. The eigenoperators associated with the eigenvalues 1 and -1 are the identity $\mathbb{I}$ and S^z, respectively.
Consider an initial state of the form

$$\rho(0) = a\,|0\rangle\langle 0| + (1-a)\,|1\rangle\langle 1|, \tag{4.10}$$

with $a \in [0, 1]$. This state can be rewritten in the Floquet asymptotic subspace $\{\mathbb{I}, S^z\}$ as

$$\rho(0) = \frac{1}{2}\left(\mathbb{I} + (2a-1)S^z\right). \tag{4.11}$$

The stroboscopic dynamics is then given by

$$\rho(nT) = \mathcal{E}_\mathrm{F}^n\big(\rho(0)\big) = \frac{1}{2}\left(\mathbb{I} + (-1)^n(2a-1)S^z\right). \tag{4.12}$$

Equivalently, this can be expressed as

$$\rho(nT) = a\,|0 \oplus n\rangle\langle 0 \oplus n| + (1-a)\,|1 \oplus n\rangle\langle 1 \oplus n|, \tag{4.13}$$

where $\oplus$ denotes addition modulo 2. This result reveals a period-doubled subharmonic response. Indeed, using S^z as an order parameter, one finds

$$S^z(nT) = \mathrm{Tr}\big(S^z \rho(nT)\big) = (-1)^n(2a-1), \tag{4.14}$$

showing oscillations with period $2T$ and amplitude $2a-1$, while the expectation values of S^x and S^y vanish over time. For instance, starting from the initial state $|0\rangle\langle 0|$ ($a = 1$), the oscillation amplitude is maximal and equal to 1, as illustrated in Figure 4.1b. Importantly, this subharmonic behavior persists indefinitely, as the Floquet gap Δ_F vanishes.
Furthermore, it is important to emphasize that the subharmonic oscillation emerges independently of the chosen initial state. Indeed, the Liouvillian (4.5) induces decoherence, which suppresses the off-diagonal elements of the density matrix in the standard basis. Physically, these off-diagonal terms encode quantum coherence between different states; their decay therefore corresponds to the loss of phase coherence and the transition toward a classical probabilistic mixture. In contrast, the diagonal elements of the density matrix, which represent the populations, remain invariant under the Liouvillian evolution and are entirely determined by the initial condition. This is a consequence of the fact that S^z is a strong symmetry of the system. As a result, the system retains memory of its initial populations even as coherence is lost. The action of the periodic kick is then to alternate the sign associated with these populations, effectively inducing a nontrivial dynamical modulation of the state.

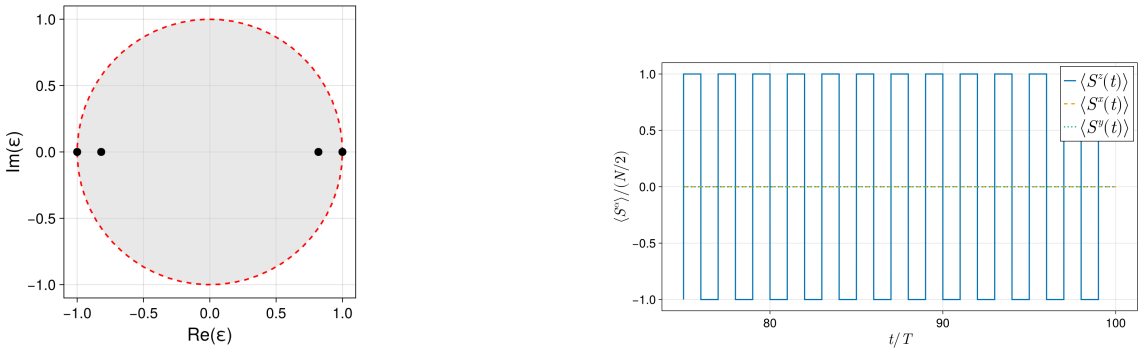

(a) (b)

Figure 4.1: Qubit ($N = 1$). (a) Spectrum of the Floquet propagator (4.8) for $\kappa = 0.1$ and $T = 1$. The peripheral spectrum is highlighted with a dashed red line, while the decaying subspace is shown in gray. (b) Subharmonic oscillations of the normalized order parameter $\langle S^z\rangle/(N/2)$ over the time interval $t/T \in [75, 100]$.

Since the first and third conditions for realizing a discrete time crystal are satisfied, we now turn to the question of rigidity. To this end, we consider a perturbed kick corresponding to a rotation error,

$$U_{\mathrm{K,pert}} = \exp\left(-i(\tfrac{\pi}{2} + \eta)S^x\right), \tag{4.15}$$

where η parametrizes the strength of the perturbation. The corresponding Floquet map becomes

$$\mathcal{E}_{\mathrm{F,pert}} = U_{\mathrm{K,pert}} \otimes U^*_{\mathrm{K,pert}}\ \exp\left(\mathcal{L}T\right). \tag{4.16}$$

Its spectrum can be evaluated perturbatively as

$$\{\varepsilon_i\} = \{1, -1, e^{-2\kappa T}, e^{-2\kappa T}\} + \mathcal{O}(\eta^2). \tag{4.17}$$

We can then compute the susceptibility $\mathcal{X}^{(1)}$ associated with the eigenvalue -1. It vanishes, since this eigenvalue is affected only at second order in η.
In Figure 4.2a, the decay of the subharmonic response is illustrated by examining the amplitude, using the same time window and initial state as in Figure 4.1b, but with a finite rotation error $\eta = 0.1$. Furthermore, Figure 4.2b shows how the dissipative Floquet gap $\Delta_{\mathrm{F}}(\eta)$ evolves as a function of the perturbation strength η.

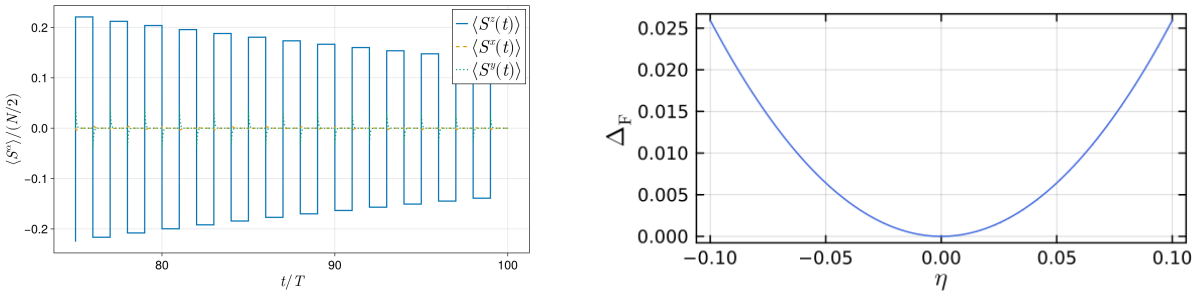

(a) (b)

Figure 4.2: Qubit ($N = 1$). (a) Decaying subharmonic oscillations of the normalized order parameter $\langle S^z\rangle/(N/2)$ over the time interval $t/T \in [75, 100]$, with $\kappa = 1$, $\eta = 0.1$ and an initial amplitude equal to 1. (b) Evolution of the dissipative Floquet gap Δ_{F} as a function of the perturbation parameter η with $\kappa = 1$.

Qudit (spin-$j > 1/2$)
Let us consider a single qudit of spin 1 subjected to pure dephasing. The dynamics is therefore governed by the Liouvillian (4.5), with the spin operators now acting on the spin-1 Hilbert space. The spectrum of the Liouvillian is given by

$$\left\{0, -8\kappa + i, -2\kappa + \frac{1}{2}i, -2\kappa - \frac{1}{2}i\right\}, \tag{4.18}$$

where the eigenvalue 0 is threefold degenerate and the other eigenvalues are twofold degenerate. The asymptotic subspace is given by:

$$\mathrm{As}(\mathcal{H}) = \{|-1\rangle\langle -1|,\ |0\rangle\langle 0|, |1\rangle\langle 1|\}. \tag{4.19}$$

Now consider applying a unitary kick that performs a cyclic permutation of the states $|-1\rangle \to |0\rangle \to |1\rangle$, of the form

$$U_{\mathrm{K}} = \begin{pmatrix} 0 & 0 & 1 \\ 1 & 0 & 0 \\ 0 & 1 & 0 \end{pmatrix}, \tag{4.20}$$

in the spin-1 basis $\{|-1\rangle, |0\rangle, |1\rangle\}$. The Floquet propagator of this system is

$$\mathcal{E}_{\mathrm{F}} = U_{\mathrm{K}} \otimes U_{\mathrm{K}} \exp(\mathcal{L}T), \tag{4.21}$$

and its eigenvalues located on the peripheral spectrum are

$$\{\varepsilon_i^*\} = \{1, \mathrm{e}^{i\pi/3}, \mathrm{e}^{i2\pi/3}\}, \tag{4.22}$$

and all the eigenvalues of $\mathcal{E}_{\mathrm{F}}$ can be observed in Figure 4.3a for $\kappa = 0.1$ and $T = 1$. Furthermore, the eigenoperators spanning the Floquet asymptotic subspace, represented in the standard basis, are

$$\mathbb{I} = \begin{pmatrix} 1 & 0 & 0 \\ 0 & 1 & 0 \\ 0 & 0 & 1 \end{pmatrix}, \quad A = \begin{pmatrix} \mathrm{e}^{i2\pi/3} & 0 & 0 \\ 0 & \mathrm{e}^{-i2\pi/3} & 0 \\ 0 & 0 & 1 \end{pmatrix}, \quad A^\dagger = \begin{pmatrix} \mathrm{e}^{-i2\pi/3} & 0 & 0 \\ 0 & \mathrm{e}^{i2\pi/3} & 0 \\ 0 & 0 & 1 \end{pmatrix}, \tag{4.23}$$

associated with the eigenvalues 1, $e^{i\pi/3}$, and $e^{-i\pi/3}$, respectively.
Consider an initial state of the form

$$\rho(0) = a\,|-1\rangle\langle -1| + b\,|0\rangle\langle 0| + (1-a-b)\,|1\rangle\langle 1|, \tag{4.24}$$

with $a, b \in [0,1]$ and $a+b \leq 1$. This state can be rewritten in the Floquet asymptotic subspace $\{\mathbb{I}, A, A^\dagger\}$ as

$$\rho(0) = \frac{1}{3}\left[(1-a-b)\mathbb{I} + (2a+b-1)A + (2b+a-1)A^\dagger\right]. \tag{4.25}$$

The stroboscopic dynamics is then given by

$$\rho(nT) = \mathcal{E}_{\mathrm{F}}^n\big(\rho(0)\big) = \frac{1}{3}\left[(1-a-b)\mathbb{I} + e^{in\pi/3}(2a+b-1)A + e^{-in\pi/3}(2b+a-1)A^\dagger\right]. \tag{4.26}$$

Equivalently, this can be expressed as

$$\rho(nT) = \begin{cases} a\,|-1\rangle\langle -1| + b\,|0\rangle\langle 0| + (1-a-b)\,|1\rangle\langle 1|, & n \equiv 0 \pmod 3 \\ a\,|0\rangle\langle 0| + b\,|1\rangle\langle 1| + (1-a-b)\,|-1\rangle\langle -1|, & n \equiv 1 \pmod 3 \\ a\,|1\rangle\langle 1| + b\,|-1\rangle\langle -1| + (1-a-b)\,|0\rangle\langle 0|, & n \equiv 2 \pmod 3 \end{cases} \tag{4.27}$$

This result reveals a period-tripled subharmonic response. Indeed, using S^z as an order parameter, one finds

$$S^z(nT) = \mathrm{Tr}\big(S^z\rho(nT)\big) = \begin{cases} 1-2a-b, & n \equiv 0 \pmod 3 \\ -1+a+2b, & n \equiv 1 \pmod 3 \\ a-b, & n \equiv 2 \pmod 3 \end{cases}, \tag{4.28}$$

showing oscillations with period $3T$ and an amplitude that depends on the values of a and b, while the expectation values of S^x and S^y vanish over time. For instance, starting from the initial state $|-1\rangle\langle -1|$ (i.e., $a=1$ and $b=0$), the oscillation amplitude is maximal and equal to 1, as illustrated in Figure 4.3b. Importantly, this subharmonic behavior persists indefinitely, as the Floquet gap Δ_{F} vanishes for both eigenvalues $e^{i\pi/3}$ and $e^{i2\pi/3}$.

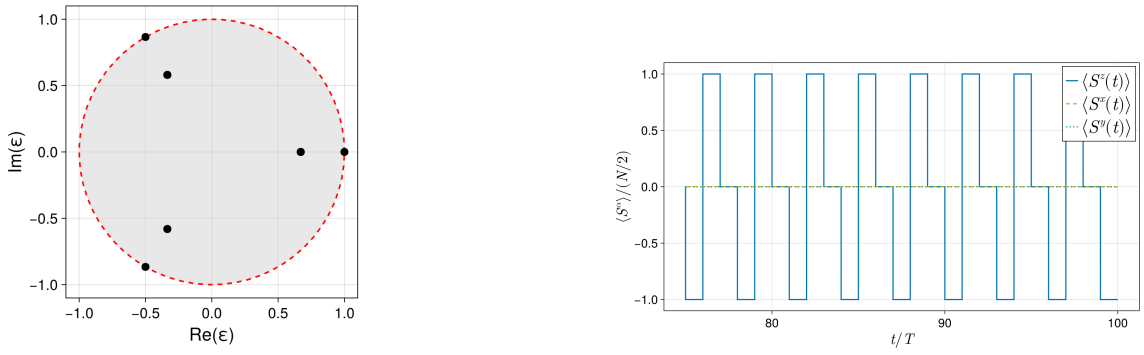

(a) (b)

Figure 4.3: Spin-1 ($N=2$) (a) Spectrum of the Floquet propagator (4.21) for $\kappa = 0.1$ and $T=1$. The peripheral spectrum is highlighted with a dashed red line, while the decaying subspace is shown in gray. (b) Subharmonic oscillations of period $3T$ of the normalized order parameter $\langle S^z\rangle/(N/2)$ over the time interval $t/T \in [75, 100]$.

As we can see, the first and third conditions for being a discrete time crystal are also fulfilled for a spin-1 qudit subject to dephasing. Let us now study the rigidity of this system by considering a rotation-error perturbation. To this end, we consider the generator G of the cyclic permutation induced by the unitary kick U_{K}, given by:

$$G = \frac{2}{\sqrt{3}} \begin{pmatrix} 0 & -i & i \\ i & 0 & -i \\ -i & 0 & i \end{pmatrix}, \tag{4.29}$$

in the spin-1 basis $\{|-1\rangle, |0\rangle, |1\rangle\}$. Hence, the generator G produces a permutation of the spin states through a rotation by $\pi/3$ in the spin-1 space:

$$U_{\mathrm{K}} = \exp(-i\pi G/3). \tag{4.30}$$

Thus, let us introduce a parameter η characterizing a rotation error, which therefore induces an error in the cyclic-permutation kick:

$$U_{\mathrm{K,pert}} = \exp\left(-i\left(\frac{\pi}{3} + \eta\right) G\right), \tag{4.31}$$

such that the new Floquet propagator is therefore given by

$$U_{\mathrm{F}} = U_{\mathrm{K,pert}} \otimes U_{\mathrm{K,pert}} \exp(\mathcal{L}T). \tag{4.32}$$

However, the eigenvalues cannot be computed analytically, since the characteristic polynomial $\mathrm{cp}(z;\eta) = \det(U_{\mathrm{F}}(\eta) - z\mathbb{I}) = 0$ is of degree nine in z, for which there is no general analytical method of solution. Nevertheless, we can gain some insight into the order at which the perturbation η enters the eigenvalues, and hence assess whether the second condition for a discrete time crystal is satisfied. Let the eigenvalues of $U_{\mathrm{F}}(\eta)$ be denoted by $\varepsilon_j(\eta)$, with $j = 1, \ldots, 9$. The characteristic polynomial can then be written as

$$\mathrm{cp}(z;\eta) = c(z - \varepsilon_1(\eta))...(z - \varepsilon_9(\eta)), \tag{4.33}$$

where c a constant and the ε_i denote the different eigenvalues. Let us assume that for $\eta \ll 1$ all the eigenvalues are non-degenerate, as we observe numerically. Differentiating with respect to η and evaluating at $\eta = 0$ gives

$$\begin{aligned} \left.\frac{\partial \mathrm{cp}(z;\eta)}{\partial \eta}\right|_{\eta=0} &= -c\left[\left.\frac{\partial \varepsilon_1}{\partial \eta}\right|_{\eta=0} (z - \varepsilon_2(\eta))...(z - \varepsilon_9(\eta)) + \ldots + \left.\frac{\partial \varepsilon_9}{\partial \eta}\right|_{\eta=0} (z - \varepsilon_1(\eta))...(z - \varepsilon_8(\eta))\right], \\ &= 0 \end{aligned}$$

where the second equality follows from an exact calculation performed using Mathematica, based on $\mathrm{cp}(z;\eta) = \det(U_{\mathrm{F}}(\eta) - z\mathbb{I}) = 0$, with $U_{\mathrm{F}}(\eta)$ given by Eq. (4.32). However, the first line vanishes if and only if $\partial\varepsilon_j/\partial\eta|_{\eta=0} = 0$ for all j. Indeed, evaluating the polynomial identity at $z = \varepsilon_j(0)$ isolates the j-th term. This amounts to saying that the eigenvalues depend on η at least up to the second order, which indicates a certain rigidity in the face of perturbations. Nevertheless, we should emphasize that the second partial derivative of $\mathrm{cp}(\eta)$ around 0 is nonzero, which indicates that the eigenvalues must have a second-order dependence on η; therefore, the spin-1 qudit does not appear to be more robust than the qubit.

A second, more concrete piece of evidence for the rigidity of this time crystal is provided by the evolution of the dissipative Floquet gap as a function of the error η, shown in Figure 4.4a. A first remark is that the evolution of the dissipative gap is the same for both eigenvalues other than 1 that were initially in the peripheral spectrum. We can then clearly see that, in the case of a spin-1 qudit, this evolution reaches a minimum value at $\eta = 0$, which supports the fact that the peripheral eigenvalues depend on η at least at second order. Furthermore, Figure 4.4b shows how the eigenvalues other than 1 in the peripheral spectrum leave it and move into the decaying spectrum when a rotation error $\eta = 0.25$ is considered.

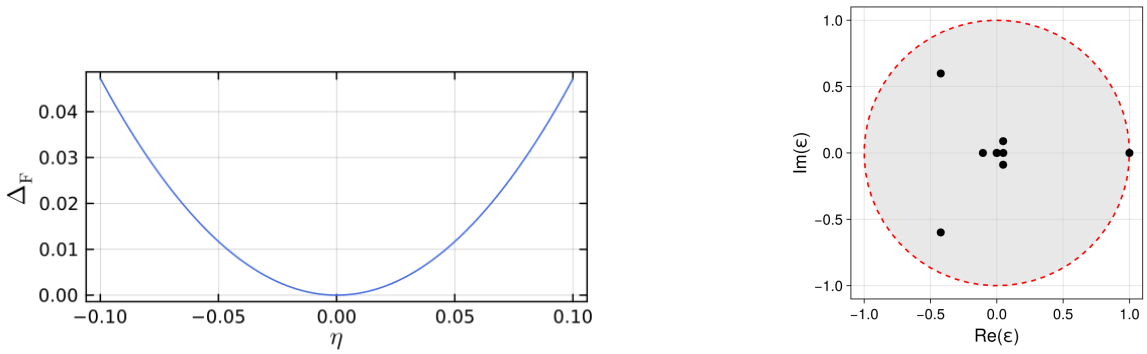

(a) (b)

Figure 4.4: Spin-1 ($N = 2$). (a) Evolution of the dissipative Floquet gap Δ_F for the two eigenvalues $e^{i\pi/3}$ and $e^{-i\pi/3}$ as a function of the perturbation parameter η, with $\kappa = 1$. (b) Spectrum of the Floquet propagator (4.32) for $\kappa = 1$, $T = 1$, and $\eta = 0.25$. The eigenvalues $e^{i\pi/3}$ and $e^{-i\pi/3}$ of the unperturbed Floquet propagator (4.21) move away from the peripheral spectrum.

Comments

The first point we wish to emphasize is that the two time crystals described here should be regarded as 'weak' discrete time crystals in OQS, as their eigenvalues of the peripheral spectrum are only linearly robust against rotation errors. Nevertheless, this shows that a subharmonic response can be achieved in a single-spin system, albeit with limited robustness, and not necessarily in a many-body system. Thus, this kind of system can serve as a useful introduction to more complex systems, providing a fully quantum characterization of discrete time crystals in OQS in terms of the Floquet spectrum and the Floquet dissipative gap, rather than relying solely on a mean-field description of the discrete time crystal. However, to obtain a genuine discrete time crystal, one should consider collective open quantum systems, since the rigidity must persist as the size of the system increases for the phenomenon to be regarded as a phase of matter[1]. Moreover, the subharmonic oscillations exhibited by this system should be regarded as a dynamical curiosity arising from the strong S^z symmetry of the system, rather than as the emergence of spontaneous breaking of the discrete time-translation symmetry.

We expect that the behavior observed in the previous examples can be generalized to higher spins subject to dephasing, so that different higher-period subharmonic responses can be observed, depending on the value of the spin considered. Indeed, Figure 4.5a shows that a $6T$ subharmonic response can be achieved for a dephasing spin-3 qudit, and Figure 4.5b shows that the Floquet gaps associated with all the peripheral-spectrum eigenvalues (other than 1) are linearly robust, since the Floquet gap reaches a minimum at $\eta = 0$.

Furthermore, a spin-s of dimension $2s+1$ can also exhibit a kT subharmonic response, provided that $2s + 1$ is divisible by k. For instance, in the case of a spin-6 qudit, one can observe not only a $6T$ subharmonic response but also $3T$ and $2T$ responses. This depends on the kick U_K considered. Indeed, to obtain a $(2s + 1)T$ subharmonic response, we should choose a U_K that permutes the diagonal elements so as to form an $(N + 1)$-cycle, whereas to obtain a $\frac{2s+1}{k}T$ response, we should choose a U_K that permutes the diagonal elements in blocks so as to form a $\frac{2s+1}{k}$-cycle.

Hence, here are the steps to construct a time crystal from a dephasing spin-s qudit: we can build a time crystal fulfilling the spectral definition of the discrete time crystal given in section 4.1 by generalizing the dephasing of a qubit to higher spin:

[1]We emphasize that a dissipative discrete time crystal in a non-interacting system exhibiting robust subharmonic oscillations has been proposed only recently in Ref. [88], opening a promising route toward robust time-crystalline behavior in open quantum systems.

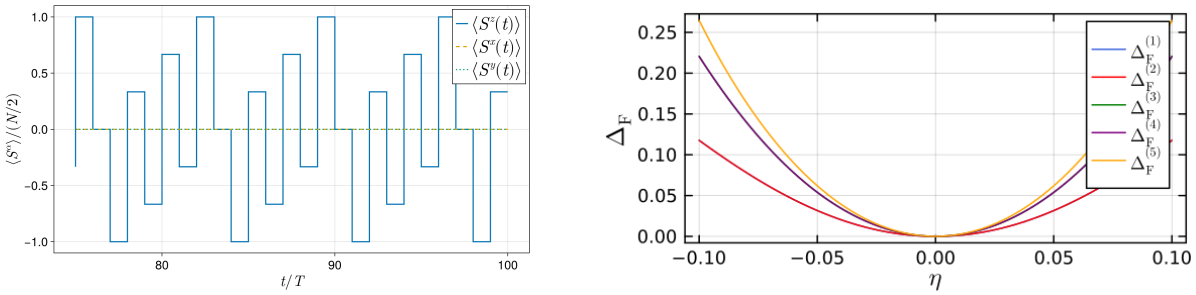

(a) (b)

Figure 4.5: Spin-3 ($N = 6$). (a) Time evolution of the normalized order parameter $\langle S^z\rangle/(N/2)$ over the interval $t/T \in [75, 100]$ for $\kappa = 1$ and $T = 1$, showing robust oscillations with a period of $6T$. (b) Dissipative Floquet gaps $\Delta_F^{(i)}$, associated with the fifth eigenvalues of the peripheral spectrum, as a function of the perturbation strength η for $\kappa = 1$. All Floquet gaps reach their minimum at $\eta = 0$. The pairs $\Delta_F^{(1)}$ and $\Delta_F^{(2)}$, as well as $\Delta_F^{(3)}$ and $\Delta_F^{(4)}$, exhibit identical evolution throughout the explored parameter range.

1. Choose the desired subharmonic response n by applying a kick to a spin system subject to dephasing, such that the response has periodicity nT.

2. Write the Liouvillian
$$\mathcal{L}(\rho) = \frac{1}{2}\left[S^z, \rho\right] + \kappa\left(S^z \rho S^z - \rho\right), \tag{4.34}$$
characterizing the dephasing of the spin-s qudit in a Hilbert space of dimension $N + 1$. We must have $n = N + 1$ in order to exhibit the nT subharmonic response.

3. Define the kick U_K of size $(N + 1) \times (N + 1)$ as
$$U_K = \begin{pmatrix} 0 & 1 \\ I & 0 \end{pmatrix}, \tag{4.35}$$
where I is the identity matrix of size $N \times N$, and then determine the generator G of the kick:
$$U_K = \exp(-i2\pi/(2s + 1)G). \tag{4.36}$$
In the case where the dimension $N + 1$ of the spin space has one or more divisors k, we can use the kick
$$U_K = \exp(-i2\pi k/(2s + 1)G), \tag{4.37}$$
to create a $\frac{n}{k}T$ subharmonic response.
The Floquet propagator is then given by:
$$U_F = U_K \otimes U_K^* \exp(\mathcal{L}T), \tag{4.38}$$
and the eigenvalues in its peripheral spectrum will therefore be 1 and $\exp(m\pi k/(2s + 1))$, with $m = 1, \ldots, \frac{n}{k} - 1$ and k a divisor of n.

4. The last step is to study the rigidity of the system by considering a rotation error η in the cyclic permutation,
$$U_K = \exp\left(-i\left(\frac{2\pi k}{(2s + 1)} + \eta\right)G\right), \tag{4.39}$$
for which we expect the system to be linearly robust at any spin.

4.2 Continuous (quasi) time crystals

The evolution of the original concept of time crystals introduced by Frank Wilczek led to the development of discrete time crystals in both isolated and open quantum systems. This evolution emerged following the no-go theorem established by Watanabe and Oshikawa [9], which rules out the existence of continuous time crystals in equilibrium quantum systems. Nevertheless, their work also pointed out that the original idea of time crystals could remain relevant in non-equilibrium settings, thereby paving the way for the concept of discrete time crystals.
Another important development of the time-crystal concept was proposed in 2018 by F. Iemini *et al.* [28]. In this work, the authors predicted a novel non-equilibrium phase of matter that spontaneously breaks time-translation symmetry, referred to as Boundary Time Crystals (BTCs). More precisely, a BTC consists of a boundary system coupled to a bulk environment, which together form an isolated macroscopic system. Denoting by N_b and N_B the degrees of freedom for the boundary and the bulk systems respectively, we consider the case in which a macroscopic fraction of the universe, the boundary system ($N_\mathrm{b} \to \infty$), breaks spontaneously time-translational invariance. The thermodynamic limit is performed with N_b, $N_\mathrm{B} \to \infty$, with the ratio $N_\mathrm{b}/N_\mathrm{B} \to 0$. In other words, the boundary system is macroscopic, but still small compared to the global system. This scaling is the crucial feature to define a boundary phenomenon. Hence, the boundary must exhibit robust periodic dynamics for infinite large times. Its dynamics can be described within the framework of open quantum systems, and in our case through the GKSL master equation, provided that the volume and the interaction between it and the boundary are correctly modeled. Furthermore, dissipative time crystals has also been introduced which is a many-body quantum system coupled to a noise inducing environment which exhibits non-trivial periodic motion in some observable at late time for generic initial conditions [89–91]. Thus, dissipative time crystals can be distinguished from related boundary time crystals which are usually taken to be single-body systems that exhibit persistent oscillations despite dissipation, which therefore constitute a new type of continuous time crystal. However, given that in both cases we will study their dynamics using GKSL's master equation and observe the same types of time-crystal signatures, we will set these distinctions aside and use the term 'continuous time crystal' (CTC) for both cases in this thesis; furthermore, we will refer only to open quantum systems and not to open classical systems, as this term can sometimes appear in literature [31].
In such systems, the steady state is generically non-thermal; consequently, the no-go theorem of Watanabe and Oshikawa does not apply. This implies that a Hamiltonian system may, in principle, spontaneously break time-translation symmetry when subjected to dissipation. Hence, CTCs correspond to open quantum systems described by a time-independent Liouvillian and characterized by persistent and robust periodic oscillations of an observable acting as an order parameter. In the thermodynamic limit, these oscillations must persist for infinitely long times.
More recently, another concept has been proposed theoretically, namely Continuous Quasi Time Crystals (CQTCs) [32]. These systems are globally based on the same idea as CTCs, except that the oscillations exhibited by the system are aperiodic and its dynamic is chaotic rather than strictly periodic. Such behavior can also be interpreted as a form of time-translation symmetry breaking: although the governing equations remain time-translation invariant, their persistent aperiodic solutions in the thermodynamic limit do not share this symmetry.
In the following, we will investigate the properties of both CTCs and CQTCs from mean-field theory, which will prove to be a particularly insightful framework for studying these phases. We will then analyze the Liouvillian spectrum and the dissipative gap in order to characterize realistic finite-size systems. Finally, we will provide formal definitions of CTCs and CQTCs before presenting two different collective-spin systems that exemplify these phenomena.

4.2.1 Definitions and properties

When theorizing about discrete time crystals in closed quantum systems, the question naturally arises of how the introduction of an environment would affect the system. Indeed, it was unclear whether the environment would destroy the discrete time-crystalline signatures or, on the contrary, help to stabilize the phenomenon. In fact, the discrete time crystal appearing in a disordered one-dimensional Ising spin chain, described in section 2.2.3, cannot survive the coupling to an environment [24], which led us to the discussion of the concept of discrete time crystals in open quantum systems presented in section 4.1. However, the dissipation induced by an environment makes it possible to recover part of the original concept of a time crystal characterized by the spontaneous breaking of continuous time-translation symmetry, gives rise to a dissipative continuous time crystal if the system exhibits a robust and persistent periodic oscillation, or to a dissipative continuous quasi-time crystal if the system exhibits robust and persistent aperiodic oscillations and chaotic behavior.
As usual, the thermodynamic limit is the theoretical framework used to characterize phases of many-body systems. Hence, continuous time crystals (and also continuous quasi-time crystals) in this limit have been characterized using a mean-field approach as a first tool. Briefly, it consists in neglecting the quantum correlations between different local observables A_i of an N-body system by factorizing the expectation values of operator products into products of expectation values:

$$\langle A_i A_j \rangle \approx \langle A_i \rangle \langle A_j \rangle.$$

This approximation becomes accurate in the thermodynamic limit, where collective observables such as

$$M = \frac{1}{N} \sum_{i=1}^{N} A_i$$

have fluctuations typically scaling as

$$\Delta M \sim \frac{1}{\sqrt{N}},$$

so that the relative fluctuations vanish for $N \to \infty$. This is, for example, a valid method in the case of the collective spin systems that we will study in the following sections. In this approach, the dynamics of the collective observables can be described semi-classically as a system of coupled differential equations. The continuous time-crystalline phase can then emerge in the form of a limit-cycle phase, which in nonlinear classical dynamics corresponds to a closed phase-space trajectory asymptotically approached by at least one neighboring trajectory [30]. However, it is not necessarily characterized by a limit cycle, but may also correspond to simple periodic trajectories around a steady state in phase space [38]. It corresponds to self-sustained oscillations of the system, even in the absence of any external periodic or aperiodic influence. Hence, in the mean-field characterization of open quantum systems, the continuous time-crystalline phase, and the transition from a non-oscillating steady-state phase to it, can be characterized and highlighted using nonlinear classical system theory.
However, we are also interested in the properties of the open quantum system that allow it to be characterized as a continuous time crystal. In this respect, the Liouvillian $\mathcal{L}$ governing the open quantum system is of the utmost importance, and more precisely its spectral structure. Indeed, we saw in section 3.3 that the system evolves into an equilibrium steady state if the only eigenvalue with a vanishing real part is zero, whereas the system possesses an oscillating steady state if there is at least one other eigenvalue with a vanishing real part. Thus, in order to have a continuous time crystal, $\mathcal{L}$ must possess at least two purely imaginary eigenvalues in the thermodynamic limit, and these must be equally spaced (i.e. the separation between neighboring eigenvalues is constant) in order to have a periodic—commensurate—oscillating steady state. In the case of a continuous quasi-time crystal, these eigenvalues must not be equally spaced, in order to have an aperiodic oscillating steady state. A judiciously chosen observable must

then be selected so as to exhibit robust and persistent oscillations when the system is in the continuous time-crystalline (or continuous quasi-time-crystalline) phase, and equilibrium when it is in the equilibrium phase. When the system is considered to be finite, rather than in the thermodynamic limit, the steady state is not time-periodic. Increasing the size of the system causes the real parts of more and more eigenvalues to converge to 0 in the thermodynamic limit. Hence, for finite systems, the dissipative Liouvillian gap Δ is useful in informing us about the decay of the periodic behavior into the equilibrium steady state.

In practical studies and applications, the thermodynamic limit is unattainable, and finite-size effects are inevitable. Thus, even if the thermodynamic limit provides a convenient theoretical framework to study CTCs (and CQTCs)—in particular to define the phase transition of an open quantum system into the (quasi-)time-crystalline behavior, its critical exponents, and its parameter survival range—it may conceal quantum correlations that persist under finite-size conditions and that can affect the dynamical behavior of the system. While exact diagonalization can serve this purpose for small system sizes being limited by insufficient numerical power, a unified and practically useful analytical framework that can reliably capture the long-time dynamics of CTCs (and CQTCs) in finite-size systems is still required. Such a study has been carried out for the case of continuous time crystals in collective spin systems, which we will briefly discuss in the following section [92].

Let us summarize what defines a continuous time crystal and a continuous quasi-time crystal, and then provide a formal definition in terms of the Liouvillian. The first condition for an open quantum system to be considered a continuous time crystal is that the system must possess a continuous time-translation symmetry but exhibit, via an order parameter $\mathcal{O}(t) = \mathrm{tr}(O\rho_{\mathrm{ss}})$, a periodic oscillation; for a continuous quasi-time crystal, the oscillation must instead be aperiodic. The second condition is that the periodic or aperiodic oscillation should exist over a wide range of parameters and without fine-tuned Hamiltonians. Furthermore, it is worth mentioning that the robustness of a CTC phase refers to the persistence of a periodic evolution in the thermodynamic limit, and not necessarily to the rigidity of its period. The main difference with respect to Floquet systems is that, there, since one is breaking a discrete symmetry, rigidity is intimately related to the period of the driving; in our case, by contrast, since the dynamics is time-invariant, such a timescale is not present, and the period of oscillation is allowed to change within the symmetry-broken phase. This is a direct analog of the fact that, in spatial crystals, the spatial periodicity can be changed by changing the particle-particle interaction. The last condition is that the periodic or aperiodic oscillation must persist indefinitely in the thermodynamic limit. Hence, let us define all these conditions in terms of the Liouvillian [28, 93]:

CTCs Liouvillian definition:

An open quantum system whose dynamics is governed by a GKSL master equation with a time-independent Liouvillian $\mathcal{L}$ is said to exhibit continuous time-crystalline behavior if $\mathcal{L}$ satisfies:

1. At least one eigenvalue different from 0 must be purely imaginary in the thermodynamic limit. The imaginary eigenvalues of the low-lying Liouvillian excitations are organized into bands, separated by a fundamental frequency.
2. The imaginary band structure must be present over a wide range of parameters. Furthermore, the period of oscillation is allowed to change depending on the system parameters.
3. The dissipative gap Δ must be equal to zero in the thermodynamic limit.

In the case of continuous quasi-time crystals, we would like to emphasize that it is perhaps too "soon" to define this phase solely on the basis of the Liouvillian spectral properties (the non-commensurability of the purely imaginary eigenvalues) since this can also correspond to aperiodic oscillations without necessarily implying chaotic dynamics, and more hindsight on

this newly identified phase of matter is needed.
Furthermore, we can define the continuous time-crystalline phase based on the correlation function in the thermodynamic limit define in section 4.1, $C_M^\infty(t)$ [34, 94]:

Correlation-based definition of continuous time crystals:
Continuous time crystals are defined by the persistence of a finite order parameter, $C_M^\infty(0) > 0$, together with persistent oscillations of the correlation function, i.e. $C_M^\infty(t) = C_M^\infty(t+T)$ with T the periodicity of the oscillation.

An important comment about dissipative quantum systems that exhibit time-crystalline behavior is that the majority of systems exhibiting this kind of behavior have been subjected to a continuous external driving, so that it was the "competition" between driving and dissipation that led to such behavior [28, 94, 95]. However, very recently, a dissipative time crystal without external driving has been proposed [96]. Indeed, the authors provide a theoretical mean-field analysis of a spin-1/2 Heisenberg XYZ model subjected to dissipation, in which each spin undergoes an incoherent downward-flipping process, such that the dynamics of the system can be described by the GKSL master equation.
The concepts of continuous time crystals and continuous quasi-time crystals are not confined to the theoretical stage, since continuous time crystals have been observed experimentally. They can be observed in the form of a limit-cycle phase exhibited by an observable in the context of open quantum systems. Thus, while limit cycles are well established in classical nonlinear physics [97], there are two essential conditions for limit cycles in open quantum systems to form a CTC. Firstly, the formation of the limit cycle must be associated with the spontaneous breaking of continuous time-translation symmetry; that is, the relative temporal phase of the oscillations takes random values between 0 and 2π across repeated realizations [30]. Secondly, the limit-cycle phase must be robust against temporal perturbations of a technical or fundamental character, such as quantum noise and, for open systems, fluctuations associated with dissipation [30]. Thus, a limit-cycle phase has been observed in a continuously pumped dissipative Bose–Einstein condensate of Rb^{87} atoms placed inside a transversely pumped high-finesse optical cavity operating in the recoil-resolved regime [30]. The time-crystalline behavior manifested as emergent oscillations in the intracavity photon number.
A more recent realization has been observed in spin gases [29]. A laser polarizes Rb^{87} atoms, which then transfer their energy to polarize Xe^{129} gas inside a magnetic field. A second laser measures the xenon's state and uses these data to constantly adjust the system through a magnetic feedback loop. This feedback mechanism induces nonlinear interactions between Xe^{129} atoms, which are essential for the generation of CTCs. Furthermore, by controlling the magnetic field, they observed a dynamical phase characterized by quasi-periodic oscillations and random temporal phases, indicating the emergence of a continuous time quasi-crystal for the first time. The oscillations manifest as persistent limit-cycle oscillations of nuclear spins, with coherence times exceeding several hours.
In what follows, we present the first system found to exhibit this kind of behavior, namely a continuously driven-dissipative collective spin system. Afterwards, we will present continuous quasi-time-crystallinity in two coupled continuously driven-dissipative collective spins.

4.2.2 Driven dissipative collective spin system

To see the properties discussed in the previous section in application, we study the boundary time crystal presented by *Imeni et al.* [28], where the Hamiltonian is given by

$$H = \omega_0 S^x, \tag{4.40}$$

and such that the dynamics of the open quantum system can be described by the following GKSL master equation ($\hbar = 1$)

$$\dot{\rho} = \mathcal{L}(\rho) = -i\,[H, \rho] + \frac{\kappa}{S}(S^- \rho S^+ - \frac{1}{2}\{S^+ S^-, \rho\}), \tag{4.41}$$

where $S^\alpha = \frac{1}{2}\sum_{j=1}^{N} \sigma_j^\alpha$, with $\alpha = x, y, z$, consist of a collection of N spin-1/2 particles whose dynamics is governed by collective spin operators satisfying the commutation relation $[S^\alpha, S^\beta] = i\varepsilon^{\alpha\beta\gamma} S^\gamma$. Here, σ_j^α are the Pauli matrices acting on spin j, and $S = N/2$ is the total spin. The operators $S^\pm = S^x \pm iS^y$ are the collective raising and lowering operators. The Hamiltonian H characterizing the unitary dynamics of the system can be interpreted as a continuous drive, with ω_0 the driving frequency. This kind of model can emerge from a periodically driven system, where the explicit time dependence of the drive can typically be removed by performing a rotating-wave approximation for a suitable driving frequency, yielding a time-independent description. Such a time-independent Hamiltonian remains physical when the driving frequency is high enough that the system can no longer resolve individual oscillation cycles, allowing one to effectively treat the driving as continuous. The dissipative part of the Liouvillian describes a collective spin-lowering process in the z direction, arising from the coupling of the system to its environment, with effective decay rate κ. At non-zero temperature, the latter is proportional to $1 + n(T)$, where $n(T)$ is the thermal occupation number, which vanishes at $T = 0\,\mathrm{K}$. Moreover, we must therefore add an additional non-unitary term, identical to the one in Eq. (4.41) but with S^+ and S^- exchanged and with an effective dissipative rate proportional to $n(T)$. It characterizes a collective spin-raising process in the z direction, through which the system absorbs energy from its environment. We will see in the following that the relevant dynamics of the system is not affected by this additional term, except that the relevant parameter is no longer κ but the difference between the two dissipative rates, which can simply be regarded as a renormalization of κ when only the dissipative term in Eq. (4.41) is considered.
We should emphasize that the total spin of the system is conserved, since $[\mathbf{S}^2, S^\alpha] = [\mathbf{S}^2, S^+] = [\mathbf{S}^2, S^-] = 0$, and that it is a strong symmetry of the system. Since $\mathbf{S}^2$ is a strong symmetry of the dynamics, the Liouvillian $\mathcal{L}$ block-diagonalizes in the respective spin-J eigenbases, such that $\mathcal{L} = \bigoplus_J \mathcal{L}_J$. Therefore, the dynamics is constrained within each spin-J subspace. The maximum angular-momentum value $J = S = N/2$ corresponds to the totally symmetric Dicke subspace, while lower values of J correspond to asymmetric subspaces. The spin-J irreducible representation has dimension $2J + 1$.

Mean-field analysis

The dynamics of this system in the thermodynamic limit $S \to \infty$ can be well understood using mean-field theory. Indeed, we can first derive the evolution of the expectation value of any operator O of the system within the Heisenberg picture:

$$\frac{d\langle O\rangle}{dt} = \frac{d}{dt}\mathrm{Tr}\,(O\rho) = \mathrm{Tr}([H, O]\rho) + \frac{\kappa}{2S}\mathrm{Tr}\left(\left([S^+, O]S^- + S^+[O, S^-]\right)\rho\right), \tag{4.42}$$

where we have used the cyclic property of the trace to arrive at this result. Then, if we are interested in the evolution of the collective spin S^α, we find

$$\begin{aligned}
\frac{d}{dt}\langle S^x\rangle &= \frac{\kappa}{2S}\left(\langle S^x S^z\rangle + \langle S^z S^x\rangle + \langle S^x\rangle\right) \\
\frac{d}{dt}\langle S^y\rangle &= -\omega_0\langle S^z\rangle + \frac{\kappa}{2S}\left(\langle S^y S^z\rangle + \langle S^z S^y\rangle - \langle S^y\rangle\right) \\
\frac{d}{dt}\langle S^z\rangle &= \omega_0\langle S^y\rangle - \frac{\kappa}{S}\left(\langle (S^x)^2\rangle + \langle (S^y)^2\rangle + \langle S^z\rangle\right).
\end{aligned}$$

In the thermodynamic limit, we can define the rescaled macroscopic spin operator $m^\alpha = \langle S^\alpha \rangle / S$, with the commutation relation $[m^\alpha, m^\beta] = i\varepsilon^{\alpha\beta\gamma} m^\gamma / S$. Hence, when $S \to \infty$, these operators commute and the quantum correlations between them vanish, so that $\langle m^\alpha m^\beta \rangle \approx \langle m^\alpha \rangle \langle m^\beta \rangle$. The three equations above can therefore be written in the thermodynamic limit as

$$\begin{aligned} \dot{m^x} &= \kappa m^x m^z \\ \dot{m^y} &= -\omega_0 m^z + \kappa m^y m^z \\ \dot{m^z} &= \omega_0 m^y - \kappa \left((m^x)^2 + (m^y)^2 \right), \end{aligned} \tag{4.43}$$

where the mean-field dynamics is characterized by a set of coupled nonlinear differential equations. Since the total spin is a conserved quantity of the system, at the mean-field level this means that $(m^x)^2 + (m^y)^2 + (m^z)^2 = m^2$ is conserved, since correlations are assumed to vanish. We can associate each of the spin-J subspaces with the mean-field total angular-momentum value $m = J/S$. The states with $m < 1$ belong to the asymmetric angular-momentum sectors, whereas the states with $m = 1$ belong to the symmetric Dicke subspace, which is the case we will consider for the moment. Hence, we can find the steady state of the system by solving the system of differential equations (4.43) with the time derivatives set to zero. By doing so, we find two distinct phases for the steady state.
In the case $\omega_0/\kappa < 1$, there are two steady states

$$(m^x, m^y, m^z) = \left(0, \frac{\omega_0}{\kappa}, \pm \sqrt{1 - \left(\frac{\omega_0}{\kappa} \right)^2} \right), \tag{4.44}$$

and when we insert these two solutions into the Jacobian matrix $\mathcal{J} = \partial \dot{m^\alpha} / \partial m^\beta$:

$$\mathcal{J} = \begin{pmatrix} \kappa m_z & 0 & \kappa m_x \\ 0 & \kappa m_z & -\omega_0 + \kappa m_y \\ -2\kappa m_x & \omega_0 - 2\kappa m_y & 0 \end{pmatrix}, \tag{4.45}$$

the positive solution is characterized by two positive eigenvalues and one zero eigenvalue, which tells us that this steady state is unstable, whereas the negative solution is characterized by two negative eigenvalues and one zero eigenvalue, which tells us that this steady state is stable, thereby leading to a unique steady state for the long-time dynamics.
In the case $\omega_0/\kappa > 1$, there are again two steady states

$$(m^x, m^y, m^z) = \left(\pm \sqrt{1 - \left(\frac{\kappa}{\omega_0} \right)^2}, \frac{\kappa}{\omega_0}, 0 \right), \tag{4.46}$$

and when we insert these two solutions into $\mathcal{J}$ given in (4.45), we find the same eigenvalues for both solutions, namely $\lambda_1 = 0$ and $\lambda_{2,3} = \pm i\sqrt{\omega_0^2 - \kappa^2}$. Thus, on crossing the critical point at $\omega_0/\kappa = 1$, we observe neither the standard pitchfork bifurcation (in which a stable fixed point becomes unstable and two stable fixed points are born) nor a Hopf bifurcation (in which a fixed point turns into a limit cycle attracting the system to a periodic orbit). The phase space consists of two families of periodic trajectories circulating around each of the steady-state solutions (4.46). Moreover, the dynamics has a periodicity $T = 2\pi/\sqrt{\omega_0^2 - \kappa^2}$.
Hence, when $\omega_0/\kappa < 1$, the classical description tells us that the system is in a melted phase, meaning that its dynamics converges to a unique steady state, whereas when $\omega_0/\kappa > 1$, the system is in the CTC phase, so that its infinite-time dynamics exhibits persistent periodic oscillations. We can visualize this by examining the phase portrait obtained from the dynamics in spherical coordinates, corresponding to the parametrization [98]

$$m = (\sin\theta \cos\varphi, \sin\theta \sin\varphi, \cos\theta), \tag{4.47}$$

with the dynamics constrained to the surface of the Bloch sphere. Figure 4.6a shows the phase portrait when $\omega_0/\kappa < 1$, where the repulsive and attractive fixed points can be seen. Figure 4.6b shows the phase portrait when $\omega_0/\kappa > 1$, where the two periodic orbits around the two fixed points can be clearly observed. Furthermore, the oscillation is around $m^z = 0$.

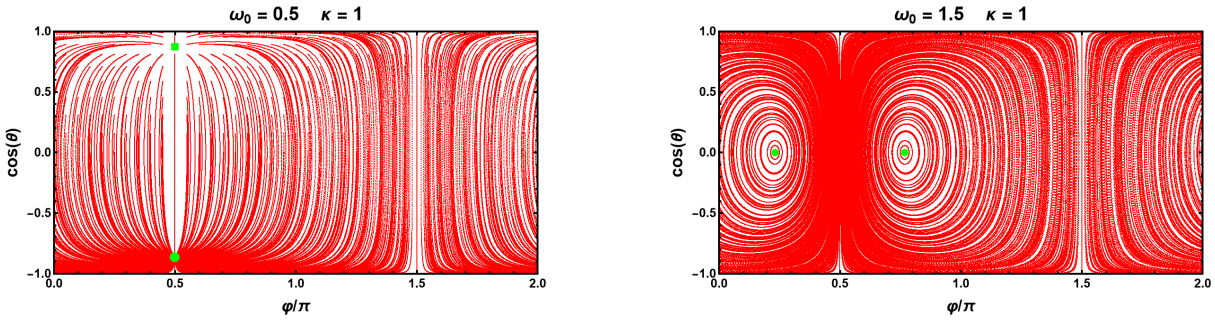

(a) (b)

Figure 4.6: Phase portraits obtained by solving the set of differential equations (4.43). (a) $\omega_0 = 0.5$ and $\kappa = 1$ with the unstable steady state (green square) $m = (0, 1/2, \sqrt{3}/2)$ and the stable steady state (green point) $m = (0, 1/2, -\sqrt{3}/2)$ ($\cos\theta = \pm\sqrt{3}/2$ and $\varphi/\pi = 1/2$). (b) $\omega_0 = 1.5$ and $\kappa = 1$ with the two fixed points at the center of the periodic orbits (green points) $m = (\pm\sqrt{3}/2, 1/2, 0)$ ($\cos\theta = 0$ and $\varphi \approx \{0.7297, 2.4119\}$).

Finite-size analysis

Having explored the classical limit of the system, we now turn to a full quantum description. To this end, we will examine the spectral properties of the Liouvillian, as well as the dynamics of the system for different finite system sizes. We should emphasize that the following computations of the Liouvillian spectrum and of the dynamical behavior have been carried out by restricting the system to the symmetric Dicke subspace, so that the Hilbert space of the system has dimension $N + 1$ rather than 2^N.

In Figure 4.7a, we can see the Liouvillian spectrum for the phase $\omega_0/\kappa < 1$ while in Figure 4.7b, it corresponds to the phase $\omega_0/\kappa > 1$, for $N = 40$. In the melted phase, the spectrum is gaped and the eigenvalues with the largest real parts have no imaginary part. However, the spectrum in the CTC phase converges to the imaginary axes and the eigenvalues with the largest real parts have a non-zero imaginary part. A more detailed analysis can be seen in Figure 4.7c. Indeed, the evolution of the seven eigenvalues with the smallest real parts in the CTC phase is depicted as a function of the system size N. We can see that the real parts of all the eigenvalues seem to converge to zero in the thermodynamic limit, following a power law with different rates. In Figure 4.7d, the imaginary parts converge when the system size increases to form bands separated by a fundamental frequency $\Gamma_{\omega_0/\kappa}$, which depends on the parameters ω_0 and κ. In fact, these bands are separated by the oscillation frequency $\sqrt{\omega_0^2 - \kappa^2}$ of m^z found previously in the mean field analysis depicted by the distance between the red dashed lines. These properties of the spectrum are responsible for the appearance of the time-periodic evolution that lasts indefinitely in the thermodynamic limit and does not require a specific choice of initial conditions. These features satisfy the definition of a CTC that we proposed.

In Figure 4.8, we can observe the time evolution of the correlation function $C_M(t)$ in the CTC phase. In the context of this system, the normalized order parameter is $\langle S^z \rangle / S$ and the correlation function is therefore given by

$$C_M(t) = \frac{\langle S^z(t) S^z(0) \rangle_{\text{ss}}}{S^2}. \tag{4.48}$$

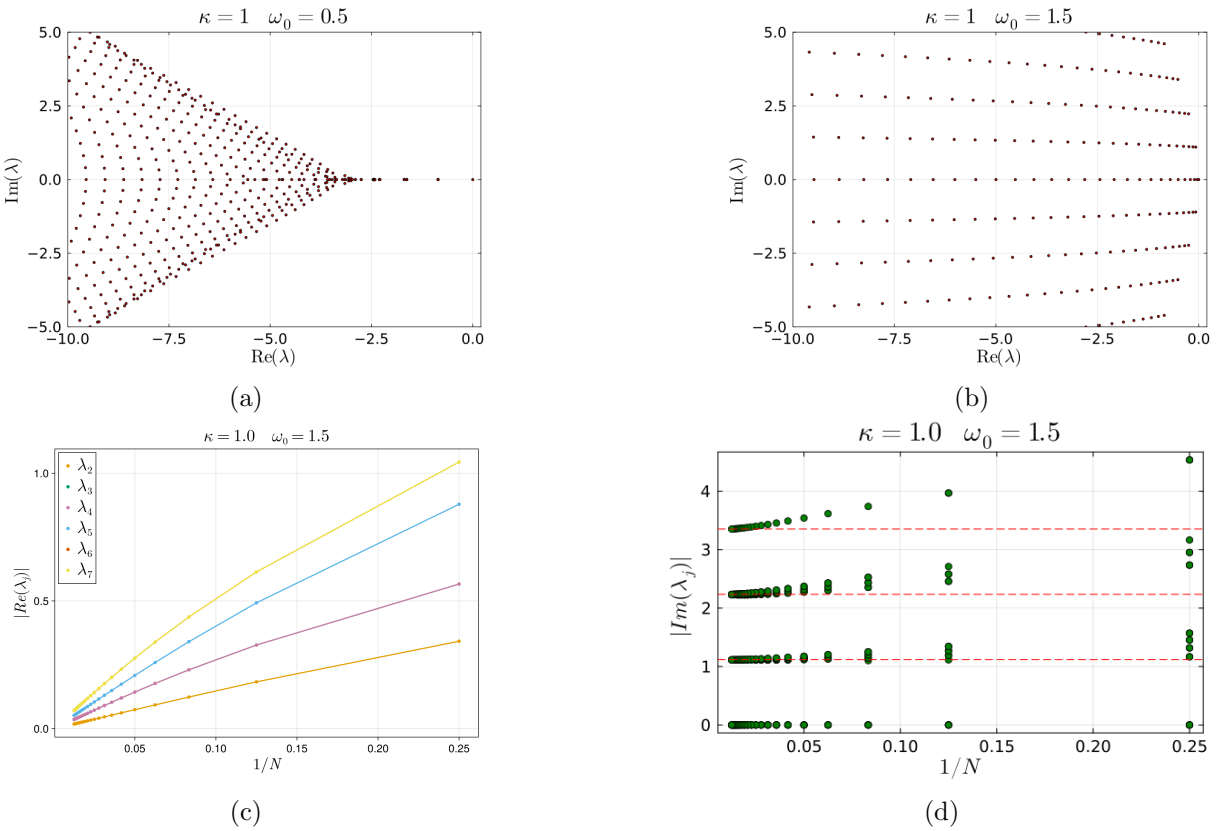

Figure 4.7: Eigenvalues of the Liouvillian given by Eq. (4.41) (a) in the strong dissipation regime $\omega_0/\kappa = 0.5$ and (b) in the weak dissipation regime $\omega_0/\kappa = 1.5$. (c) Finite-size scaling of Liouvillian eigenvalues in the CTC phase. The eigenvalues λ_j are ordered according to increasing real part, $|\mathrm{Re}(\lambda_j)| \leq |\mathrm{Re}(\lambda_{j+1})|$, with $j = 0$ corresponding to the zero eigenvalue. The real parts scale to zero as a power law of the inverse system size N. (d) The imaginary parts exhibit a band structure with a fundamental frequency separation represented by the distance between the red dashed lines that correspond to the frequency given by the mean-field analysis. For a fixed excitation threshold (selecting only eigenvalues such that $j^2/N \leq 0.025$), the band width remains finite in the thermodynamic limit.

Hence, as the size of the system increases, we see that the periodic oscillation of $C_M(t)$ persists for longer and longer times, whereas in the mean-field limit the periodic oscillation must persist indefinitely. Moreover, the period of the oscillation predicted by the mean-field limit, which is given by the distance between the two red dashed lines, agrees with that obtained in the full quantum description, so that we expect the frequency to be independent of the system size.
An additional property exhibited by continuous time crystals is the behavior of the steady-state quantum fluctuations of the order parameter $\langle S^z \rangle$. In this context, it can be defined as

$$F^2 = \frac{\langle (S^z)^2 \rangle_{\mathrm{ss}} - \langle S^z \rangle_{\mathrm{ss}}^2}{S^2}. \tag{4.49}$$

This quantity measures the normalized fluctuations of S^z around its steady-state mean, and thus characterizes the strength of quantum fluctuations of the magnetization along the z-direction. For CTCs, it has been observed that this quantity behaves as

$$F^2 = C_M^{\infty}(0)\, S, \tag{4.50}$$

implying a linear divergence with the total spin value S [25, 94]. We therefore computed F^2 as a function of S and we observe that this scaling is also observed in the present CTC, as shown

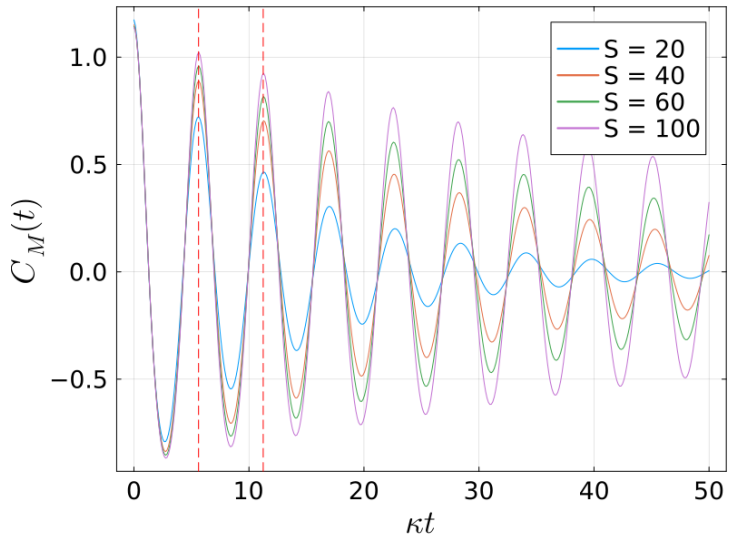

Figure 4.8: Time evolution of $C_M(t)$ given by Eq. (4.48) for different system size $N = 20$, $N = 40$, $N = 60$ and $N = 100$. The persistence of the periodic oscillation increase with N.

in Figure 4.9a. This indicates that the integrated fluctuations of S^z are extensive, i.e., they scale with the number of degrees of freedom rather than remaining bounded. Such a divergence signals the presence of strong, system-wide correlations rather than purely local fluctuations. In Figure 4.9b, the equal-time correlation function $C_M(0)$ converges to a finite value, which is $C_m^{\infty}(0)$ in the thermodynamic limit. This asymptotic value is indicated by the red dashed line and corresponds to the slope of F^2 in Figure 4.9a, thereby confirming the relation given in Eq. (4.50).

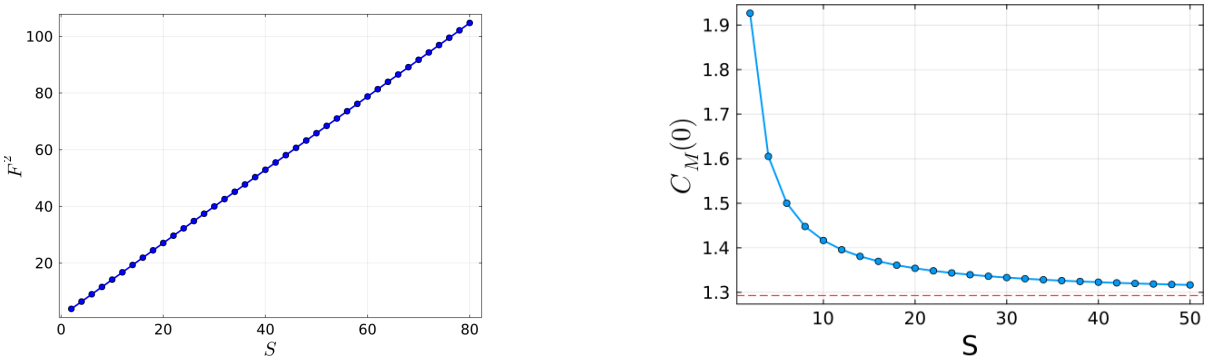

(a) (b)

Figure 4.9: Evolution of the quantum fluctuations F^2 given by Eq. (4.49) as a function of the size of the system N. F^2 grows linearly with N.

Comments

While the results presented here constitute the basic properties of a continuous time crystal, there are several comments we can make in order to go further in the description of continuous time crystals in driven collective spin systems.

One might wonder about the effect of perturbations in the unitary part of the dynamics, and therefore consider a Hamiltonian of the form:

$$H = \omega_0 S^x + \frac{\omega_x}{S}(S^x)^q + \frac{\omega_z}{S}(S^z)^p, \tag{4.51}$$

with $p, q \in \mathbb{N}^+$. For instance, let us consider for the moment the case $p = q = 2$. In the mean-field limit, we can derive the set of differential equations for the macroscopic observables m^α:

$$\begin{aligned} \dot{m^x} &= -2\omega_z m^y m^z + \kappa m^x m^z \\ \dot{m^y} &= 2(\omega_z - \omega_x) m^x m^z - \omega_0 m^z + \kappa m^y m^z \\ \dot{m^z} &= 2\omega_x m^x m^y + \omega_0 m^y - \kappa \left((m^x)^2 + (m^y)^2 \right). \end{aligned} \tag{4.52}$$

When we consider the case $\omega_x = 0$ in the CTC phase ($\omega_0/\kappa > 1$), by setting the derivatives to zero and $m = 1$, we find the following fixed points:

$$(m^x, m^y, m^z) = \left(0, \frac{\kappa}{\omega_0}, \pm\sqrt{1 - \left(\frac{\kappa}{\omega_0}\right)^2} \right), \tag{4.53}$$

and

$$(m^x, m^y, m^z) = \left(\frac{2\omega_z\omega_0}{\sqrt{\kappa^2 + 4\omega_z^2}}, \frac{\kappa\omega_0}{\kappa^2 + 4\omega_z^2}, \pm\sqrt{1 - \frac{\omega_0^2}{\sqrt{\kappa^2 + 4\omega_z^2}}} \right). \tag{4.54}$$

For the last two fixed points (4.54) to exist, the condition $\sqrt{\kappa^2 + 4\omega_z^2} \geq \omega_0$ must hold, which sets the threshold for the survival of the CTC phase [28]. This tells us that the CTC phase remains stable even for a non-zero value of ω_z.
However, when we consider the case $\omega_x \neq 0$, this has the effect of improving the stability of the time crystal, as can be seen from the phase portraits displayed in Figure 4.10. As we can see, when ω_z is below the threshold ($\sqrt{\kappa^2 + 4\omega_z^2} \leq \omega_0$), the two periodic orbits are preserved in the phase portraits, whereas when ω_z exceeds the threshold, one of the two periodic orbits breaks, becoming a stable steady state toward which some initial states converge. However, for the same value of ω_z, as we increase ω_x we recover the two periodic orbits, which shows how ω_x stabilizes the CTC phase [28, 98].
In Ref. [98], the authors performed a detailed mean-field study, supported by a finite-size analysis, of the quantum model of a p, q-spin interaction system—a generalized p-spin interaction system—which is the collective driven spin system described by equation (4.41) with the Hamiltonian (4.51) and $\omega_0 = 0$. Hence, based on symmetry considerations, they identified two conditions that determine for which forms of perturbation in the Hamiltonian (4.51), together with collective dissipation, such a system still exhibits a CTC phase:

- **Symmetry:** A CTC phase exists only for even values of p, while q can be either even or odd [98]. Indeed, the Hamiltonian must possess a $\mathbb{Z}_2$ symmetry generated by $G = \prod_j \sigma_j^x$, which commutes with the Hamiltonian (4.51) but acts as $GS^\pm G^\dagger = S^\mp$ on the jump operators. This corresponds to an effective switch of the preferred alignment of the spins. Thus, the dissipative part breaks the $\mathbb{Z}_2$ symmetry of the system.

- **Collective dissipation:** The mean-field dynamics of the p, q-spin interaction system displays CTC behavior only in the presence of collective dissipation [98]. If we instead consider a set of jump operators $S^\pm = \sum_i^{N_s} \sigma_i^\pm$ with $N_s \leq N$, time-crystallinity is lost. In the latter case, $\mathbf{S}^2$ is no longer a strong symmetry of the system. We therefore expect that the total spin must remain a conserved quantity for such a system to exhibit a CTC phase.

However, we should emphasize that these conditions apply only to driven-dissipative spin systems. Indeed, the breaking of a discrete symmetry is not necessary, as in the dissipative Bose–Hubbard model of Ref. [99], where the system possesses a $\mathbb{Z}_2$ strong symmetry that is therefore not broken by the dissipation. Moreover, a CTC can be induced by local dissipation through long-range interactions [94].

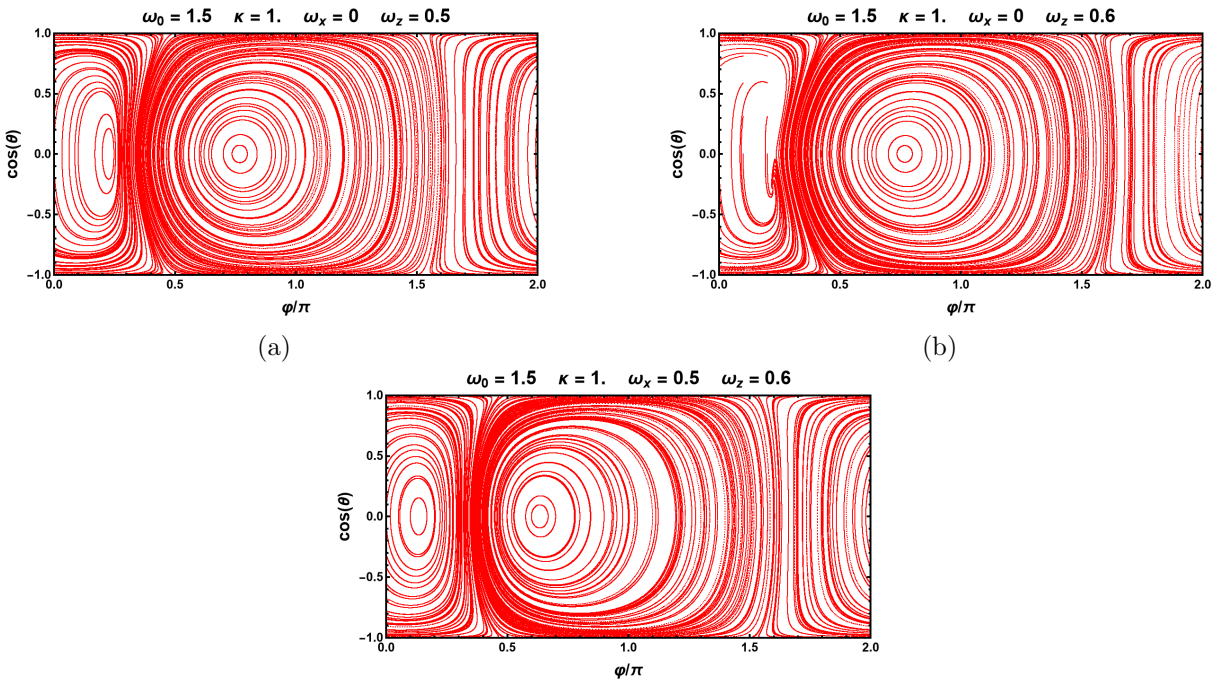

Figure 4.10: Phase portraits obtained by solving the set of differential equations (4.52), (a) for $\omega_0 = 1.5$, $\kappa = 1$, $\omega_x = 0$ and $\omega_z = 0.5$, (b) for $\omega_0 = 1.5$, $\kappa = 1$, $\omega_x = 0$ and $\omega_z = 0.6$, (c) for $\omega_0 = 1.5$, $\kappa = 1$, $\omega_x = 0.5$ and $\omega_z = 0.5$. The continuous time crystal remain stable for $\omega_z \neq 0$ and is stabilized by increasing ω_x.

The continuous time crystals corresponding to driven-dissipative collective spin systems have mostly been studied within the symmetric Dicke subspace. A first reason why studies are restricted to this subspace is the collective nature of the system, which is characterized by a permutational symmetry that is a strong symmetry of the underlying open quantum system. Moreover, as already mentioned, $\mathbf{S}^2$ is a strong symmetry of the Liouvillian in Eq. (4.41), which reduces the dimension of the relevant Hilbert space from 2^N to $N + 1$, making it possible to study the system in the thermodynamic limit via a mean-field approximation. However, in reference [100], the authors investigated the effect of including the asymmetric subspaces on the dynamics of CTCs in a driven-dissipative spin model. They found that the inclusion of asymmetric subspaces leads to time-crystal behavior even when ω_0/κ is less than one. Another result they found is that taking the asymmetric subspaces into account leads to multistability: depending on the parameter values, the system can exhibit either a time-crystal or a melted phase for different initial states. A similar result was also observed in the p, q-spin interaction system for $p = 2$, $q = 1$, for instance [98].

A final comment about this CTC is that its analysis has been restricted to a classical treatment via a mean-field approximation for $N \to \infty$, or to numerical simulations of small finite systems. More precisely, mean-field theory fails to predict the long-time dynamics of the system, since it sustains undamped oscillations, which are unachievable for a realistic finite-size system [101]. On the other hand, studies of the dynamical behavior including finite-size effects are limited in system size, owing to insufficient numerical performance and to the lack of an analytical solution for the dynamics. Hence, *Liu et al.* [92] developed an effective approach, called the stroboscopic rotating-wave approximation, which provides a good approximation to the state describing the long-time evolution of boundary time crystals under strong driving. This approach divides the

system evolution into long-time evolution at stroboscopic points and short-time evolution between adjacent stroboscopic points. Thus, they were able to provide analytical expressions for the dynamics of $\langle S^z \rangle$, its decay rate, and the steady state in the strong-driving regime.

4.2.3 Two coupled driven dissipative collective spin systems

Now that we have presented an open quantum system that exhibits spontaneous breaking of the continuous time-translation symmetry into robust periodic oscillations, let us present a system that can exhibit spontaneous breaking of the continuous time-translation symmetry into chaotic oscillations, which can be referred to as a CQTC.
We consider a system consisting of two coupled driven-dissipative collective spins, evolving under the unitary dynamics characterized by the following Hamiltonian

$$H = \Omega(S_A^x + S_B^x) + \frac{\Gamma}{2S}(S_A^+ S_B^- + S_A^- S_B^+), \tag{4.55}$$

where the parameter Γ determines the strength of the coherent coupling between the subsystems and the parameter Ω is the driving frequency of the two subsystems when uncoupled ($\Gamma = 0$). Hence, the addition of the dissipative dynamics yields the following GKSL master equation ($\hbar = 1$)

$$\dot{\rho} = -i\,[H, \rho] + \frac{\kappa}{S}\mathcal{D}[S_A^-]\rho + \frac{\kappa}{S}\mathcal{D}[S_B^+]\rho, \tag{4.56}$$

where κ is the decay (excitation) rate for subsystem A (B). The operators $(\mathbf{S}_j)^2$, with $j = A, B$, are strong symmetries of the dynamics, which means that the total spin is a conserved quantity in both subsystems. Thus, as for the CTC described in the previous section, we restrict our analysis to the totally symmetric Dicke subspace, such that $S = N/2$ for both subsystems. This system has been studied in depth in Refs. [32, 33], and we will present here the main results.

Mean-field analysis

For any generic operator O, we can write the Heisenberg evolution of its expectation value, associated with the system (4.56), as

$$\frac{d}{dt}\langle O \rangle = i\mathrm{Tr}([H, O]\rho) + \frac{\kappa}{2S}\mathrm{Tr}\Big(\Big(S_A^+[O, S_A^-] + [S_A^+, O]S_A^- + S_B^-[O, S_B^+] + [S_B^-, O]S_B^+\Big)\rho\Big) \tag{4.57}$$

If we consider the above equation for the collective spin components S_j^α with $\alpha = x, y, z$ and $j = A, B$, then, in the thermodynamic limit, we can define the rescaled macroscopic spin operators $m_j^\alpha = \langle S_j^\alpha \rangle / S$ and, using the same arguments as in the mean-field analysis of the previous section, derive the following set of differential equations in the thermodynamic limit

$$\begin{aligned}
\dot{m_x^A} &= \kappa_A m_x^A m_z^A + \Gamma m_z^A m_y^B, \\
\dot{m_y^A} &= -\Omega m_z^A + \kappa_A m_y^A m_z^A - \Gamma m_z^A m_x^B, \\
\dot{m_z^A} &= \Omega m_y^A - \kappa_A \left[\left(m_x^A\right)^2 + \left(m_y^A\right)^2\right] + \Gamma(m_y^A m_x^B - m_x^A m_y^B),
\end{aligned} \tag{4.58}$$

where $\kappa_A = \kappa$. The same equations hold for subsystem B, swapping the indices A and B, with $\kappa_B = -\kappa$.
A relevant tool for revealing chaotic behavior of this system in the classical limit is the largest Lyapunov exponent (LLE)[2], which is defined as the limit of the logarithmic rate of separation of two initially close trajectories in phase space

$$\Lambda_L = \lim_{d_0 \to 0} \lim_{t \to \infty} \frac{1}{t} \ln\left(\frac{d(t)}{d_0}\right), \tag{4.59}$$

[2]The LLE is the largest of the Lyapunov exponents, whereas LE refers to the full set of Lyapunov exponents associated with the different directions in phase space.

where d_0 is the initial distance between the two trajectories and $d(t)$ is the distance at time t [97, 102]. Depending on the value taken by Λ_L, we can distinguish different behaviors:

- $\Lambda_L < 0$ **:** Nearby trajectories converge exponentially. The system evolves toward a stable fixed point. The dynamics is non-chaotic.
- $\Lambda_L = 0$ **:** Nearby trajectories neither converge nor diverge exponentially. This corresponds to neutral stability, typical of limit cycles and periodic orbits. In our context, it corresponds to CTCs.
- $\Lambda_L > 0$ **:** Nearby trajectories diverge exponentially in time. The system is sensitive to initial conditions and exhibits chaotic behavior. In our context, it corresponds to CQTCs.

Furthermore, Λ_L refers to a single initial state. Thus, we denote by $\langle \Lambda_L \rangle$ the average LLE over different initial states. In the following, we consider initial states of the form $m = (\alpha, \beta, \sqrt{1-\alpha^2-\beta^2})$, so that $|m| = 1$, with $\alpha, \beta \in [-1, 1]$. The variables α and β are jointly uniformly distributed over a disk of radius a, meaning that their joint probability density function is

$$p(\alpha, \beta) = \frac{1}{\pi a^2}. \tag{4.60}$$

Figure 4.11 represents the phase diagram of the LLE of the nonlinear system (4.58) over different values of the parameters Ω, Γ, and κ. Panel (a) corresponds to the phase diagram for the initial state $\alpha = \beta = 0$, while panels (b) and (c) show the phase diagram averaged over different initial states, with $a = 0.1$ and $a = 1$, respectively. Let us focus on panel (a) to examine the different regimes.
The blue region in the bottom left of the figure corresponds to the melted phase, with a negative value of Λ_L, meaning that the system converges to a stable steady state.
The first CTC region, in the upper right, described by $\Lambda_L = 0$, corresponds to the CTC described in the previous section, with the phase transition at $\Omega/\kappa = 1$ when there is no coupling ($\Gamma = 0$). Thus, this CTC survives when we add a small coupling, but the dynamics becomes quasi-periodic. In the middle of the figure, there is a new CTC region where neither the driving Ω nor the coupling Γ dominates. In this region, the macroscopic z-spin component m_A^z of subsystem A oscillates around a non-zero value, while m_B^z oscillates around zero.
Then, there is a red region—the one of interest in this section—characterized by a positive value of Λ_L, meaning that the dynamics does not converge to a fixed point. Instead, the system sustains persistent oscillations that remain non-periodic. This behavior originates from the competition between two distinct ordering mechanisms encoded in the set of differential equations (4.58), which become relevant in this parameter regime. On the one hand, one contribution favors oscillations involving both m_x and m_y. On the other hand, the competing term tends to enforce oscillatory dynamics restricted primarily to the y-z plane. As the relative strength of these contributions becomes comparable, the system is subjected to competing and non-commensurate ordering tendencies. This frustration between the two mechanisms ultimately leads to chaotic dynamics, giving rise to a CQTC regime.
We can see in panels (b) and (c) of Figure 4.11 that all the regimes remain clearly visible even when we average over many initial conditions, although they appear smeared out, which confirms the robustness of the phase diagram with respect to the choice of initial state.

Finite size analyzis

In Ref. [32], the authors performed a dynamical analysis of the system (4.56) to go beyond the mean-field analysis for large finite system sizes, by introducing the truncated Wigner approximation (TWA) for open quantum spins. The first step is to rewrite the master equation (4.56) in terms of bosonic operators by performing the Schwinger-boson transformation [103, 104] on the collective spins of subsystems A and B. The TWA is then a technique to transform the time

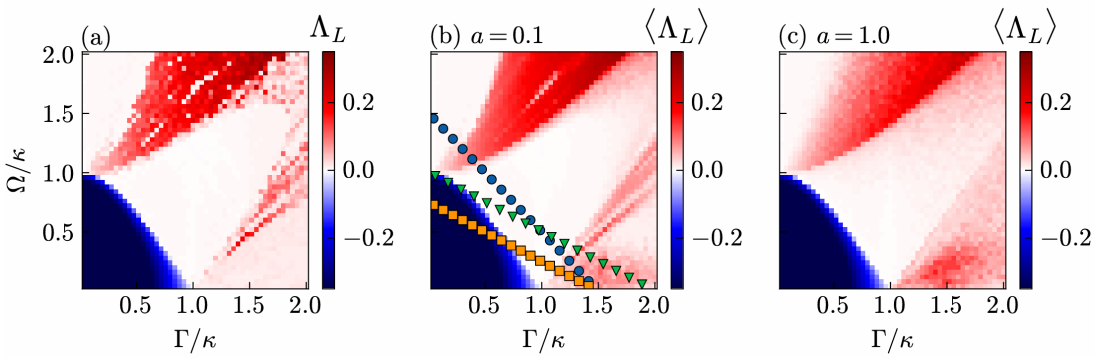

Figure 4.11: Largest Lyapunov exponent Λ_L versus Γ and Ω. (a) Initial conditions $m_j^z = 1$ and $m_j^{x,y} = 0$ for all j. (b) Averaged over 50 random initial conditions with $a = 0.1$, (c) with $a = 1$. Reprinted from Ref. [33].

evolution of the bosonic system into a set of stochastic (Itô) differential equations. While the derivation of these equations is not of interest here, the numerical results are, and can be seen in Figure 4.12. Panels (a) and (b) show the dynamics of the average z-spin component, $\langle m_A^z\rangle$ and $\langle m_B^z\rangle$ respectively, for different finite system sizes obtained using the TWA, together with the mean-field dynamics for subsystems A and B, in the CQTC phase ($\Omega/\kappa = 2$ and $\Gamma/\kappa = 1.4$). We can see that the CQTCs approach the mean-field limit as the system size is increased within the TWA. The advantage of the TWA is that it is expected to capture correlations beyond the mean-field ones. However, only quantum fluctuations at the lowest order in $\hbar$ are included. We emphasize that the TWA also works in the CTC regime of this system. In panel (c), the Fourier transform of the dynamics of $\langle m_A^z\rangle$ shown in (a) is computed over a time $\kappa t = 10^2$, while in panel (d) it is computed over a time $\kappa t = 10^3$. The chaotic behavior manifests itself as a broad, random distribution of frequencies.

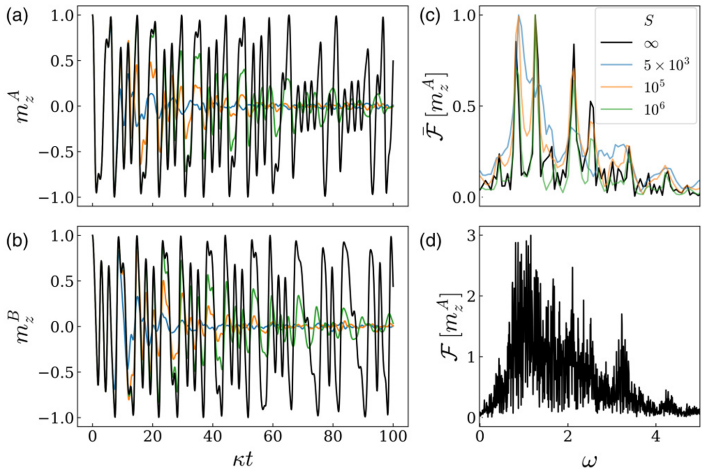

Figure 4.12: (a,b) Chaotic evolution of subsystems A and B over time obtained using mean-field dynamics (black line) and the TWA (color lines), for $\Gamma/\kappa = 2$ and $\Omega/\kappa = 1.4$. (c,d) Normalized emission spectrum corresponding to the dynamics of m_A^z shown in (a). The spectrum in (c) is obtained from the Fourier transform over a time interval $\kappa t = 10^2$, while (d) corresponds to $\kappa t = 10^3$. Reprinted from Ref. [32].

Let us check whether this CQTC satisfies the conditions on the Liouvillian spectrum given in section 4.2.1. In Figure 4.13, the left panels show the evolution of the imaginary parts of three different eigenvalues λ_1, λ_2, and λ_3 as a function of the system size S, while the right panels

show the evolution of the real parts of the same three eigenvalues. We can see that the real parts of the three eigenvalues approach zero in the thermodynamic limit, with different decay rates d_k. As for the imaginary parts, it can be observed that those of these three eigenvalues take incommensurate values in the thermodynamic limit, since $\mathrm{Im}[\lambda_3^\infty]-\mathrm{Im}[\lambda_2^\infty] \neq n\,\mathrm{Im}[\lambda_3^\infty]-\mathrm{Im}[\lambda_1^\infty]$ for any integer n. Hence, these observations confirm the closing of the spectral gap, together with incommensurate purely imaginary eigenvalues, for the CQTC phase.

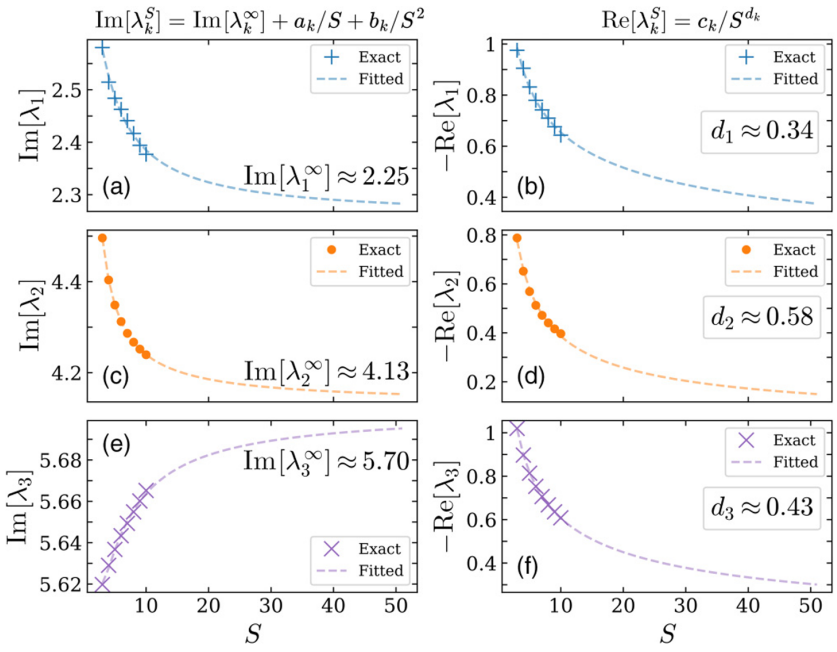

Figure 4.13: Spectrum of the Liouvillian given by Eq. (4.56) in the chaotic phase. Scaling of the imaginary (a,c,e) and real (b,d,f) parts of three distinct eigenvalues λ_1, λ_2, and λ_3 as a function of the system size $S_A = S_B = S$. The data are fitted using the scaling forms introduced in Fig. 5. We use $\Gamma/\kappa = 2$ and $\Omega/\kappa = 1.4$. The imaginary parts are fitted with $\mathrm{Im}[\lambda_k^S] = \mathrm{Im}[\lambda_k^\infty] + \frac{a_k}{S} + \frac{b_k}{S^2}$, where $\mathrm{Im}[\lambda_k^\infty]$ denotes the extrapolated thermodynamic limit $S \to \infty$. The real parts are fitted using $\mathrm{Re}[\lambda_k^S] = c_k S^{-d_k}$, where d_k characterizes the finite-size scaling and indicates the vanishing of $\mathrm{Re}[\lambda_k]$ in the thermodynamic limit. Reprinted from Ref. [32].

4.3 Time glasses

If we summarize, for the moment, the different concepts of time crystals that we have in open quantum systems, we first saw in Section 4.1 that the concept of the discrete time crystal has been generalized, even with the introduction of dissipation, where the discrete time-translation symmetry can be broken into robust and persistent subharmonic oscillations in the thermodynamic limit.

We then saw the concept of the continuous time crystal in open quantum systems in Section 4.2, where the continuous time-translation symmetry can be broken in a non-equilibrium quantum system through the competition between continuous driving and dissipation, which induces robust and persistent periodic oscillations in the thermodynamic limit. In parallel, we also introduced the concept of the continuous quasi-time crystal, which is characterized by the breaking of continuous time-translation symmetry such that the open quantum system exhibits robust and persistent aperiodic oscillations and, most importantly, chaotic behavior.

An interesting question now is the following: if we return to a dissipative open quantum system subjected to periodic driving, is it also possible to find a phase in which the system breaks the discrete time-translation symmetry such that it exhibits robust and persistent aperiodic oscilla-

tions and chaotic behavior, as an analog of the continuous quasi-time crystal but in a periodic system? The answer is yes; this was introduced and described theoretically very recently by *T. Haiga*, leading to the concept of time glasses [34].
In this section, we will therefore present the main properties of time glasses and their signatures, as presented in Ref. [34], and study a simple system exhibiting this kind of behavior, which is a kicked collective spin system, by performing a mean-field analysis and studying its quantum properties in the finite-size case.

4.3.1 Properties

We begin by emphasizing that the content of this section is entirely based on Ref. [34], as time glasses constitute a recently proposed non-equilibrium phase of matter.
The time glass extends the idea of discrete time crystals by replacing subharmonic oscillation with aperiodic oscillation and chaotic dynamics. In this phase, the microscopic constituents remain synchronized but the collective order parameter evolves in an irregular and unpredictable manner. Despite its chaotic nature, this behavior is remarkably robust: the characteristic timescale of the dynamics increases with system size, allowing the chaotic motion to persist indefinitely in the thermodynamic limit. As a result, the time glass represents a minimal and physically realizable example of macroscopic chaos, combining collective synchronization with sustained chaotic temporal evolution. The difference with continuous quasi time crystals and time glasses is that for the latter the system is subjected to a periodic driving such that is has a discrete time translation symmetry.
Since the thermodynamic limit is time and again the appropriate framework to describe spontaneous symmetry breaking, mean-field theory is again an easy framework to work with to describe the property of the relevant observables thanks to deterministic non-linear differential equations which provide us nice identification of the different phase and its transitions point, the critical exponents and an easy first study of the chaotic behavior of the system thanks to classical chaotic theory already well known.
Furthermore, we can characterize the behavior of time glasses through the correlation function. Hence, by using the autocorrelation function $C_M^{\infty}(t)$ in the thermodynamic limit, we can characterize time glasses:

Correlation-based definition of time glasses:
Time glasses are characterized by a nonzero equal-time correlation function, $C_M^{\infty}(0) > 0$, while their temporal correlations decay at long times, $C_M^{\infty}(t) \to 0 \quad \text{as} \quad t \to \infty$. This contrasts with discrete time crystals, which display persistent subharmonic oscillations. The decay in time glasses results from the chaotic dynamics that governs the evolution of the order parameter.

In the case of a Floquet open quantum system, we can focus only on the stroboscopic evolution to facilitate the analyzes, via the Floquet propagator, of an observable $\mathcal{O}$ associated with an operator O acting as an order parameter such that the stroboscopic evolution in the Heisenberg picture is given by

$$O(nT) = (\mathcal{E}_F^{\dagger})^n O, \tag{4.61}$$

and the corresponding stroboscopic correlation function is

$$C_M(nT) = \langle O(nT)O(0)\rangle_{ss} = \mathrm{Tr}\big[O(\mathcal{E}_F^n O\rho_{ss})\big]. \tag{4.62}$$

The correlation function provides a useful tool, as for discrete time crystals, to characterize the dynamical behavior of time glasses and to distinguish them from other phases such as discrete time crystals, static ordered states, and disordered phases. A central question is how time glasses can be identified from the structure of their Floquet spectrum and, more generally,

from their spectral properties. A key feature of the time glass phase is the coexistence of spontaneous symmetry breaking with a finite spectral gap. This is particularly unusual, since in typical many-body systems symmetry breaking is accompanied by a closing of the gap. In open quantum systems described by a Lindblad master equation, for instance, symmetry-broken steady states are generally associated with a vanishing Floquet gap Δ_F in the thermodynamic limit. Thus, the time glass phase exhibits symmetry breaking while maintaining a nonzero gap, making this behavior a distinctive and robust signature of the phase. Time glasses exhibit a fundamentally different spectral structure. Their dynamics is characterized by chaotic temporal fluctuations, leading to a continuous Fourier spectrum.
The relevant relaxation timescale, denoted τ_{rel}, quantifies the duration over which these chaotic oscillations persist. Remarkably, this timescale increases only logarithmically with system size, $\tau_{\text{rel}} \sim \ln N$. At first sight, the divergence of τ_{rel} in the thermodynamic limit appears to contradict the presence of a finite Floquet gap, since a nonzero gap typically implies exponential relaxation with a finite characteristic timescale set by the inverse gap. This apparent paradox is resolved by distinguishing between asymptotic relaxation and transient dynamical behavior. While Δ_{F} governs the ultimate approach to the steady state, the observed relaxation time can be strongly influenced by system-size dependent overlaps with slow modes (coefficients). In particular, if the projection of the initial state onto eigenmodes with small decay rates increases with system size, the effective relaxation time may grow significantly, even in the presence of a finite spectral gap.
These are the main properties exhibited by time glasses, and we will therefore present a simple kicked collective spin system that exhibits this kind of behavior, as developed in Ref. [34].

4.3.2 Discrete quasi time crystals

Before studying the kicked collective-spin system, we briefly discuss discrete quasi-time crystals. In particular, one may wonder why this phase is not referred to as a discrete quasi-time crystal, by analogy with continuous quasi-time crystals. In fact, this is because this nomenclature has already been used and is already quite ambiguous whether it be in closed or open quantum system. While most papers define a discrete quasi-time crystal as a system with discrete time-translation symmetry whose response further breaks the time-translation symmetry of the drive, exhibiting robust and persistent aperiodic oscillations in the thermodynamic limit [36, 87, 105], other works use the term differently. In particular, some papers refer to discrete quasi-time crystals as systems subjected to an aperiodic drive that nevertheless display a periodic response [106, 107], or a distinct aperiodic response [108]. However, it is not related to any kind of chaotic behavior. If we refer to the most common definition of discrete quasi time crystal, the property of the system that exhibits this kind of behavior must possess quite the same property as that of a discrete time crystal (see section 4.1 for a reminder). Indeed, the discrete quasi time crystal phase is also characterized by a limit cycle or an aperiodic orbit around a stable state in the phase space but the oscillations of the order parameter are aperiodic. In this case it leads to a discrete Fourier spectrum composed of sharp Bragg-like peaks. Furthermore, the signature of discrete quasi time crystals based on the correlation function $C_M(t)$ are almost the same as discrete time crystals except that $C_M(t)$ must exhibit aperiodic oscillations and not subharmonic oscillations. Last but not least, the Floquet spectrum of a discrete quasi time crystal must contain eigenvalues in the peripheral spectrum of the Floquet map whose phases are incommensurate. The interference between these modes then gives rise to aperiodic oscillations. In addition, the system must exhibit a Floquet dissipative gap that closes in the thermodynamic limit. Hence it is instructive to contrast this behavior with that of time glasses briefly discussed in the previous section in order to clearly distinguish between them.
We have therefore chosen to focus primarily on time glasses, in which the aperiodicity of the response is synonymous with chaotic behavior, rather than on discrete time quasi crystals, whose concept is rather unclear in the literature and which do not really exhibit properties or behaviors

richer than those of discrete time crystals, except that they exhibit aperiodic oscillations.

4.3.3 Kicked dissipative collective spin system

A simple system exhibiting a time glass phase is a collective spin system subjected to a periodic sequence of instantaneous kicks rather than a continuous drive. Its Hamiltonian is

$$H = \omega_z S^z + \frac{\omega_{xx}}{S}(S^x)^2 \sum_n \delta(t - nT), \qquad n \in \mathbb{Z}, \tag{4.63}$$

where $S = N/2$ denotes the total spin, ω_z is the frequency associated with the energy splitting of the underlying two-level system, and ω_{xx} characterizes the strength of the kicks. The system receives an instantaneous kick every period T; throughout this work, we set $T = 1$. As before, our analysis is restricted to the symmetric Dicke subspace. The dissipative dynamics is described by the usual GKSL master equation ($\hbar = 1$),

$$\dot{\rho} = \mathcal{L}(\rho) = -i[H, \rho] + \frac{\kappa}{S}\left(S^- \rho S^+ - \frac{1}{2}\{S^+ S^-, \rho\}\right). \tag{4.64}$$

This model possesses the strong $\mathbf{S}^2$ symmetry, implying conservation of the total spin quantum number, as well as a weak $\mathbb{Z}_2$ symmetry corresponding to a rotation by π about the z-axis. The stroboscopic evolution is therefore characterized by the following Floquet map

$$\mathcal{E}_F = e^{-i\omega_{xx}(S^x)^2/S} e^{\mathcal{L}} e^{i\omega_{xx}(S^x)^2/S}. \tag{4.65}$$

Mean-field analysis

As already discussed, in the thermodynamic limit $S \to \infty$ we can define the macroscopic spin observables $m^\alpha = S^\alpha/S$, such that, in the mean-field limit, the dissipative dynamics of the macroscopic spin observables is governed by a set of nonlinear differential equations:

$$\begin{aligned} \dot{m^x} &= -\omega_z m^y + \kappa m^x m^z, \\ \dot{m^y} &= \omega_z m^x + \kappa m^y m^z, \\ \dot{m^z} &= -\kappa\left((m^x)^2 + (m^y)^2\right). \end{aligned} \tag{4.66}$$

These equations of motion preserve the norm of the spin vector $\mathbf{m}$, and we take $|\mathbf{m}| = 1$, so that the dynamics remains confined to the surface of the Bloch sphere. The coherent contribution associated with the term ω_z generates a precession around the z-axis, whereas the dissipative terms controlled by κ progressively align the spin along the negative z direction. Consequently, the state $\mathbf{m} = (0, 0, -1)$ acts as an attracting fixed point, while $\mathbf{m} = (0, 0, 1)$ is unstable.
To determine the effect of the periodic kick, it is useful to introduce an auxiliary time variable ($t \in [0, 1]$) and to interpret the kick as a continuous unitary evolution governed by

$$\dot{\rho} = -i\left[\frac{\omega_{xx}}{S}(S^x)^2, \rho\right]. \tag{4.67}$$

The transformation induced by a single kick is then obtained by integrating this equation over the interval ($t \in [0, 1]$). In the mean-field limit, the corresponding equations for the macroscopic spin observables m^α take the form

$$\begin{aligned} \dot{m}^x &= 0, \\ \dot{m}^y &= -2\omega_{xx} m^x m^z, \\ \dot{m}^z &= 2\omega_{xx} m^x m^y. \end{aligned} \tag{4.68}$$

These equations also preserve the norm of the spin vector $\mathbf{m}$. They describe a rotation around the x-axis with an angular velocity proportional to ω_{xx}. As a result, points located in the hemispheres $m^x > 0$ and $m^x < 0$ rotate in opposite directions, producing a nonlinear twisting of the Bloch sphere around the x-axis. One period of the stroboscopic evolution is obtained by first evolving the system under the dissipative dynamics for one unit of time and subsequently applying the kick evolution.
Figure 4.14 shows the bifurcation diagrams of the macroscopic spin observables m^α as a function of the parameter ω_{xx}. It has been computed by integrating the dynamics of Eq. (4.66) for a time $t_0 = 1$, then the dynamics of Eq. (4.68) for a time $t_1 = 1$, and so on periodically, while discarding the transient dynamics, for $\omega_z = \pi/2$ and $\kappa = 1$. We can distinguish three different dynamics:

- $\omega_{xx} \lesssim 1.5$: The system relaxes to the stable fixed point $\mathbf{m} = (0, 0, -1)$. This corresponds to a disordered phase in the x-y plane.
- $1.5 \lesssim \omega_{xx} \lesssim 2.3$: The system undergoes spontaneous symmetry breaking, and a subharmonic period-2 limit cycle emerges for the observables m^x and m^y. This corresponds to a discrete time-crystal phase.
- $\omega_{xx} \gtrsim 2.3$: The system exhibits chaos, characterizing a time-glass phase.

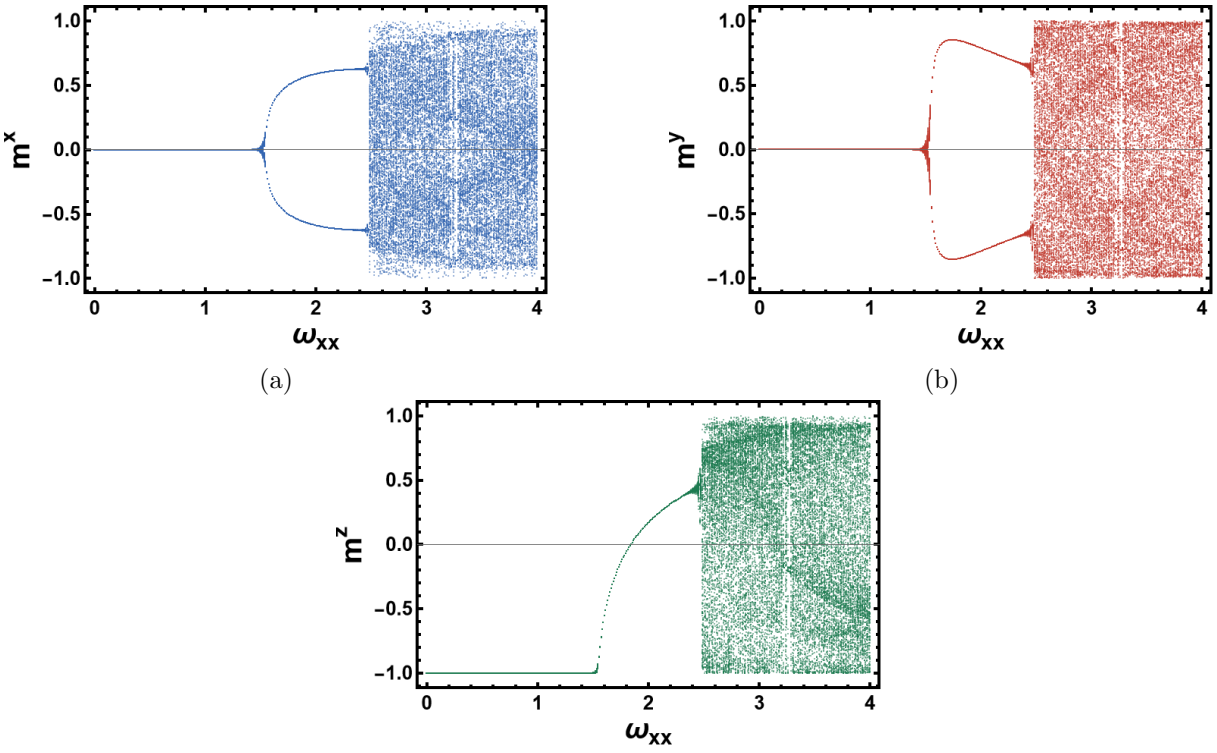

(a) (b) (c)

Figure 4.14: Bifurcation diagrams of the macroscopic spin observables: (a) m^x, (b) m^y, and (c) m^z, as functions of the kick strength ω_{xx}, for $\omega_z = \pi/2$ and $\kappa = 1$. The diagrams are obtained from the stroboscopic dynamics generated by alternating evolution under Eq. (4.66) for a duration $t_0 = 1$ and under Eq. (4.68) for a duration $t_1 = 1$. As ω_{xx} increases, the system undergoes a sequence of dynamical transitions from a stable fixed point to periodic limit cycles via period-doubling bifurcations, and eventually to chaotic behavior.

In addition to the bifurcation diagrams, we can also compute the largest Lyapunov exponent

(LLE) to detect chaos. To do so, we computed the latter with Mathematica using the standard Benettin algorithm [109]. Two initially nearby trajectories are evolved according to Eq. (4.66) during time $t_0 = 1$ and then according to Eq. (4.68) during time $t_1 = 1$ such that one period of the dynamic is $T = t_0 + t_1$. After discarding an initial transient to ensure convergence to the asymptotic dynamics, the distance d_n between the trajectories is measured after each forcing period T. The quantity $\ln(d_n/d_0)$ is recorded, where d_0 denotes the initial separation. The perturbed trajectory is then renormalized along the separation vector to restore the distance d_0, and the procedure is iterated. The Lyapunov exponent is finally estimated as

$$\Lambda_L = \frac{1}{KT} \sum_{n=1}^{K} \ln\left(\frac{d_n}{d_0}\right), \tag{4.69}$$

where K is the number of periods used for averaging after the transient has been removed. Hence, in Fig. 4.15a, we compute a phase diagram of the LLE as a function of ω_z and ω_{xx} for $\kappa = 1$, starting from the initial condition $m^x = 1$ and $m^{y,z} = 0$. The black dashed line indicates the parameter path along which the LLE shown in Figure 4.15b was evaluated with $\omega_z = \pi/2$. Along this path, the LLE remains negative in the region corresponding to the stable fixed-point phase and approaches zero at the critical point where the bifurcation diagram in Figure 4.14 signals the transition to the discrete time crystal (DTC) phase. Upon further increasing ω_{xx}, the LLE becomes positive at the transition between the DTC phase and the chaotic phase, again in agreement with the bifurcation analysis of Figure 4.14.
More generally, the phase diagram in Figure 4.15a clearly reveals the presence of the three distinct dynamical regimes. These regions are separated by the white regions corresponding to vanishing LLE. In particular, the transition between the static phase and the discrete time-crystal phase is given by the black curve, which encode the relation between the critical values ω_z^c and ω_{xx}^c,

$$\omega_z^c = \arccos\left(\frac{-\cosh\kappa}{\sqrt{1+(\omega_{xx}^c)^2}}\right) - \arctan(\omega_{xx}^c). \tag{4.70}$$

This relation follows from a linear stability analysis of the steady fixed point: it locates the parameters at which the fixed point loses stability through a period-doubling bifurcation, signaling the onset of the subharmonic period-$2T$ response that characterizes the discrete time crystal. Furthermore, this relation is defined for $\omega_{xx}^c > \sinh(\kappa)$. For the particular value $\omega_z = \pi/2$, Eq. (4.70) reduces to the critical point

$$\omega_{xx}^c = \frac{e^{2\kappa}+1}{2e^{\kappa}} = \cosh\kappa, \tag{4.71}$$

in agreement with the value given in Ref. [34]. Hence, the diagram demonstrates that both the discrete time crystal phase and the time-glass phase persist away from the special point $\omega_z = \pi/2$, indicating that these phases exist over a finite range of parameters.

Finite size system analysis

Let us now investigate the behavior of this system outside the thermodynamic limit by considering finite-size effects.
We can start by analyzing the behavior of the correlation function applied to this system. Here, we will define the order parameter as $\langle S^x\rangle/S$, such that the correlation function is given by

$$C_M(t) = \frac{\langle S^x(t)S^x(0)\rangle_{\text{ss}}}{S^2}, \tag{4.72}$$

and let us look at its behavior when we increase the system size S in Figure 4.16, for different values of the kick-intensity parameter ω_{xx}. Figures a, b, and c correspond to kick strengths

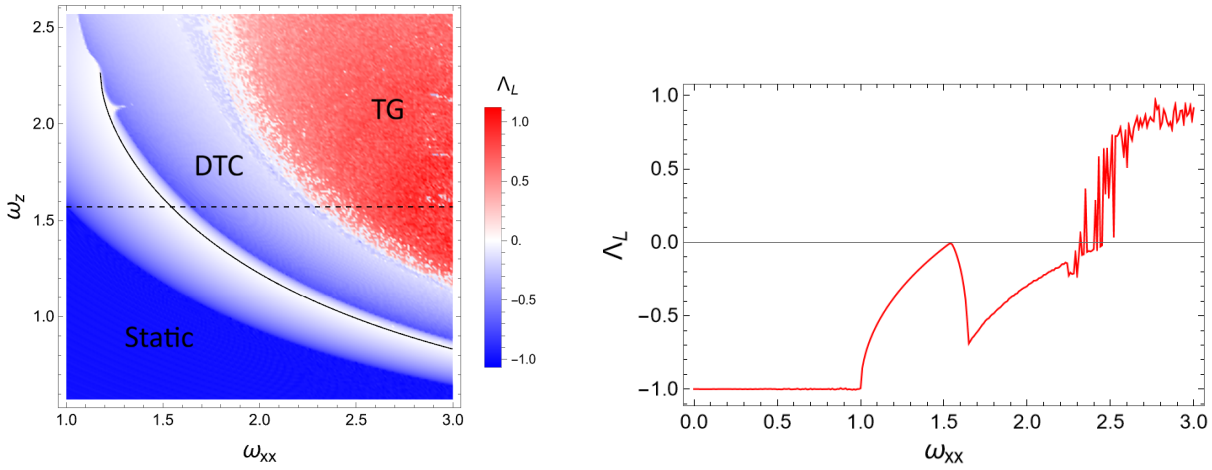

(a) (b)

Figure 4.15: (a) Phase diagram of the LLE Λ_{L} as a function of ω_z and Ω, for $\kappa = 1$ and initial conditions $m^x = 1$, $m^{y,z} = 0$. The different dynamical regimes (stable fixed point, discrete time crystal, and time glass) are separated by the white curves corresponding to vanishing LLE. The black curve corresponds to the transition between the static order and the discrete time crystal order given by Eq. (4.70). (b) Evolution of the LLE as a function of ω_{xx} for $\omega_z = \pi/2$, corresponding to the black dashed line in panel (a).

$\omega_{xx} = 1$, 2, and 3, respectively. According to the bifurcation diagram in Figure 4.14, Figures a, b, and c correspond to the disordered phase, the discrete time-crystal phase, and the time-glass phase, respectively.
Hence, in Figure 4.16a, we can observe that $C_M(t)$ decays as $\propto S^{-1}$ when we increase S, which is confirmed by the decay of $C_M(0)$ in Figure 4.16d. As a result, we can conclude that $C_M^{\infty}(t) = 0, \quad \forall t$, which is a signature of the disordered phase.
In Figure 4.16b, $C_M(t)$ exhibits subharmonic period-2 oscillations whose persistence increases as S increases. Moreover, in Figure 4.16d, we can see that $C_M(0) \neq 0$ and remains constant as S increases. We can conclude that $C_M^{\infty}(t)$ must exhibit persistent period-2 subharmonic oscillations at infinite time, and that $C_M^{\infty}(0) \neq 0$ in the thermodynamic limit, which is a signature of the discrete time-crystal phase (see section 4.1).
In Figure 4.16c, $C_M(t)$ decreases immediately for all S, and we can observe in Figure 4.16d that $C_M(0) \neq 0$ and remains constant as S increases. We can conclude that $C_M^{\infty}(t) = 0$ for $t \neq 0$ and $C_M^{\infty}(0) \neq 0$ in the thermodynamic limit, which is a signature of the time-glass phase.
Let us now analyze the spectral properties of the Floquet map characterized by Eq. (4.65). We begin by examining the Floquet spectrum of the kicked collective spin. Figure 4.17 shows the eigenvalues $\{\lambda_\alpha\}$ of the Floquet map for $\omega_{xx} = 1$ (Figure 4.17a-c), $\omega_{xx} = 2$ (Figure 4.17d-f), and $\omega_{xx} = 3$ (Figure 4.17g-i).
For $\omega_{xx} = 1$, where the classical limit supports a stable fixed point, the Floquet gap converges to a nonzero, finite value as S grows, as indicated by the red arrow. The eigenvalue λ_1 shifts only slightly with increasing S, which makes this convergence apparent. The remaining eigenvalues λ_α ($\alpha > 1$) likewise appear to settle toward definite values in the limit $S \to \infty$.
For $\omega_{xx} = 2$, corresponding to the discrete time-crystal phase, $\lambda_1 \to -1$ as $S \to \infty$, as the red arrows indicate. This limit signals that the system develops period-2 subharmonic oscillations, in accordance with the definition of discrete time crystals in section 4.1.
For $\omega_{xx} = 3$, corresponding to the time-glass phase, the data indicate that the Floquet gap stays non-zero as $S \to \infty$. We note that, for both $\omega_{xx} = 2$ and $\omega_{xx} = 3$, the eigenvalues λ_α ($\alpha > 1$) show no clear tendency to converge to definite values up to $S = 32$.
Focusing now on the discrete time-crystal phase for $\omega_{xx} = 2$, we can clearly see in Figure 4.18b

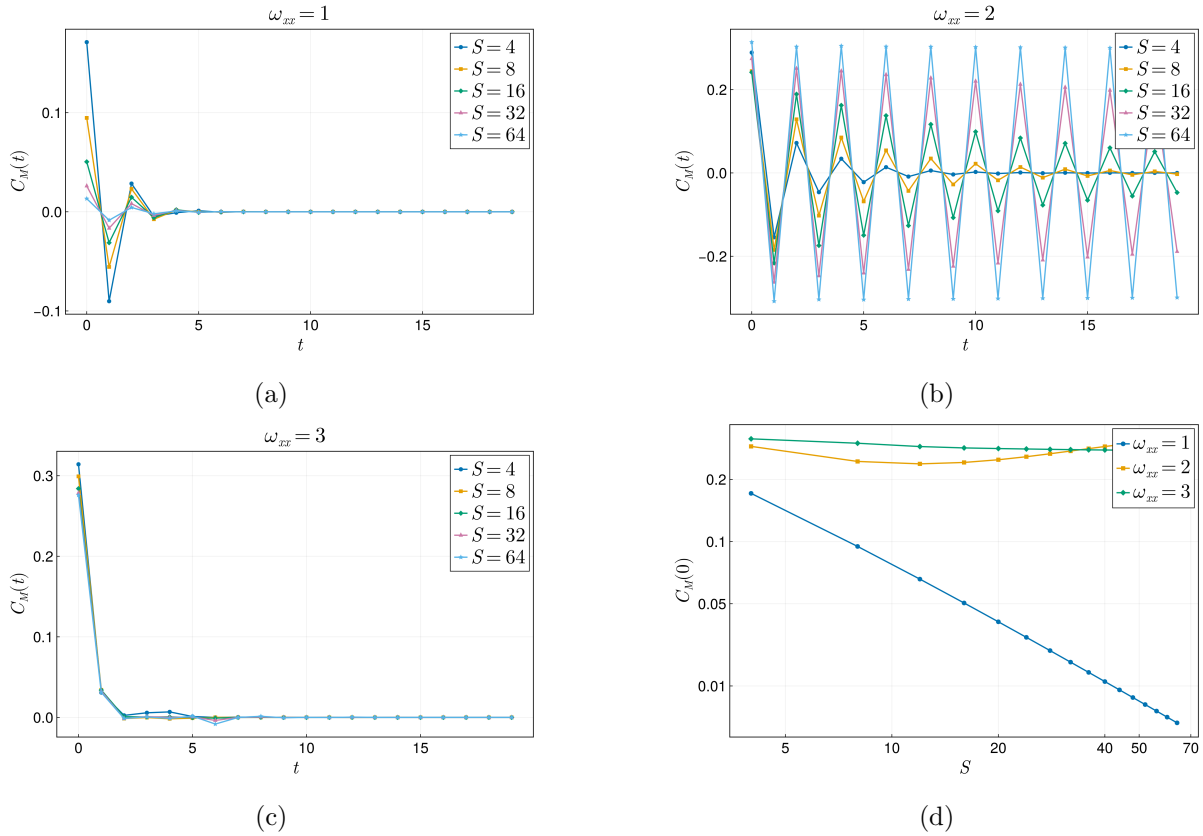

Figure 4.16: Time evolution of the correlation function $C_M(t)$, given by Eq. (4.72), for (a) the disordered phase ($\omega_{xx} = 1$), (b) the discrete time-crystal phase ($\omega_{xx} = 2$), and (c) the time-glass phase ($\omega_{xx} = 3$). (d) Evolution of $C_M(0)$ as a function of S for $\omega_{xx} = 1, 2, 3$. Data obtained from the GitHub repository provided in Ref. [34].

that the Floquet gap Δ_F decreases exponentially as a function of S, tending to 0 in the thermodynamic limit, in accordance with the property of discrete time crystals defined in section 4.1. This behavior is in contrast to the case $\omega_{xx} = 1$ in Figure 4.18a, where Δ_F appears to tend to a finite value in the thermodynamic limit. Furthermore, in the time glass phase, we can clearly observe in Figure 4.18c that the Floquet gap tends to a finite value
Figure 4.18d shows how the Floquet gap Δ_F evolves with the kick strength ω_{xx} for increasing system size S. For $\omega_{xx} \lesssim 1.5$, the gap remains pinned close to unity and is essentially independent of S: this is the disordered phase, where a single stable fixed point governs the dynamics and the gap stays finite. As ω_{xx} increases past the dashed line, the gap collapses, and over the window where $\Delta_F \to 0$ the finite-S curves converge onto the classical result. This vanishing gap is the signature of the discrete time-crystal phase. For larger ω_{xx}, the gap reopens and does not close cleanly but instead remains finite, corresponding to the chaotic behavior of the time-glass phase. The boundaries between these three regimes coincide with the transitions seen in the bifurcation diagrams of Figure 4.14.

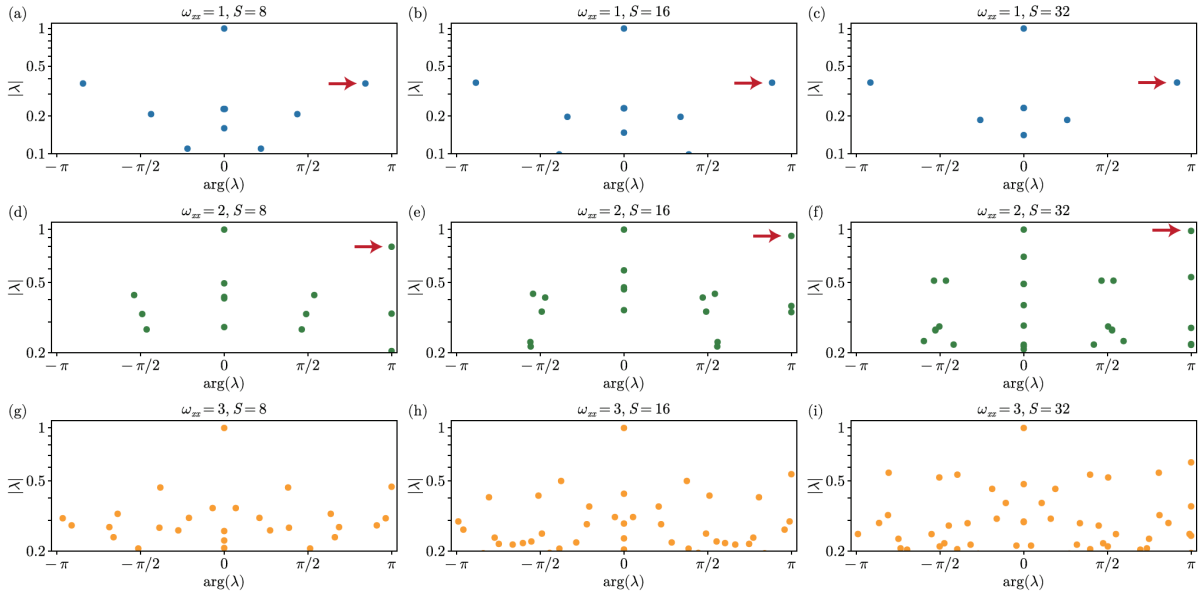

Figure 4.17: Spectrum λ_α of the Floquet map of the kicked collective spin system given by Eq. (4.65). Panels (a)-(c) show the spectra for kick strength $\omega_{xx} = 1$ with $S = 8$, 16, and 32, respectively. Panels (d)-(f) show the spectra for kick strength $\omega_{xx} = 2$, and panels (g)-(i) for $\omega_{xx} = 3$. In all cases, the remaining parameters are fixed at $\omega_z = \pi/2$ and $\kappa = 1$. Reprinted from Ref. [34]

.

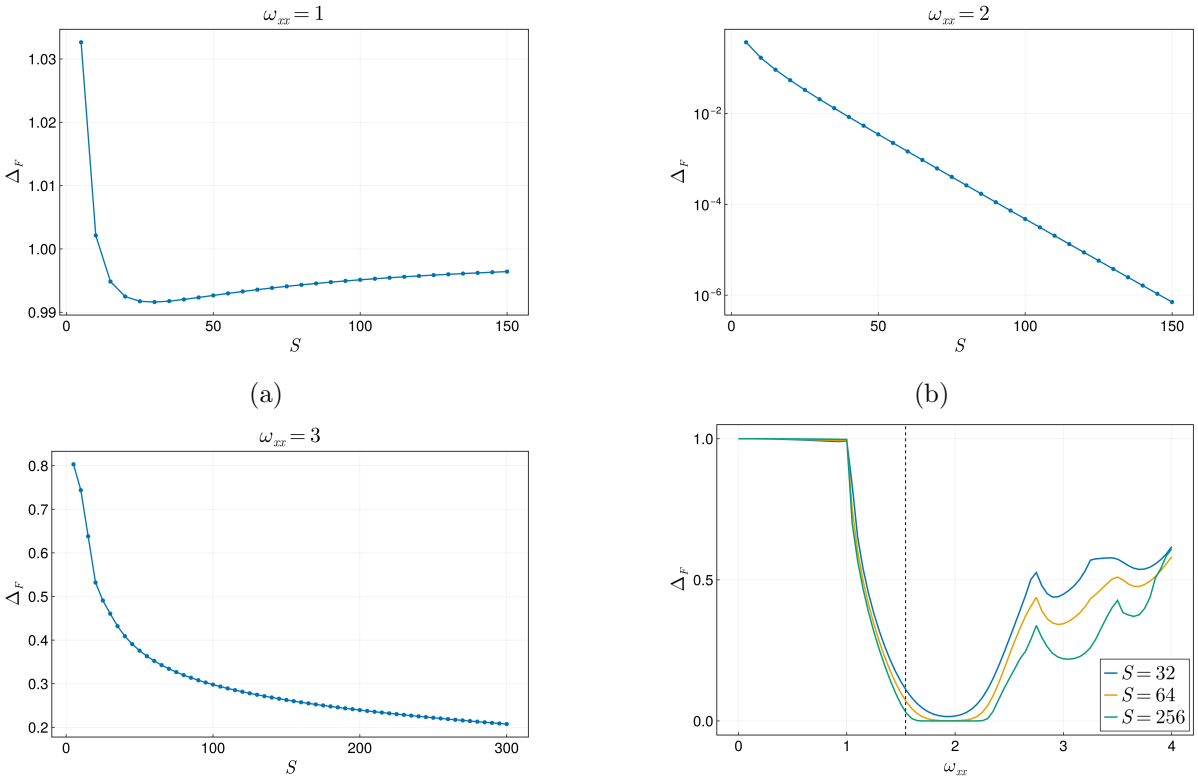

Figure 4.18: Evolution of the Floquet gap Δ_F as a function of S with (a) $\omega_{xx} = 1$, (b) $\omega_{xx} = 2$ and (c) $\omega_{xx} = 3$, with $\kappa = 1$ and $\omega_z = \pi/2$. (d) Floquet gap Δ_F of the Floquet map given by Eq. (4.65), as a function of the kick strength ω_{xx}, with $S = 32$, 64, 128, and 256. The dashed vertical line marks the critical kick strength at which the fixed point loses stability and a limit cycle appears given by Eq. (4.71). Data obtained from the GitHub repository provided in Ref. [34].

Conclusion

The aim of this thesis was to give a unified and pedagogical overview of the different time crystals that arise in open quantum systems. We close by retracing the path we followed and by indicating where the most promising open questions lie.

We began with discrete time crystals in closed quantum systems. The intention there was not to give an exhaustive technical treatment, but rather a reasonably complete conceptual picture, enough to make the subsequent transition to open systems natural. The core idea is that a discrete time crystal extends the principle of spontaneous symmetry breaking into the time dimension: under a periodic drive, an interacting many-body system spontaneously breaks the residual discrete time-translation symmetry and responds at a subharmonic of the driving frequency, in a way that is rigid against perturbations and persistent in the thermodynamic limit. Its very existence is a response to the no-go theorems that forbid time crystals in equilibrium: by leaving equilibrium through periodic driving, and by relying on a mechanism such as many-body localisation to avoid the generic heating of Floquet systems, time-crystalline order becomes possible as a genuine non-equilibrium phase of matter, with appealing prospects as a robust resource for quantum memory and metrology. This closed-system picture, however, is an idealisation: any realistic platform is coupled to an environment, which is precisely what motivated the rest of this work.

Property	**Time crystals in closed quantum systems**	
	DTC	**Prethermal DTC**
Symmetry	Discrete time-translation induced by a periodic driving T, i.e. $H(t) = H(t+T),\ \forall t$	
SSB	Subharmonic oscillation of the order parameter: period nT, $n \in \mathbb{Z}$, $n \geq 2$	
Rigidity	Rigid: subharmonic locking survives generic drive imperfections	
Persistence	Infinite lifetime	Finite lifetime in the thermodynamic limit but exponentially long with the drive frequency
Stabilization mechanism	Many-body interactions: MBL, long-range interactions, mean-field nonlinear interactions,...	High driving frequency
Paradigmatic model	Driven disordered spin chain	Driven clean Ising spin chain

Table I: Comparative table between DTC and prethermal DTC in closed quantum systems.

We therefore turned to open quantum systems, focusing on the Markovian regime governed by the Gorini–Kossakowski–Sudarshan–Lindblad (GKSL) master equation, and we developed the associated tools, the Liouville-space formulation and the spectral analysis of the Liouvillian, that the analysis of dissipative time crystals requires.

With this framework in place, we entered the core of the thesis. We first treated discrete time crystals (DTC) in open quantum systems, presenting their defining properties and a precise definition built on the correlation function of the order parameter and on the spectrum of the Floquet map. We then generalised the dephasing spin qubit of Ref. [71] to larger spins. These

systems provide a useful introduction to a fully quantum, rather than mean-field, description of DTCs in open quantum systems. They also show that dissipation can, in a certain sense, remove the need for many-body interactions in order to obtain time-crystalline behaviour. At least from the standpoint of Ref.[71], a discrete time crystal may emerge in a system without many-body interactions, with dissipation playing a role analogous to that played by interactions in the closed-system case.

We next presented continuous time crystals (CTC) and continuous quasi time crystals (CQTC). For the CTC, a mean-field treatment reduces the order-parameter dynamics to a set of nonlinear differential equations, and the phase is defined through the correlation function together with the spectrum of the Liouvillian, the signature being the emergence of purely imaginary eigenvalues in the thermodynamic limit, corresponding to a stable limit cycle. The CQTC is a much more recent notion and still calls for further study before a fully satisfactory definition can be settled. We argued that the natural characterisation should likewise rest on the Liouvillian spectrum and the correlation function, and it may ultimately parallel the one that applies to time glasses, for the moment, however, the analysis relies mainly on the Fourier spectrum of the dynamics and on the mean-field description. We illustrated both phases through reference systems, a driven collective spin for the CTC [28] and two coupled driven, dissipative collective spins for the CQTC [32, 33], in order to exhibit their characteristic signatures and properties.

We then introduced the very recent concept of the time glass [34], which can be understood as the Floquet (periodically driven) counterpart of the CQTC. We presented its properties and a definition based on the correlation function and the spectrum of the Liouvillian, and we emphasized the distinction from the discrete quasi time crystal: in a discrete quasi time crystal the temporal order is aperiodic yet regular, whereas in a time glass it is genuinely chaotic. Finally, for a reference kicked collective-spin model [34], we contributed an original mean-field analysis in the form of a phase diagram of the largest Lyapunov exponent. This diagram demonstrates that both the time-glass and the discrete-time-crystal orders of this system are robust over an extended region of parameter space, rather than being confined to fine-tuned points, the hallmark, as throughout this work, of a genuine phase rather than an accidental resonance and presented the finite size analyzes also.
Several directions naturally extend the present study. A first is to move beyond the Markovian, GKSL setting and to ask how each of these phases behaves under non-Markovian system–environment coupling, where memory effects of the bath may either protect or degrade the temporal order, as performed in Ref. [25]. A second is to deepen the understanding of these phases as resources, in particular for quantum metrology and sensing [21, 110], quantum clocks [111], and to sharpen the still-incomplete definitions, most notably that of the continuous quasi time crystal.

A further, avenue concerns time-crystalline order that does not require the thermodynamic limit. Recent works have shown that systems endowed with a strong dynamical symmetry, in the time-independent case, and with a Floquet dynamical symmetry, in the driven case, can sustain persistent oscillations even at finite size [112]: the undamped oscillation is then protected by the symmetry structure, which guarantees purely imaginary Liouvillian eigenvalues regardless of system size, rather than by a collective effect emerging only in the thermodynamic limit. This mechanism offers an attractive route to robust temporal order in small, experimentally accessible systems. We note that a discrete time crystal has already been proposed along the Floquet-dynamical-symmetry line [113], but in our view it remains limited: the discrete time crystal appears only for fine-tuned parameters, whereas away from fine-tuning the robust phase is rather a discrete quasi time crystal.

Taken together, these results follow a single thread. The spontaneous breaking of time-translation symmetry, forbidden in equilibrium, becomes possible out of equilibrium, and dissipation, far from being merely a source of decoherence, emerges as a constructive ingredient

Property	Time Crystals in Open Quantum Systems			
	DTC	Time Glass	CTC	CQTC
Framework	Dynamic generated by a periodic Liouvillian $\mathcal{L}_t$ and characterized by a Floquet map $\mathcal{E}_F$		Dynamic generated by a time-independent Liouvillian $\mathcal{L}$	
Symmetry	Discrete time translation, $\mathcal{L}_t = \mathcal{L}_{t+T}$		Continuous time translation	
Order-parameter response	Subharmonic oscillation: period nT, $n \geq 2$	Chaotic behavior	Periodic oscillation: period T	Chaotic behavior
Correlation function $C_M^\infty(t)$	$C_M^\infty(t) = C_M^\infty(t+nT)$ $C_M^\infty(0) \neq 0$	$C_M^\infty(t) \to 0$, for $t \to \infty$ $C_M^\infty(0) \neq 0$	$C_M^\infty(t) = C_M^\infty(t+T), \forall t$ $C_M^\infty(0) \neq 0$	Not defined
Spectrum property	$\Delta_F \to 0$ in the thermodynamic limit	$\Delta_F \neq 0$ in the thermodynamic limit	$\Delta \to 0$ in the thermodynamic limit	$\Delta \to 0$ in the thermodynamic limit
Rigidity	Rigid: the order-parameter behavior survives for generic, non-fine-tuned parameters of the system.			
Persistence	Infinite lifetime in the thermodynamic limit			
Stabilization mechanism	Many-body interactions, collective dynamics and dissipation			
Paradigmatic model	Single spin-s with dephasing	Kicked driven dissipative collective spin system	Driven dissipative collective spin system	Two coupled driven-dissipative collective spin systems

Table II: Comparative table of time crystals in open quantum systems.

that can stabilize, and even create, temporal order. What results is a rich and still-expanding landscape of phases of matter in time, periodic, quasiperiodic, and chaotic, whose classification and physical realization remain a vivid and open field.

Bibliography

[1] R. Moessner and J. E. Moore, *Topological phases of matter* (Cambridge University Press, 2021).

[2] A. J. Beekman, L. Rademaker, and J. van Wezel, SciPost Phys. Lect. Notes , 11 (2019).

[3] A. S. T. Pires, in *Theoretical Tools for Spin Models in Magnetic Systems*, 2053-2563 (IOP Publishing, 2021) pp. 1–1 to 1–16.

[4] P. Anderson, *Basic Notions Of Condensed Matter Physics* (CRC Press, 2018).

[5] A. Shapere and F. Wilczek, Phys. Rev. Lett. **109**, 160402 (2012).

[6] F. Wilczek, Phys. Rev. Lett. **109**, 160401 (2012).

[7] P. Bruno, Phys. Rev. Lett. **110**, 118901 (2013).

[8] P. Bruno, Phys. Rev. Lett. **111**, 070402 (2013).

[9] H. Watanabe and M. Oshikawa, Phys. Rev. Lett. **114**, 251603 (2015).

[10] K. Sacha, Phys. Rev. A **91**, 033617 (2015).

[11] D. V. Else, B. Bauer, and C. Nayak, Phys. Rev. Lett. **117**, 090402 (2016).

[12] F. Alet and N. Laflorencie, Comptes Rendus Physique **19**, 498 (2018), quantum simulation / Simulation quantique.

[13] S. A. Parameswaran and R. Vasseur, Reports on Progress in Physics **81**, 082501 (2018).

[14] D. A. Abanin, E. Altman, I. Bloch, and M. Serbyn, Rev. Mod. Phys. **91**, 021001 (2019).

[15] P. Ponte, Z. Papić, F. m. c. Huveneers, and D. A. Abanin, Phys. Rev. Lett. **114**, 140401 (2015).

[16] A. Russomanno, F. Iemini, M. Dalmonte, and R. Fazio, Phys. Rev. B **95**, 214307 (2017).

[17] B. Huang, Y.-H. Wu, and W. V. Liu, Phys. Rev. Lett. **120**, 110603 (2018).

[18] A. Pizzi, J. Knolle, and A. Nunnenkamp, Nature Communications **12**, 2341 (2021).

[19] S. Choi, J. Choi, R. Landig, G. Kucsko, H. Zhou, J. Isoya, F. Jelezko, S. Onoda, H. Sumiya, V. Khemani, C. von Keyserlingk, N. Y. Yao, E. Demler, and M. D. Lukin, Nature **543**, 221 (2017).

[20] R. E. Barfknecht, S. E. Rasmussen, A. Foerster, and N. T. Zinner, Phys. Rev. B **99**, 144304 (2019).

[21] R. Ghosh, B. Das, and V. Mukherjee, Physical Review B **113**, 10.1103/hym6-j655 (2026).

[22] P. Frey and S. Rachel, Science advances **8**, eabm7652 (2022).

[23] D. Zhang, X. Li, Y. Guo, H. Yu, Y. Jin, and Z.-Q. Yin, arXiv preprint arXiv:2508.15230 (2025).

[24] A. Lazarides and R. Moessner, Phys. Rev. B **95**, 195135 (2017).

[25] F. Carollo and I. Lesanovsky, Phys. Rev. A **105**, L040202 (2022).

[26] A. Lazarides, S. Roy, F. Piazza, and R. Moessner, Phys. Rev. Res. **2**, 022002(R) (2020).

[27] Z. Gong, R. Hamazaki, and M. Ueda, Phys. Rev. Lett. **120**, 040404 (2018).

[28] F. Iemini, A. Russomanno, J. Keeling, M. Schirò, M. Dalmonte, and R. Fazio, Phys. Rev. Lett. **121**, 035301 (2018).

[29] Y. Huang, T. Wang, H. Yin, M. Jiang, Z. Luo, and X. Peng, Nature Communications **16**, 9375 (2025).

[30] P. Kongkhambut, J. Skulte, L. Mathey, J. G. Cosme, A. Hemmerich, and H. Keßler, Science **377**, 670–673 (2022).

[31] T. L. Heugel, M. Oscity, A. Eichler, O. Zilberberg, and R. Chitra, Phys. Rev. Lett. **123**, 124301 (2019).

[32] P. Solanki and F. Minganti, Phys. Rev. B **112**, 134311 (2025).

[33] E. Postavová, G. Passarelli, P. Lucignano, and A. Russomanno, New Journal of Physics **28**, 034502 (2026).

[34] T. Haga, Phys. Rev. Res. **8**, 013257 (2026).

[35] M. P. Zaletel, M. Lukin, C. Monroe, C. Nayak, F. Wilczek, and N. Y. Yao, Rev. Mod. Phys. **95**, 031001 (2023).

[36] X. Luo, Y. Zhou, Z. Xu, and W. Jiang, Discrete time quasi-crystal in rydberg atomic chain (2025), arXiv:2505.09117 [quant-ph] .

[37] K. Sacha and J. Zakrzewski, Reports on Progress in Physics **81**, 016401 (2017).

[38] K. Sacha, *Time Crystals*, Springer Series on Atomic, Optical, and Plasma Physics (Springer International Publishing, 2020).

[39] D. V. Else, C. Monroe, C. Nayak, and N. Y. Yao, Annual Review of Condensed Matter Physics **11**, 467–499 (2020).

[40] V. Khemani, R. Moessner, and S. L. Sondhi, A brief history of time crystals (2019), arXiv:1910.10745 [cond-mat.str-el] .

[41] R. Zwicky, *Symmetries of Quantum Mechanic* (University od Edinburgh, 2015).

[42] W.-K. Tung, *Group Theory in Physics* (1985).

[43] B. C. Hall, An elementary introduction to groups and representations (2000), arXiv:math-ph/0005032 [math-ph] .

[44] P. Etingof, Lie groups and lie algebras (2026), arXiv:2201.09397 [math.RT] .

[45] K. Ōshika and K. Ōshika, *Discrete groups*, Vol. 207 (American Mathematical Soc., 2002).

[46] V. Bargmann, Journal of Mathematical Physics **5**, 862 (1964).

[47] L. Pacheco, *Quantum Theory for Mathematicians*, Graduate Texts in Mathematics, Vol. 265 (Springer, 2013).

[48] M. Bukov, L. D'Alessio, and A. Polkovnikov, Advances in Physics **64**, 139 (2015), https://doi.org/10.1080/00018732.2015.1055918 .

[49] J. van Wezel, J. Zaanen, and J. van den Brink, Phys. Rev. B **74**, 094430 (2006).

[50] S. Blundell, *Magnetism in Condensed Matter*, reprint ed., Oxford Master Series in Condensed Matter Physics No. 4 (Oxford Univ. Press, Oxford, 2014).

[51] H. J. Lipkin, N. Meshkov, and A. J. Glick, Nuclear Physics **62**, 188 (1965).

[52] D. Stein and C. Newman, *Spin Glasses and Complexity*, Primers in Complex Systems (Princeton University Press, 2013).

[53] N. D. Mermin and H. Wagner, Phys. Rev. Lett. **17**, 1133 (1966).

[54] P. C. Hohenberg, Phys. Rev. **158**, 383 (1967).

[55] D. I. Khomskii, *Basic Aspects of the Quantum Theory of Solids: Order and Elementary Excitations* (Cambridge University Press, 2010).

[56] P. Fazekas, *Lecture Notes on Electron Correlation and Magnetism* (WORLD SCIENTIFIC, 1999) https://www.worldscientific.com/doi/pdf/10.1142/2945 .

[57] H. Bruus and K. Flensberg, *Many-Body Quantum Theory in Condensed Matter Physics: An Introduction*, Oxford Graduate Texts (OUP Oxford, 2004).

[58] J. van Wezel and J. van den Brink, American Journal of Physics **75**, 635 (2007).

[59] Y. Aharonov and D. Bohm, Phys. Rev. **115**, 485 (1959).

[60] P. Nozières, Europhysics Letters **103**, 57008 (2013).

[61] A. Syrwid, J. Zakrzewski, and K. Sacha, Phys. Rev. Lett. **119**, 250602 (2017).

[62] V. K. Kozin and O. Kyriienko, Physical Review Letters **123**, 210602 (2019).

[63] V. Khemani, R. Moessner, and S. L. Sondhi, Comment on "quantum time crystals from hamiltonians with long-range interactions" (2020), arXiv:2001.11037 [cond-mat.str-el] .

[64] V. K. Kozin and O. Kyriienko, Reply to "comment on "quantum time crystals from hamiltonians with long-range interactions"" (2020), arXiv:2005.06321 [quant-ph] .

[65] G. Floquet, Annales scientifiques de l'École Normale Supérieure **12**, 47 (1883).

[66] J. H. Shirley, Phys. Rev. **138**, B979 (1965).

[67] C. Delaive, *Dynamical tunneling in time crystals*, Unpublished master's thesis, Université de Liège, Liège, Belgique (2024).

[68] M. Sato and T. N. Ikeda, J. Phys. Soc. Jap. **94**, 111007 (2025), arXiv:2508.01783 [cond-mat.str-el] .

[69] D. V. Else, B. Bauer, and C. Nayak, Phys. Rev. X **7**, 011026 (2017).

[70] V. Khemani, C. W. von Keyserlingk, and S. L. Sondhi, Phys. Rev. B **96**, 115127 (2017).

[71] A. Riera-Campeny, M. Moreno-Cardoner, and A. Sanpera, Quantum **4**, 270 (2020).

[72] L. D'Alessio and M. Rigol, Phys. Rev. X **4**, 041048 (2014).

[73] P. Ponte, A. Chandran, Z. Papić, and D. A. Abanin, Annals of Physics **353**, 196–204 (2015).

[74] A. Russomanno, A. Silva, and G. E. Santoro, Physical Review Letters **109**, 10.1103/physrevlett.109.257201 (2012).

[75] A. Lazarides, A. Das, and R. Moessner, Phys. Rev. Lett. **112**, 150401 (2014).

[76] S. Notarnicola, F. Iemini, D. Rossini, R. Fazio, A. Silva, and A. Russomanno, Phys. Rev. E **97**, 022202 (2018).

[77] V. Khemani, A. Lazarides, R. Moessner, and S. L. Sondhi, Phys. Rev. Lett. **116**, 250401 (2016).

[78] W. C. Yu, J. Tangpanitanon, A. W. Glaetzle, D. Jaksch, and D. G. Angelakis, Phys. Rev. A **99**, 033618 (2019).

[79] C. W. von Keyserlingk, V. Khemani, and S. L. Sondhi, Phys. Rev. B **94**, 085112 (2016).

[80] F. M. Surace, A. Russomanno, M. Dalmonte, A. Silva, R. Fazio, and F. Iemini, Phys. Rev. B **99**, 104303 (2019).

[81] N. Y. Yao, A. C. Potter, I.-D. Potirniche, and A. Vishwanath, Phys. Rev. Lett. **118**, 030401 (2017).

[82] F. Damanet and J. Martin, Open quantum systems, Lecture course PHYS3136-1, University of Liège (2025), academic year 2024–2025.

[83] D. Gu, Z. Wang, and Z. Wang, Phys. Rev. B **112**, 245123 (2025).

[84] F. M. Gambetta, F. Carollo, M. Marcuzzi, J. P. Garrahan, and I. Lesanovsky, Phys. Rev. Lett. **122**, 015701 (2019).

[85] B. Zhu, J. Marino, N. Y. Yao, M. D. Lukin, and E. A. Demler, New Journal of Physics **21**, 073028 (2019).

[86] K. Chinzei and T. N. Ikeda, Phys. Rev. Res. **4**, 023025 (2022).

[87] X. Feng, S. Liu, S. Chen, and S.-X. Zhang, Tunable discrete quasi-time crystal from a single drive (2025), arXiv:2512.10303 [quant-ph] .

[88] G. Das, S. Saha, and R. Bhattacharyya, Phys. Rev. A **113**, 042216 (2026).

[89] F. Russo and T. Pohl, Phys. Rev. Lett. **135**, 110404 (2025).

[90] G. Passarelli, P. Lucignano, R. Fazio, and A. Russomanno, Phys. Rev. B **106**, 224308 (2022).

[91] H. Keßler, J. G. Cosme, C. Georges, L. Mathey, and A. Hemmerich, arXiv 10.1088/1367-2630/ab9fc0 (2020).

[92] Z. Liu, Y. Li, Z. Fei, and X. Wang, Boundary time crystals: Beyond mean-field theory (2025), arXiv:2510.03028 [quant-ph] .

[93] Z. Wang, R. Gao, X. Wu, B. Buča, K. Mølmer, L. You, and F. Yang, Phys. Rev. Lett. **135**, 230401 (2025).

[94] Z. Wang, R. Gao, X. Wu, B. Buča, K. Mølmer, L. You, and F. Yang, Phys. Rev. Lett. **135**, 230401 (2025).

[95] M. Esencan, A. I. Lvovsky, and B. Buča, Time crystals as passively protected oscillating qubits (2026), arXiv:2602.20269 [quant-ph] .

[96] S. Yang, Z. Wang, L. Fu, and J. Jie, Communications Physics **8**, 10.1038/s42005-025-02040-1 (2025).

[97] S. H. Strogatz, *Nonlinear dynamics and chaos*, 2nd ed. (CRC Press, London, England, 2019).

[98] G. Piccitto, M. Wauters, F. Nori, and N. Shammah, Phys. Rev. B **104**, 014307 (2021).

[99] Y. Nakanishi and T. Sasamoto, Phys. Rev. A **107**, L010201 (2023).

[100] P. Solanki, M. Krishna, M. Hajdušek, C. Bruder, and S. Vinjanampathy, Phys. Rev. Lett. **133**, 260403 (2024).

[101] A. Mukherjee, Y. Ibrahim, M. Hajdušek, and S. Vinjanampathy, Phys. Rev. A **110**, 012220 (2024).

[102] A. Pikovsky and A. Politi, *Lyapunov Exponents: A Tool to Explore Complex Dynamics* (Cambridge University Press, 2016).

[103] J. Schwinger, *ON ANGULAR MOMENTUM*, Tech. Rep. (Harvard Univ.; Nuclear Development Associates, Inc. (US), 1952).

[104] A. Auerbach, *Interacting Electrons and Quantum Magnetism*, Graduate Texts in Contemporary Physics (Springer Science & Business Media, 2012).

[105] X. Chen and J. Wu, Discrete time crystal and perfect many-body tunneling in a periodically driven heisenberg spin chain (2025), arXiv:2507.15565 [cond-mat.str-el] .

[106] S. Anisur, W. V. Liu, and S. Choudhury, Entropy **27**, 609 (2025).

[107] D. V. Else, W. W. Ho, and P. T. Dumitrescu, Phys. Rev. X **10**, 021032 (2020).

[108] S. Anisur and S. Choudhury, Dissipative dicke time quasicrystals (2026), arXiv:2602.05994 [quant-ph] .

[109] G. Benettin, L. Galgani, A. Giorgilli, and J.-M. Strelcyn, Meccanica **15**, 21 (1980).

[110] D. Gribben, A. Sanpera, R. Fazio, J. Marino, and F. Iemini, SciPost Phys. **18**, 100 (2025).

[111] L. Viotti, M. Huber, R. Fazio, and G. Manzano, Phys. Rev. Lett. **136**, 110401 (2026).

[112] H. Yoshida and R. Hamazaki, Theory of steady states for lindblad equations beyond time-independence: Classification, uniqueness and symmetry (2026), arXiv:2602.13095 [quant-ph] .

[113] K. Chinzei and T. N. Ikeda, Phys. Rev. Lett. **125**, 060601 (2020).